Title
The Double Copy: From Scattering to Radiation

Author
Chester, David Alan

Publication Date
2018

Peer reviewed|Thesis/dissertation

UNIVERSITY OF CALIFORNIA
Los Angeles

The Double Copy:
From Scattering to Radiation

A dissertation submitted in partial satisfaction
of the requirements for the degree
Doctor of Philosophy in Physics

by

David Alan Chester III

2018

ABSTRACT OF THE DISSERTATION

The Double Copy:
From Scattering to Radiation

by

David Alan Chester III
Doctor of Philosophy in Physics
University of California, Los Angeles, 2018
Professor Zvi Bern, Chair

This thesis discusses consequences of color-kinematics duality and applications towards computing quantum scattering amplitudes and classical radiation fields. Stemming from this duality, tree-level Bern-Carrasco-Johansson amplitude relations can be extended to one-loop integral coefficient relations for scattering in Yang-Mills theory. The double copy, which also follows from color-kinematics duality, allows for graviton scattering amplitudes to be found from scattering amplitudes in Yang-Mills theory. Additionally, a classical radiative double copy for obtaining gravitational waves in various theories is discussed. As a warm-up, a classical double copy of the Lienard-Wiechert potential in electrodynamics is found within a specific context, which allows for gravitational waves in linearized gravity to be found. Next, radiation in Yang-Mills and Yang-Mills-biadjoint-scalar theories is found, and the radiative double copy of these results allows for radiation in general relativity and Einstein-Yang-Mills theory, repsectively. In light of the recent detection of gravitational waves by the LIGO collaboration, this motivates the search of efficient analytic techniques for computing gravitational radiation. The double copy offers a way to apply methods from particle physics to gravitational-wave astronomy.

The dissertation of David Alan Chester III is approved.

Eric D'Hoker

Burt Totaro

Zvi Bern, Committee Chair

University of California, Los Angeles

2018

This thesis is dedicated to my family, friends, and colleagues.

TABLE OF CONTENTS

LIST OF FIGURES

ACKNOWLEDGMENTS

This work was accomplished via constant support from various individuals and institutions. First, I am thankful for the love and financial support of my parents that have allowed me to pursue higher education. If it wasn't for Alejandro Rodriguez, I may never have been inspired enough to study theoretical physics at MIT for undergraduate studies. I am thankful to Stephen Goodman, Vinay Ramasesh, and Emily Davis for providing early motivation in pursuing high energy theory. I would like to thank Erotokritos Katsavounidis and Brennen Hughey for initial research opportunities related to gravitational waves at LIGO roughly ten years ago. I also am thankful to Peter Bermel, Joeseph Formaggio, and Sophia Cisneros for fostering the development of my research skills, as well as Hong Liu for teaching a sophisticated treatment of renormalization in quantum field theory.

A successful graduate career was due to countless interactions with many excellent educators and researchers. I am particularly thankful to Zvi Bern for his constant guidance throughout graduate school, as well as many others at UCLA. In particular, I would like to thank Scott Davies, Josh Nohle, Alex Edison, Julio Parra-Martinez, Jared Claypoole, Walter Goldberger, Alexander Ridgway, Jedidiah Thompson, Donal O'Connell, Isobel Nicholson, Andres Luna, and Alexander Ochirov for various discussions related to this research. Without these conversations, this thesis would have never come to fruition. I would like to thank all of my professors who have lectured me in various courses and have answered a countless number of questions. Finally, I would like to thank Mani Bhaumik and Zvi Bern for opening the Mani L. Bhaumik Institute of Theoretical Physics, which has allowed me to attend lectures from many world-renowned physicists.

VITA

2012 B.S. Physics, Concentration in Theoretical Physics and Music
Massachusetts Institute of Technology, Massachusetts Ave, Cambridge, MA , USA

PUBLICATIONS

This thesis includes portions of the previously published work outlined below.

D. Chester, "Bern-Carrasco-Johansson relations for one-loop QCD integral coefficients," Phys. Rev. D 93, no. 6, 065047 (2016). [arXiv:1601.00235 [hep-th]].

D. Chester, "Radiative double copy for Einstein-Yang-Mills theory," Phys. Rev. D 97, 084025 (2018). [arXiv:1712.08684 [hep-th]].

CHAPTER 1

Introduction

Physicists are looking for the relationship between the four fundamental forces of nature. The standard model successfully describes the quantum field theory of electromagnetic, weak, and strong interactions, which includes Maxwell's linear electrodynamics and Yang-Mills theory, a nonlinear gauge theory. Gravity is accurately described by Einstein's theory of general relativity, and string theory contains a high-energy completion of gauge theory and general relativity. While the Lagrangians and equations of motion for Yang-Mills theory and general relativity appear to be different, the solutions of the two theories remarkably seem to be related. The "double copy" construction discussed in this thesis uses gauge theory solutions to find gravity solutions for quantum scattering amplitudes and classical radiation fields.

The double copy originates from ideas in string theory. The tree-level Kawai-Lewellen-Tye (KLT) relations in string theory relate the scattering amplitudes of closed strings to two copies of open-string amplitudes [1]. By taking the low-energy limit, it was then realized that similar relations hold at tree-level for quantum field theory, which relate gravitons to gluons [2]. This was applied to loop level of quantum field theories via generalized unitarity [3, 4], which led to various studies of perturbative quantum gravity and the UV properties of various supergravity theories [5–10].

Shortly after KLT relations were found, factorization of color and kinematics simplified Yang-Mills amplitudes for specific gluon scattering processes [11–14]. As particle colliders scattered nucleons at high energies, theorists pursued precision quantum corrections due to gluon background processes, which led to efficient recursive methods [15]. Over a decade later, investigations of string theory in twistor space [16] inspired modern on-shell recursive methods for computing tree-level amplitudes that exploits factorization of color and kinemat-

ics [17–20]. A systematic bootstrapping of one-loop QCD amplitudes had phenomenological applications for colliders [21–23], including detailed analysis of QCD jets in search of new physics [23–27] prior to the LHC's detection of the Higgs boson [28, 29].

A kinematic analog of the Jacobi identity for color factors was found, which led to the Bern-Carrasco-Johannson (BCJ) relations between tree-level color-ordered partial amplitudes in Yang-Mills theory [30–32]. This included the development of the double copy at tree level, a procedure for finding gravity amplitudes from gauge theory amplitudes. The double copy helps with understanding the relationship between supersymmetric gauge and gravity theories at loop level [33–48]. In particular, the double copy helped compute additional UV properties of supergravity theories [49–55]. Related progress was made in string theory, including the development of additional monodromy relations and loop-level KLT relations [56–66].

Color-kinematics duality and the double copy have simplified and related scattering amplitudes amongst a wide class of theories, including the nonlinear sigma model and Born-Infeld theory [67–71]. A biadjoint scalar field theory can be added to Yang-Mills theory to find scattering amplitudes in Einstein-Yang-Mills theory [72–74]. The CHY formalism allows for KLT/string-inspired amplitude relations between Yang-Mills and general relativity [75–77], which also shows how Einstein-Yang-Mills theory, Dirac-Born-Infeld theory, special Galileon theory, the nonlinear sigma model, and biadjoint scalar theory are all interrelated [69, 78–81]. Additionally, Z-theory has been proposed to bring additional double copy structure to string theory amplitudes [82–84].

While progress has been made to investigate the origins of the double copy [85–89], the precise relationship between gauge and gravity theories is not fully understood. More practically, the double copy could be useful for computations of gravitation radiation from physical sources [90–92]. As LIGO continues to collect more gravitational wave data, ever more complex precision calculations will be needed. The double copy approach offers the possibility of greatly simplifying such computations, given that gauge-theory calculations are simpler than those in general relativity. We look to address this topic by first introducing color-kinematics duality and the double copy for scattering amplitudes in quantum field

theory, followed by a brief overview of gravitational radiation and the radiative double copy for classical gravitational waves.

1.1 Color-Kinematics Duality and the Double Copy for Scattering Amplitudes

The double copy is based on the duality between color and kinematics. Factorization of color and kinematics allows for Yang-Mills tree amplitudes to have the following representation,

$$\mathcal{A}_n^{\text{tree}} = g^{n-2} \sum_{i \in \Gamma} \frac{1}{S_i} \frac{n_i c_i}{D_i}, \tag{1.1}$$

where g is the coupling constant, i sums over all Feynman diagrams Γ with only three-point vertices, S_i is the symmetry factor associated with the ith diagram, n_i is a kinematic numerator, c_i is a color numerator, and D_i is a denominator comprised of inverse propagators. The color factors c_i are comprised of the structure constants f^{abc} from the non-Abelian gauge theory with SU(N) symmetry. Since the structure constants satisfy Jacobi relations, various color factors also satisfy the following simple identity,

$$c_i + c_j + c_k = 0, \tag{1.2}$$

where i, j, and k are labels for three different diagrams which have color factors satisfying a Jacobi relation.

Since the four-point gluon vertex contains two factors of f^{abc}, these contributions can be represented by combinations of two three-point gluon vertices which only contain one factor of f^{abc}. As such, summing over all Feynman diagrams contains redundant information, and the tree-level amplitudes are spanned by a basis with only trivalent graphs Γ_3. Once this representation is chosen, the kinematic numerators are found to satisfy the following relationship dual to the Jacobi relations,

$$n_i + n_j + n_k = 0. \tag{1.3}$$

This color-kinematics duality also led to the discovery of tree-level Bern-Carrasco-Johansson (BCJ) amplitude relations [30]. At four points, this leads to the following simple BCJ

relationship for color-stripped partial amplitudes A_n^{tree},

$$s_{24}A_4^{\text{tree}}(1,2,4,3) = s_{14}A_4^{\text{tree}}(1,2,3,4), \tag{1.4}$$

where $s_{ij} = (p_i + p_j)^2$ are inverse propagators in terms of external momenta. The BCJ amplitude relations are most easily noticed when the amplitudes are put in a representation that allows the kinematics factors to satisfy relations analogous to the color-factor Jacobi relations, which can occur when all contributions are represented as trivalent graphs. Whenever such a representation is found, graviton amplitudes can be found perturbatively via the double copy, which was later extended to loop level via unitarity methods [35].

To introduce the double copy, the general form of an n-point L-loop gauge theory amplitude in d dimensions is put in the following representation

$$\mathcal{A}_n^{(L)} = i^L g^{n-2+2L} \sum_{i\in\Gamma_3} \int \prod_{l=1}^{L} \frac{d^d p_l}{(2\pi)^d} \frac{1}{S_i} \frac{n_i c_i}{D_i}, \tag{1.5}$$

where i sums over all diagrams Γ_3 with at most three-point vertices, L loop momenta are integrated over for perturbative quantum corrections. This representation of the amplitude is not unique, as generalized gauge transformations allow for the transfer of terms between the different n_i. In this representation, contact terms such as the four-point gluon vertex are absorbed into trivalent diagrams by multiplying and dividing by appropriate propagators.

The double copy states that a gravity solution can be found by replacing color factors with appropriate kinematic factors. For scattering amplitudes, the color numerator c_i is replaced with a distinct kinematic numerator $\tilde{n}_i$ which may be found from a different gauge theory, such that

$$c_i \to \tilde{n}_i, \qquad g \to \frac{\kappa}{2}. \tag{1.6}$$

The corresponding n-point L-loop gravity amplitude is given by

$$\mathcal{M}_n^{(L)} = i^{L+1} \left(\frac{\kappa}{2}\right)^{n-2+2L} \sum_{i\in\Gamma_3} \int \prod_{l=1}^{L} \frac{d^d p_l}{(2\pi)^d} \frac{1}{S_i} \frac{n_i \tilde{n}_i}{D_i}. \tag{1.7}$$

In order to apply the double copy procedure, it was initially thought that the gauge theory amplitude must be put in a canonical BCJ form, which states that the kinematic numerators

satisfy an analogous Jacobi identity, such that the kinematic numerators and the color factors satisfy the same algebraic properties. The original conjecture states that at least one choice of numerators exists such that the duality is manifest. More recently, the color-kinematics duality constraint has been relaxed, so that the duality only needs to hold manifestly on the unitarity cuts, rather than on the entire multiloop integral [93]. This allows for more general ansatzs to be formed, making it easier to find a representation of the amplitudes that allows for a double copy. Most recently, the UV properties of $\mathcal{N} = 8$ supergravity has been found to five loops [55].

1.2 Motivating a Radiative Double Copy

Finding exact solutions in general relativity, in particular for gravitational wave emission, is often difficult. The post-Newtonian (PN) approximation was introduced by Einstein in 1916 and studied by de Sitter and Lorentz as a weak-field nonrelativistic expansion, see Ref. [94] for a more detailed history. This led to the discovery of the quadrupole moment method for finding gravitational waves in linearized gravity, presented in Section 3.1.1. The quadrupole moment method is a nonrelativistic weak-field approximation found from the linearized wave equation. The post-Newtonian (PN) approximation refers to assuming $v/c \ll 1$ and allows for relativistic corrections to be added to the solution found by the quadrupole moment method via a multipole expansion. For bound-state sources, the virial theorem states that

$$\frac{v^2}{c^2} = \frac{Gm}{rc^2}, \tag{1.8}$$

where G is Newton's gravitational constant, m is the total mass of the system, and r is the typical size of the system. Therefore, the PN approximation also expands in powers of $\sqrt{G}$, which assumes weakly interacting gravitational fields. As such, linearized gravity describes the lowest (zeroth) order of the PN approximation.

The post-Minkowskian (PM) approximation makes no assumption about v/c, yet makes a weak-field approximation by expanding in powers of $\sqrt{G}$. For weak fields, retardation effects are negligible in the near zone, which allows for the PN approximation to be utilized

for the first few lowest orders. However, radiation is in the far zone and necessitates retardation effects. Since the PN approximation to lowest order utilizes an instantaneous Green function from Newtonian gravity, naively utilizing the PN approximation to find radiation at arbitrarily high orders fails to satisfy the proper boundary conditions and causes unphysical divergences due to neglecting gravitational backreaction.

In 1986, Blanchet and Damour addressed these difficulties by considering a post-Minkowski (PM) approximation in vacuum for regions of spacetime with radii larger than d [95], corresponding to the intermediate and radiation zones. The PN approximation is utilized in the near and intermediate zones, and boundary conditions are utilized to connect this solution with the PM approximation, which allows for gravitational radiation to be found in the far zone to higher orders in v/c [96–103]. Alternatively, Will, Wiseman, and Pati have presented the Direct Integration of the Relaxed Einstein equation (DIRE) approximation [104–107], which gives equivalent results to those found by Damour and Blanchet.

While results within the PN approximation have been found up to fourth order [108–116], using the PM approximation with physical sources in the near zone and properly utilizing a retarded Green function to find radiation in the far zone has only been found to first order [117–124]. While the PN approximation is typically simpler, perturbing in two different parameters causes an explosion of terms at higher orders. If the technical difficulties of the PM approximation were properly dealt with, such a formalism may allow for more compact expressions at higher orders. Due to these technical challenges and the fact that most physically relevant sources of radiation come from bound states, the PN approximation has received more focus. However, scattering processes are not bound by the same virial theorem, which allow for the possibility of relativistic weak-field scenarios. Graviton scattering amplitudes found in perturbative quantum field theory takes a weak-field approximation similar to the PM approximation.

Even though the issue of matching boundary conditions at infinity has been solved, it is still difficult to calculate gravitational waves to high orders in perturbation theory due to complexity of general relativity. The double copy has proven to be efficient for high-order calculations of perturbative graviton scattering amplitudes. The radiative double copy

takes inspiration from the double copy of scattering amplitudes by finding rules which replace charge/color factors with appropriate kinematic factors. In particular, the charge of a particle is replaced by its corresponding momentum, as suggested from color-kinematics duality. It was first shown that any metric in Kerr-Schild form, an infinite family of classical solutions to Einstein's field equations, has a single copy in electromagnetism after subtracting away the Lienard-Wiechert potential [90].

Further investigations have been made for more exotic solutions and in higher dimensions. The electric charge density is the single copy of the Komar energy density [125]. A dyon is a single copy of the Taub-NUT spacetime, as the NUT charge is the double copy of the magnetic charge [126]. The Taub-NUT double copy is exposed when put in a double Kerr-Schild form, adding a term for the magnetic charge contributions. It was also found that the single copy of Plebanski gravity allowed for the Yang-Mills equations to be solved in curved space as well, which may be expected from the perspective of E8 unification [127–129]. The de Sitter metric can be written in a Kerr-Schild form, showing that the cosmological constant is the double copy of a uniform electric charge density.

Recent work has also generalized the static point particle solution to trajectories with arbitrary accelerations [91]. The authors also showed that the Coulomb/Schwarzschild double copy is indeed the same double copy as the scattering amplitudes double copy. The zeroth copy can be used to find a biadjoint scalar field, which allows for some promising nonperturbative studies [130]. The Kerr-Schild double copy construction was extended to curved spacetime [131, 132], as well as scattering amplitudes on background plane waves [133].

A perturbative double copy from Yang-Mills theory for arbitrary radiation metrics was introduced by Goldberger and Ridgway [92]. Within this construction, biadjoint scalar field theory solutions can give radiation in Yang-Mills theory [134], and progress has been made with bound states [135] and spinning black holes [136, 137]. Another perturbative spacetime approach allowed for a radiative double copy [138], and adding ghost fields to Yang-Mills theory allows for the dilaton to be removed from inelastic black hole scattering to lowest order [139].

1.3 Outline

This thesis focuses on consequences of color-kinematics duality. In Chapter 2, the implications of the tree-level BCJ relations are studied at next order. When a one-loop Yang-Mills amplitude is spanned by a basis of integrals with corresponding coefficients, the BCJ relations provide a wide variety of one-loop integral coefficient relations. Similar integral coefficient relations should exist at arbitrary loop order, demonstrating that color-kinematics duality helps simplify perturbative calculations. Furthermore, since the double copy holds, similar relations could be found in theories of gravity.

The rest of the thesis focuses on understanding how the double copy can be used to find gravitational waves in a perturbative weak-field approximation. Chapter 3 focuses on comparing radiation in electrodynamics to radiation in linearized gravity. While the radiation fields do not exhibit a straightforward double copy, a gravitational analogue of the Lienard-Wiechert potential is found within a specific context. Subtleties of the Lienard-Wiechert potential for relativistic phenomena are mentioned, which may be related to the difficulties of extending the PM approximation to higher orders.

In Chapter 4, radiation in nonlinear gauge and gravity theories is studied via Feynman diagrams with a worldline parametrization. A radiative double copy allows for gravitational radiation to be found from Yang-Mills radiation. Furthermore, it is shown that radiation in Yang-Mills-biadjoint-scalar theory allows for a double copy to correctly reproduce radiation in Einstein-Yang-Mills theory. Additionally, a scalar field is added to Yang-Mills, and an ansatz for its solution is found to remove the dilaton within the formalism of of Ref. [92], which is analogous to what was found in Ref. [139]. Chapter 5 states concluding remarks and potential for further development.

CHAPTER 2

Scattering Amplitudes and One-Loop Integral Coefficient Relations

This chapter reviews work previously published by the author [140], which investigates the color-kinematics duality at loop level in Yang-Mills theory.

2.1 From Trees to Loops

Devising efficient methods for calculating scattering amplitudes has been useful to confirm the validity of the Standard Model. Even at tree level, the number of Feynman diagrams dramatically increases as the number of legs increases. For seven, eight, and nine external gluons there are already 2485, 34300, and 559405 Feynman diagrams needed at tree level [141]. Of course, with modern techniques we can obtain the amplitude $\mathcal{A}_n$ without calculating any Feynman diagrams. At tree-level, the amplitude is decomposed into a color-stripped partial amplitude A_n, which separates the color from the kinematics. The Parke-Taylor formula gives simple form of maximally helicity violating (MHV) or anti-MHV partial amplitudes [11, 14]. On shell recursion developed by Britto, Cachazo, Feng and Witten (BCFW) can be used to find any helicity [17, 18]. To compute the total amplitude $\mathcal{A}_n$, we need to compute the $n!$ partial amplitudes A_n, corresponding to the different permutations of the legs. However, not all $n!$ partial amplitudes are independent. Since we have a trace over the color generators, the partial amplitudes have cyclic symmetry, leaving $(n-1)!$ independent partial amplitudes. The partial amplitudes also satisfy a reflection property and the $U(1)$ photon decoupling identity, which reduces the number of independent partial amplitudes. (See e.g. Refs. [141, 142].) Remarkably, there are more tree level partial amplitude identities. The

Kleiss-Kuijf relations [143] reduces the number of independent partial amplitudes to $(n-2)!$. Furthermore, the Bern-Carrasco-Johansson (BCJ) amplitude relations [30, 56, 57, 144] give $(n-3)!$ independent partial amplitudes. This chapter applies these ideas to reduce the number of independent integral coefficients at one loop.

At one loop, we consider on-shell diagrams instead of Feynman diagrams. We apply the unitary method finding the value of the loop amplitude with the loop momentum on-shell. Furthermore, when we apply the unitarity cuts, one-loop amplitudes with massless external legs can be reconstructed in terms of products of tree amplitudes. The coefficients of basis integrals are fully determined from four-dimensional tree amplitudes [3, 4] and rational remainders from D-dimensional ones [145–149]. For a modern review of on-shell and unitarity methods for one-loop QCD amplitudes, we refer the reader to Ref. [150].

Since tree amplitudes determine the integral coefficient within the unitarity approach, we expect that the integral coefficients satisfy similar identities as the tree amplitudes themselves. In particular, we show that the tree-level BCJ amplitude relations can be used to derive integral coefficient identities. Since the loop momenta always have two on-shell solutions, we have to decompose the integral coefficient into two pieces. It is these pieces which actually satisfy the coefficient relations, rather than the total coefficient.

We demonstrate that tree-level identities significantly decrease the total number of independent integral coefficients. These relations could be used to either improve the efficiency of one-loop amplitude calculations or to provide a stability or other cross checks for the integral coefficients (e.g. see Ref. [23]).

There has been some work of extending tree-level relations to the loop level already. Tree-level monodromy relations have been applied to create loop level relations [151]. Boels and Isermann have applied the tree-level Kleiss-Kuijf identities to one-loop partial amplitudes [152, 153]. They have also extended the BCJ relations to relate one-loop integral bases. This present chapter is somewhat similar, except we apply the BCJ relations to the coefficients. Furthermore, work has been done to relate the two-loop nonplanar amplitude to the planer amplitude through the use of a BCJ type of relation [154].

This chapter is organized as follows: To demonstrate that the one-loop integral coefficients satisfy BCJ integral coefficient relations, we start by reviewing the tree-level BCJ relations and the unitarity method in section 2.1. In section 2.2, we derive the general expressions for the one-loop BCJ integral coefficient relations from the tree-level BCJ amplitude relations. In section 2.3, we explicitly provide examples and confirm that the BCJ integral coefficient relation is satisfied.

2.1.1 Introduction to Tree-Level BCJ Amplitude Relations

In this section, we review the spinor-helicity formalism, the unitarity method, and tree-level identities. In the next section, we will show that the BCJ amplitude relations can be used with the unitarity method to find new relations between integral coefficients.

The spinor-helicity formalism allows for simple expressions of scattering amplitudes. The spinors take advantage of the isomorphism between $Spin(3,1)$ and $SL(2,\mathbb{C})$, allowing for $\mathbb{C}^2$ spinors in projective space. These two components spinors allows for dimensional analysis and spin content uniquely determine massless amplitudes. When working with three- and four-point amplitudes at tree level with the spinor-helicity formalism, the amplitudes can be uniquely written down by counting particles and their spin. Recursive techniques are used to generalize to n-point amplitudes. Unitarity methods are applied to evaluate one-loop amplitudes, which recycle tree amplitudes. On-shell recursion relations allow for finite loop amplitudes. As such, it is possible to recursively calculate any n-point one-loop gluon amplitude simply by knowing three- and four-loop amplitudes along with a couple simple recursive techniques.

Two component complex spinors are used to represent massless fermions and vector bosons. A photon or gluon is a spin-one particle, but since it has no mass, there are only two independent spin states and can be represented by a two component spinor λ^i. The 4-component Dirac field ψ and its free massive Lagrangian,

$$\mathcal{L} = \bar{\psi}(i\partial\!\!\!/ - m)\psi, \tag{2.1}$$

when varied gives the Dirac equation

$$\begin{aligned}
(i\partial\!\!\!/ - m)\psi &= 0, \\
i\partial_\mu \bar{\psi}\gamma^\mu + m\bar{\psi} &= 0, \\
\psi(x) &= u(p)e^{ipx} + v(p)e^{-ipx}, \\
(p\!\!\!/ + m)u(p) &= 0, \\
(p\!\!\!/ - m)v(p) &= 0.
\end{aligned} \tag{2.2}$$

If the particle is assumed to be massless, then the two independent helicity states $u(p)$ and $v(p)$ follow the same equation of motion, which allows for the theory to be represented in terms of spinor-helicity states with the Weyl equation,

$$p\!\!\!/ u(p) = p\!\!\!/ v(p) = 0. \tag{2.3}$$

Recall that $v_\pm$ is an outgoing antifermion, $\bar{u}_\pm$ is an outgoing fermion. For all amplitudes, the momenta will be assumed to be outgoing. The $\pm$ subscript refers to the helicity of the fermion. For massless fermions, we have $u_\pm = v_\mp$ and $\bar{v}_\pm = \bar{u}_\mp$.

The spinor-helicity formalism is introduced below,

$$\begin{aligned}
u_+(k_i) &= v_-(k_i) = \left|k_i^+\right\rangle = |i\rangle = \lambda(k_i), \\
u_-(k_i) &= v_+(k_i) = \left|k_i^-\right\rangle = |i] = \tilde{\lambda}(k_i), \\
\bar{u}_+(k_i) &= \bar{v}_-(k_i) = \left\langle k_i^+\right| = [i| = \underline{\lambda}(k_i), \\
\bar{u}_-(k_i) &= \bar{v}_+(k_i) = \left\langle k_i^-\right| = \langle i| = \underline{\tilde{\lambda}}(k_i).
\end{aligned} \tag{2.4}$$

As shown, there are 3 different notations for writing the spinors, with $|i\rangle$ being simpler than $\left|k_i^+\right\rangle$ or $\lambda(k_i)$,

$$\begin{aligned}
\langle ij\rangle &= \left\langle k_i^-\right| k_j^+\right\rangle = \bar{u}_-(k_i)u_+(k_j) = \lambda^a(k_i)\lambda_a(k_j) = \underline{\lambda}(k_i)\lambda(k_j), \\
[ij] &= \left\langle k_i^+\right| k_j^-\right\rangle = \bar{u}_+(k_i)u_-(k_j) = \tilde{\lambda}_{\dot{a}}(k_i)\tilde{\lambda}^{\dot{a}}(k_j) = \tilde{\lambda}(k_i)\underline{\tilde{\lambda}}(k_j).
\end{aligned} \tag{2.5}$$

$$\tag{2.6}$$

The spinors are nice to work with, as complex conjugation flips the helicity state. These spinors are antisymmetric,

$$\langle ij\rangle = -\langle ji\rangle, \qquad [ij] = -[ji], \qquad \langle ii\rangle = [jj] = 0. \tag{2.7}$$

Channels such as s, t, and u as well as dot products of momenta are written as

$$\langle ij\rangle\,[ji] = 2k_i\cdot k_j = (k_i+k_j)^2 = s_{ij}. \tag{2.8}$$

Charge conjugation can be applied via

$$\langle k_i|\,\gamma^\mu\,|k_j] = [k_j|\,\gamma^\mu\,|k_i\rangle\,. \tag{2.9}$$

The Gordon identity also is useful since

$$[i|\,\gamma^\mu\,|i\rangle = \langle i|\,\gamma^\mu\,|i] = 2k_i^\mu. \tag{2.10}$$

Also, projection operators are given by

$$|i\rangle\,[i| = \frac{1}{2}(1+\gamma_5)\not{k}_i, \qquad |i]\,\langle i| = \frac{1}{2}(1-\gamma_5)\not{k}_i, \qquad |i\rangle\,[i| + |i]\,\langle i| = \not{k}_i. \tag{2.11}$$

The Fierz rearrangement identity is also needed for simplification,

$$\langle i|\,\gamma^\mu\,|j]\,\langle k|\,\gamma_\mu\,|l] = 2\,\langle ik\rangle\,[lj]\,. \tag{2.12}$$

The non-linear Schouten identity is also useful for simplifying complicated amplitudes,

$$\langle ij\rangle\,\langle kl\rangle = \langle ik\rangle\,\langle jl\rangle + \langle il\rangle\,\langle kj\rangle\,. \tag{2.13}$$

Finally, momentum conservation in an n-point amplitude is written as the following,

$$\sum_{i=1,\neq j,k}^{n} [ji]\,\langle ik\rangle = 0. \tag{2.14}$$

Note that massive fermions can be represented as two massless fermions by using the light-cone decomposition. This will not be discussed, but it is possible and is discussed on pages 9 and 10 in Ref. [155].

For representing polarization vectors for massless gauge bosons of helicity ± 1,

$$\epsilon_\mu^+(k,q) = \frac{\langle q|\,\gamma_\mu\,|k]}{\sqrt{2}\,\langle qk\rangle}, \tag{2.15}$$

$$\epsilon_\mu^-(k,q) = \frac{\langle k|\,\gamma_\mu\,|q]}{\sqrt{2}\,[kq]}, \tag{2.16}$$

where k is the vector boson's momentum and q is a reference momentum containing any on-shell gauge transformation. Therefore, q is any momentum such that $\epsilon^{\pm}(k,q)\cdot q = 0$. The polarization vectors satisfy

$$\begin{aligned} \epsilon^{\pm}(k,q)\cdot k &= 0, && (2.17)\\ (\epsilon^{+}_{\mu})^{*} &= \epsilon^{-}_{\mu}, && (2.18)\\ \epsilon^{+}\cdot\epsilon^{-} &= -1, && (2.19)\\ \epsilon^{+}\cdot\epsilon^{+} &= 0. && (2.20) \end{aligned}$$

Recursive and on-shell methods will provide relations for amplitudes with more external legs and at higher orders in perturbation theory. The simplest amplitudes can be written down in terms of spinor inner products by counting essentially the spin, or the phase weight of each particle.

A scattering amplitude gives the probability on an n-point particle interaction and is a function of n momenta and spins for n external legs. The tree diagrams represent the zeroth order interactions, which only includes the classical solution in the path integral. Some quantum corrections are contained in one-loop diagrams, which contain one power of $\hbar$ from the first order of perturbation theory.

$$\mathcal{A}_n(\{\lambda_1,\tilde{\lambda}_1,h_1\},\{\lambda_2,\tilde{\lambda}_2,h_2\},\ldots,\{\lambda_n,\tilde{\lambda}_n,h_n\}) = \mathcal{A}_n^{\text{tree}} + \hbar\mathcal{A}_n^{\text{1-loop}} + \sum_{L=2}^{\infty}\hbar^L\mathcal{A}_n^{\text{L-loop}}. \quad (2.21)$$

Consider Yang-Mills theory, which has a local $SU(N)$ gauge symmetry. For example, QCD has a gluon, which is an $SU(3)$ gauge vector boson. The theory is non-Abelian and therefore has nontrivial color algebra. The gauge field A_μ can be stripped of its color, such that $A_\mu = A_\mu^a T^a$, where T^a represent the 8 generators of $SU(3)$. Similarly, the amplitudes can be stripped of color, leaving behind a partial amplitude. A trace of the color matrices averages over all possible color arrangements and factors out the color dependence of the amplitude. The remaining color-stripped partial amplitude A_n is only dependent on kinematic quantities such as momenta and helicities [142]

$$\mathcal{A}_n^{\text{tree}} = g^{n-2}\sum_{\sigma\in S_n/Z_n}\text{Tr}(T^{a_{\sigma(1)}}T^{a_{\sigma(2)}}\ldots T^{a_{\sigma(n)}})A_n^{\text{tree}}(\sigma(1),\sigma(2),\ldots,\sigma(n)), \quad (2.22)$$

where S_n/Z_n represents the $n!$ permutations of external legs divided by the n cyclic permutations which are removed because they would give the same color trace. Partial amplitudes only depend on kinematic variables, and the labels of the partial amplitude signify the momenta and helicities of the particles. For simplicity, we will only work with gluons, but a similar construction can be done to add quarks.

Working with these partial amplitudes greatly simplifies calculations. Note that this deconstruction only holds for tree-level, but there exists higher loop expressions for connecting partial amplitudes with the true amplitude. The partial amplitudes are color ordered and therefore only have poles in s channels for adjacent momenta. For example, a four-point partial amplitude $A_4^{\text{tree}}(1,2,3,4)$ can only have poles in s_{12}, s_{23}, s_{34}, or s_{41}, but not s_{13} or s_{24}. The partial amplitudes have a cyclic Z_n symmetry,

$$A_n^{\text{tree}}(1,2,\ldots,n) = -A_n^{\text{tree}}(2,1,\ldots,n) = A_n^{\text{tree}}(2,\ldots,n,1) = (-1)^n A_n^{\text{tree}}(n,\ldots,2,1). \quad (2.23)$$

One can also obtain a "photon decoupling equation" or "dual Ward identity" from considering some group theory of equation 28. The equation also holds for $U(N)$ as well as $SU(N)$, so summing over the identity must give zero,

$$0 = A_n^{\text{tree}}(1,2,3,\ldots,n) + A_n^{\text{tree}}(2,1,3,\ldots,n) + A_n^{\text{tree}}(2,3,1,\ldots,n) + \cdots + A_n^{\text{tree}}(2,3,\ldots,1,n). \quad (2.24)$$

The rest of this manuscript will work with partial amplitudes, and the term amplitude will now refer to partial amplitudes. Analytic structure and phase weight determines amplitudes explicitly. First, we will consider three-point and four-point tree amplitudes.

Due to the symmetry of the amplitudes, there are only a few independent helicity configurations. For three-point tree-level, we have $A_3^{\text{tree}}(1^-,2^-,3^-)$ and $A_3^{\text{tree}}(1^-,2^-,3^+)$ as the only two independent amplitudes. To switch all of the helicities, a complex conjugate is taken, and particle numbers can be swapped and permuted to get all other configurations. The analytic poles from adjacent external legs forces s_{12}, s_{23}, and s_{31} to be in the denominator

of the amplitude. Counting the phase weight uniquely determines the resulting numerator.

$$A_3^{\rm tree}(1^-,2^-,3^-) = 0, \tag{2.25}$$

$$A_3^{\rm tree}(1^-,2^-,3^+) = \frac{i\langle 12\rangle^4}{\langle 12\rangle\langle 23\rangle\langle 31\rangle}, \tag{2.26}$$

$$A_3^{\rm tree}(1^+,2^+,3^-) = \frac{-i[12]^4}{[12][23][31]}. \tag{2.27}$$

For four-point tree-level, we have $A_4^{\rm tree}(1^-,2^-,3^-,4^-)$, $A_4^{\rm tree}(1^-,2^-,3^-,4^+)$, and $A_4^{\rm tree}(1^-,2^-,3^+,4^+)$ as the three possibly independent amplitudes.

$$A_4^{\rm tree}(1^-,2^-,3^-,4^-) = A_4^{\rm tree}(1^-,2^-,3^-,4^+) = 0, \tag{2.28}$$

$$A_4^{\rm tree}(1^-,2^-,3^+,4^+) = \frac{i\langle 12\rangle^4}{\langle 12\rangle\langle 23\rangle\langle 34\rangle\langle 41\rangle} = \frac{i[34]^4}{[12][23][34][41]}, \tag{2.29}$$

$$A_4^{\rm tree}(1^-,2^+,3^-,4^+) = \frac{i\langle 13\rangle^4}{\langle 12\rangle\langle 23\rangle\langle 34\rangle\langle 41\rangle}. \tag{2.30}$$

There are no other independent helicity configurations. Larger n-point amplitudes can be built up by recursive methods. First, BCFW recursion will stitch diagrams together by shifting the poles in the complex plane properly. A second method is the CSW relations, which build n-point amplitudes out of on-shell MHV subamplitudes, with a leg given a complex momentum shift.

The BCJ amplitude relations at tree level are connected to color-kinematics duality [30]. The duality forces the Jacobi identity on the kinematic numerators, which naturally provide tree-level partial amplitude relations beyond what is contained in the Kleiss-Kuijf relations. The BCJ relations imply that only $(n-3)!$ of the partial amplitudes are independent. A convenient choice is to fix the first 3 legs. At four and five points, the BCJ tree amplitude relations are

$$\begin{aligned}
A_4^{\rm tree}(1,2,\{4\},3) &= A_4^{\rm tree}(1,2,3,4)\frac{s_{14}}{s_{24}}, \\
A_5^{\rm tree}(1,2,\{4\},3,5) &= \frac{A_5^{\rm tree}(1,2,3,4,5)(s_{14}+s_{45}) + A_5^{\rm tree}(1,2,3,5,4)s_{14}}{s_{24}}, \\
A_5^{\rm tree}(1,2,\{4,5\},3) &= \frac{-A_5^{\rm tree}(1,2,3,4,5)s_{34}s_{15} - A_5^{\rm tree}(1,2,3,5,4)s_{14}(s_{245}+s_{35})}{s_{24}s_{245}}
\end{aligned} \tag{2.31}$$

The original BCJ paper also includes general n-point formulas for generating the BCJ relations. Notice how the BCJ amplitude relations fixes the first three legs for the set of independent partial amplitudes.

To express amplitudes, we will use the spinor-helicity formalism, which gives remarkably compact expressions for certain tree amplitudes. Tree amplitudes with zero or one plus/minus helicities are zero (except for the three-point amplitudes). The n-point Parke-Taylor formula [11, 14] expresses the MHV partial amplitudes in a remarkably simple manner,

$$A_n^{\text{tree}}(1^+, \ldots, i^-, \ldots, j^-, \ldots, n^+) = i\frac{\langle ij\rangle^4}{\langle 12\rangle \langle 23\rangle \ldots \langle n1\rangle}. \tag{2.32}$$

To find all other helicity configurations, BCFW recursion, for example, can be applied to calculate any amplitude from the Parke-Taylor formula [17]. (See, for example, Ref. [156] for an exhaustive review with examples.)

2.1.2 Unitary Cuts and One-Loop Integral Basis Coefficients

We now review the unitarity method, which is used find one-loop amplitudes as a linear combination of integral coefficients times basis integrals. At one loop any massless amplitude can be decomposed into a set of basis integrals consisting of scalar boxes, triangles, and bubbles, plus rational terms for QCD [157–159]. This reduces the problem of calculating one-loop amplitudes to determining a set rational coefficients.

Britto, Cachazo, and Feng showed how generalized unitarity could be used to find the box coefficients [160]. The work of Ossola, Papadopolous, and Pittau [22] and Forde [161] extends this to the triangle and bubble coefficients. Unitarity cuts can be used to recycle tree amplitudes into the loop-level integral coefficients. Therefore, we can generate all one-loop amplitudes from tree amplitudes; the coefficients are simply products of tree amplitudes with loop momenta on-shell.

We will study the boxes, triangles, and bubbles necessary for massless QCD in the following subsections. In particular, we are interested in the total number of cuts needed as well as the loop momentum solutions for such cuts. In order to apply unitarity cuts to a diagram, we put the loop momenta on shell which is imposed on all internal lines in Fig. 2.1.

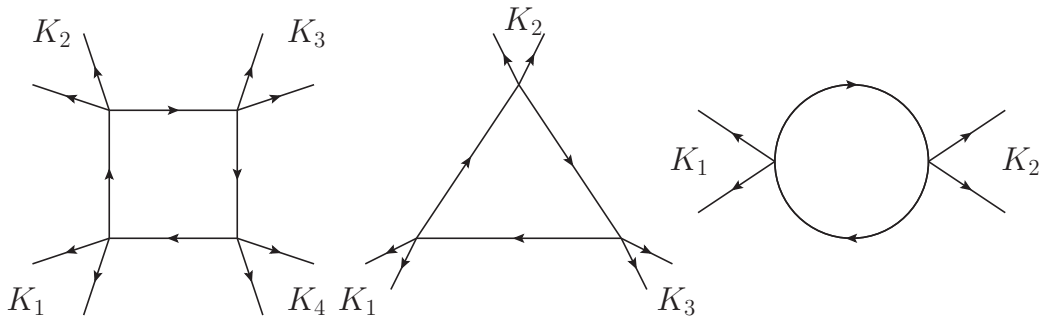

Figure 2.1: The box, triangle, and bubble cuts. At each corner there are an arbitrary of external lines.

To calculate the full one-loop amplitude, each possible unitary cut must be evaluated. Using generalized unitarity this allows us to determine the coefficients of basis integrals in terms of which the color-stripped partial amplitude is expressed,

$$A = \sum_{i=1}^{n_b} c_i \mathrm{Int}_i + R\,, \tag{2.33}$$

where i runs over the total number of basis integrals n_b, Int_i is a scalar integral, and R represents the rational terms which will be neglected throughout this chapter. Also, the word amplitude will also refer to the color-stripped partial amplitude throughout this chapter.

2.1.2.1 Box Cuts

To start our study of QCD amplitudes, we focus on the box coefficients which can be determined from the box cuts shown in Fig. 2.1. Next, we classify the different types of box cuts. There are zero-mass, one-mass, two-mass-e, two-mass-h, three-mass, and four-mass box cuts, which is shown in Fig. 2.2. Only the four-point amplitudes have a zero-mass box. There are n n-point one-mass boxes for $n \geq 5$, since there are n ways that the $n-3$ particles could be put together in the corner. For two-mass-h boxes, there are $(n-5)n$ ways with $n \geq 6$. The number of two-mass-e boxes would be the same, but we are now overcounting by a factor of two due to the symmetry of the two single legs being across from each other. Therefore, there are $(n-5)n/2$ two-mass-h boxes with $n \geq 6$. When $n \geq 7$, there are $n\binom{n-5}{2}$ three-mass

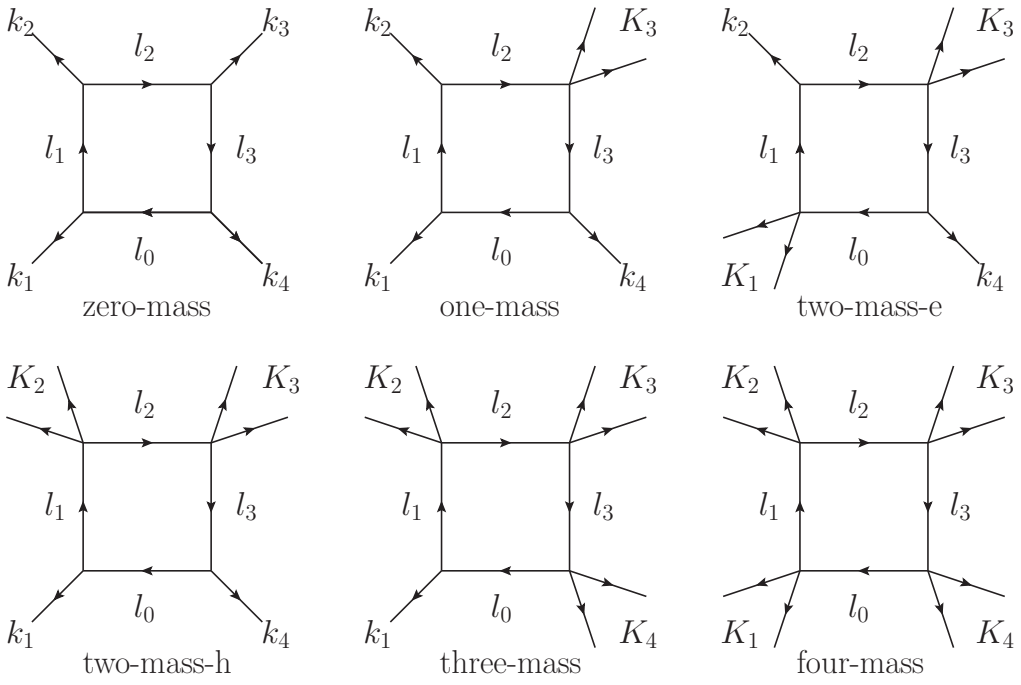

Figure 2.2: The zero-mass, one-mass, two-mass-e, two-mass-h, three-mass, and four-mass box cuts are shown above. Two-mass-e and two-mass-h stand for 'easy' and 'hard'. The K_i are sums of massless momenta and the k_i is the momentum of a single external massless leg.

boxes. For four-mass boxes, there are three contributing boxes. If $n \geq 8$ and $n \mod 4 = 0$, then there are $n/4$ contributing boxes. This corresponds to when all four corners of the box cut have the same number of legs, such as the only four-mass eight-point cut would have. If $n \geq 9$ and n is even, then there are an additional $n/2$. Finally, if $n \geq 9$, then there are $\sum_{i=1}^{n-8} n\binom{\lfloor (i+1)/2 \rfloor + 1}{2}$ additional four-mass boxes.

The unitarity cuts put the loop momenta on-shell, which gives a quadratic equation with two solutions. If there is at least one massless leg on the cut, we utilize the following compact solution [23, 162],

$$\begin{aligned} l_0^{\pm,\mu} &= \frac{\langle 1^\mp | \not{K}_2 \not{K}_3 \not{K}_4 \gamma^\mu | 1^\pm \rangle}{2 \langle 1^\mp | \not{K}_2 \not{K}_4 | 1^\pm \rangle}, \qquad l_1^{\pm,\mu} = -\frac{\langle 1^\mp | \gamma^\mu \not{K}_2 \not{K}_3 \not{K}_4 | 1^\pm \rangle}{2 \langle 1^\mp | \not{K}_2 \not{K}_4 | 1^\pm \rangle}, \\ l_2^{\pm,\mu} &= \frac{\langle 1^\mp | \not{K}_2 \gamma^\mu \not{K}_3 \not{K}_4 | 1^\pm \rangle}{2 \langle 1^\mp | \not{K}_2 \not{K}_4 | 1^\pm \rangle}, \qquad l_3^{\pm,\mu} = -\frac{\langle 1^\mp | \not{K}_2 \not{K}_3 \gamma^\mu \not{K}_4 | 1^\pm \rangle}{2 \langle 1^\mp | \not{K}_2 \not{K}_4 | 1^\pm \rangle}. \end{aligned} \tag{2.34}$$

Note that the '$-$' solution is simply the complex conjugate of the '$+$' solution. If we have a four-mass box, then we must resort to using the more lengthy solution provided by Britto, Cachazo, and Feng [160]. (See Ref. [163] for loop momentum solutions in $d = 4 - 2\epsilon$.)

To obtain an arbitrary box coefficient, we simply apply a unitarity cut and multiply the four corresponding tree amplitudes together:

$$\begin{aligned} A_n^{\text{one-loop}}\Big|_{boxes} &= \sum_{i=1}^{m} d_i \text{Box}_i = \sum_{i=1}^{m} (d_i^+ + d_i^-) \text{Box}_i, \\ d_{i;box}^{\pm} &= \frac{1}{2} A_{1,i}^{\text{tree}\pm} A_{2,i}^{\text{tree}\pm} A_{3,i}^{\text{tree}\pm} A_{4,i}^{\text{tree}\pm}, \end{aligned} \tag{2.35}$$

where the $\pm$ on the coefficients refers to the two one-loop solutions, $A_{j,i}^{\text{tree}\pm}$ are the tree amplitudes from the cuts, and m is the total number of boxes. Note that the true integral coefficient $d_{i;box}$ is the sum of the two coefficients $d_{i;box}^{\pm}$, but we must keep these separate to find the coefficient relations.

2.1.2.2 Triangles

Next consider the triangle integral coefficients. We start with the triangles by counting the number of triangle cuts. There are the one-mass, two-mass, and three-mass triangle cuts, which are shown in Fig. 2.3. Once again, there are n one-mass cuts. Similar to the two-

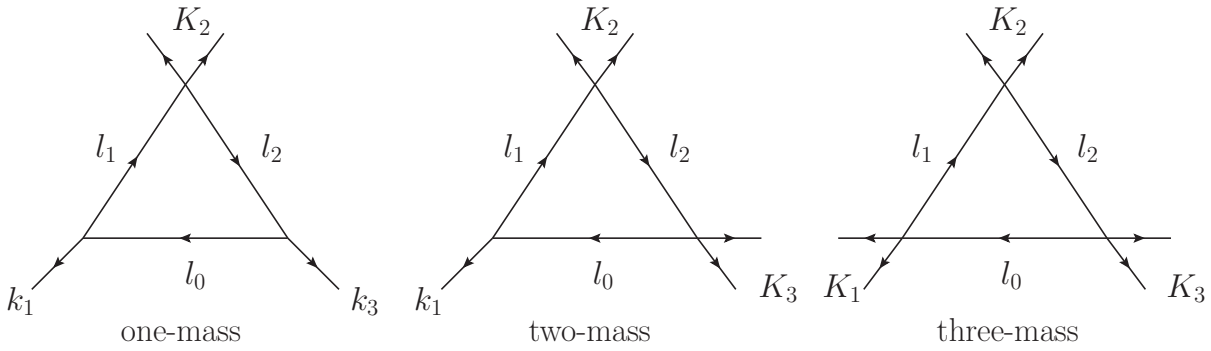

Figure 2.3: The one-mass, two-mass, and three-mass triangle cuts are shown above.

mass-e box cut, there are $(n-4)n$ two-mass triangle cuts. Finally, for the three-mass, we have an equation similar to the four-mass box cut, but no choose function is needed since it would have been choose 1. If $n \mod 3 = 0$ and $n > 5$, then we have $n/3$ contributing cuts. Furthermore, if $n > 6$, then we have an additional $\sum_{i=1}^{n-5} n\lfloor\frac{i+1}{3}\rfloor$.

For finding the loop solutions for triangle diagrams, a parameter t is introduced to represent the undetermined degree of freedom from having only three unitarity cuts. After converting Forde's loop solution [161] into our notation, we find

$$\begin{aligned}
\left\langle l_i^+\right| &= t\left\langle K_1^\flat\right| + \alpha_{i1}\left\langle K_3^\flat\right|, & \left|l_i^+\right] &= \frac{\alpha_{i2}}{t}\left|K_1^\flat\right] + \left|K_3^\flat\right], \\
\alpha_{01} &= \frac{S_1(\gamma_{13}+S_3)}{\gamma_{13}^2 - S_1S_3}, & \alpha_{02} &= -\frac{S_3(\gamma_{13}+S_1)}{\gamma_{13}^2 - S_1S_3}, \\
\alpha_{11} &= \alpha_{01} - \frac{S_1}{\gamma_{13}}, & \alpha_{12} &= \alpha_{02} - 1, \\
\alpha_{21} &= \alpha_{01} + 1, & \alpha_{12} &= \alpha_{02} + \frac{S_3}{\gamma_{13}},
\end{aligned} \tag{2.36}$$

where $i = 0, 1, 2$, $S_i = K_i \cdot K_i$, and $\gamma_{13}^\pm = K_1 \cdot K_3 \pm \sqrt{(K_1 \cdot K_3)^2 - K_1^2 K_3^2}$. The four-momentum representation of the loop momentum solution is

$$l_i^{+,\mu} = \alpha_{i2}K_1^{\flat,\mu} + \alpha_{i1}K_3^{\flat,\mu} + \frac{t}{2}\left\langle K_1^\flat\right|\gamma^\mu\left|K_3^\flat\right] + \frac{\alpha_{i1}\alpha_{i2}}{2t}\left\langle K_3^\flat\right|\gamma^\mu\left|K_1^\flat\right]. \tag{2.37}$$

We can in principle consider four triangle loop solutions, since there are two loop momenta and two gammas. However, if S_1 or $S_3 = 0$, then there is only one non-zero solution for gamma. In either case, we simply average over the two or four solutions, including the two

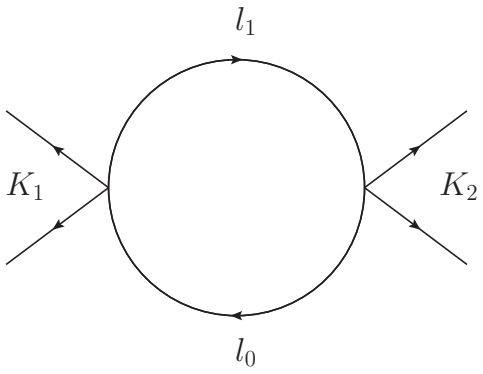

Figure 2.4: The needed two-mass bubble cut is shown above. The one-mass bubble cuts vanish.

loop momenta. To find the second loop solution, we can take the complex conjugate, or simply switch all of the angle brackets with the square brackets.

Note that our α_{ij}'s are a bit different than Forde, since we use different conventions for the loop and external momenta. Just as Forde showed, we find that $\alpha_{i1}\alpha_{i2} = \alpha_{j1}\alpha_{j2}$, for $i, j = 0, 1, 2$. Our conventions match those of Refs. [23, 163].

Following Forde's procedure to find the t-independent triangle coefficient we take

$$\begin{aligned} c^{\pm}_{i;tri}(t) &= \frac{1}{n_{\rm sol}} A^{\rm tree\pm}_{1,i} A^{\rm tree\pm}_{2,i} A^{\rm tree\pm}_{3,i}, \\ c^{\pm}_{i;tri} &= [{\rm Inf}_t c^{\pm}_{i;tri}(t)]|_{t=0}, \end{aligned} \tag{2.38}$$

where $n_{\rm sol}$ is two or four, depending on if there are one or two independent values for gamma. The symbol ${\rm Inf}_t$ instructs one to Taylor expand with respect to t around infinity and keep the $t^0 = 1$ term to obtain the triangle integral coefficients.

2.1.2.3 Bubbles

Next, we review the extraction of the bubble coefficient. Counting the number of bubble cuts is much simpler, since there are only one-mass and two-mass diagrams. There are n one-mass cuts and $\frac{n-3}{2}n$ two-mass cuts, shown in Fig. 2.4. The bubble loop momentum solution has two arbitrary parameters, t and y. Instead of using $K_2^{\flat,\mu}$, any arbitrary massless

vector χ^μ can be used. It is often convenient to choose it to be the last leg on K_1, which gives a simple $K_1^{\flat,\mu}$ and χ^μ. We define $K_1^{\flat,\mu}$ in terms of the massless spinor.

$$K_1^{\flat,\mu} = K_1^\mu - \frac{S_1}{2K_1\cdot\chi}\chi^\mu = K_1^\mu - \chi^{\flat,\mu}. \tag{2.39}$$

Now, we are ready to express the loop solution in terms of $K_1^{\flat,\mu}$ and $\chi^{\flat\mu}$.

$$\begin{aligned} \langle l_0^+| &= t\,\langle K_1^\flat| + (1-y)\,\langle\chi^\flat|\,, & |l_0^+] &= \frac{y}{t}\,|K_1^\flat] + |\chi^\flat]\,, \\ \langle l_1^+| &= \langle K_1^\flat| - \frac{y}{t}\,\langle\chi^\flat|\,, & |l_1^+] &= (y-1)\,|K_1^\flat] + t\,|\chi^\flat]\,. \end{aligned} \tag{2.40}$$

From these we can find loop momenta,

$$\begin{aligned} l_0^{+,\mu} &= yK_1^{\flat,\mu} + (1-y)\chi^{\flat,\mu} + \frac{t}{2}\,\langle K_1^\flat|\,\gamma^\mu\,|\chi^\flat] + \frac{y(1-y)}{2t}\,\langle\chi^\flat|\,\gamma^\mu\,|K_1^\flat]\,, \\ l_1^{+,\mu} &= (y-1)K_1^{\flat,\mu} - y\chi^{\flat,\mu} + \frac{t}{2}\,\langle K_1^\flat|\,\gamma^\mu\,|\chi^\flat] + \frac{y(1-y)}{2t}\,\langle\chi^\flat|\,\gamma^\mu\,|K_1^\flat]\,. \end{aligned} \tag{2.41}$$

To find a bubble coefficient, we first find the bubble cut contribution to the bubble coefficient, leaving in the y and t dependence,

$$b^\pm_{i;bub}(t,y) = \frac{1}{2}A^{\text{tree}\pm}_{1,i}(t,y)A^{\text{tree}\pm}_{2,i}(t,y). \tag{2.42}$$

To obtain the full bubble coefficient independent of y or t, one can use the methods described in Refs. [22, 23, 149, 161, 163]. The expression for the bubble cut contribution to coefficient is

$$\begin{aligned} b^\pm_{i;bub} &= [\text{Inf}_t[\text{Inf}_y b^\pm_{i;bub}(t,y)]|_{y^i=Y_i}]|_{t=0}, \\ Y_0 &= 1,\quad Y_1 = \frac{1}{2},\quad Y_2 = \frac{1}{3},\quad Y_3 = \frac{1}{4},\quad Y_4 = \frac{1}{5}. \end{aligned} \tag{2.43}$$

The bubble coefficient includes contributions from the triangles, but we will show that these contributions also satisfy the BCJ integral coefficient relations when we review the triangles. We will not review the bubble extraction in full detail, since we show that the triangle coefficient satisfies the new coefficient relations for all orders of t, implying that it hold for the total bubble coefficient as well.

Our goal is to understand how tree-level amplitude relations can be used to create loop-level integral coefficient relations. The BCJ amplitude relations are needed, since the ordering

of the two loop momenta for any tree amplitude is already fixed. Since the relations fix the third leg, we can fix one of the external legs for any of the isolated tree amplitudes. We see that one-loop integral coefficient relations naturally arise from the tree-level BCJ relations.

2.2 One-Loop Amplitude Coefficient Relations

Now that we reviewed the calculation of integral coefficients in arbitrary one-loop amplitudes, we focus on relations between these coefficients. To start, we count the number of integral coefficients needed before the BCJ integral coefficient relations are introduced.

Since the coefficient relations we will derive are independent of the external helicities, we will typically focus on MHV amplitudes for simplicity. Fixing the external helicity configuration, there are $n!$ external leg orderings, but the properties of the color trace leave only $(n-1)!/2$ to consider. The $(n-1)!$ factor comes from the cyclic symmetry and the factor of $1/2$ comes from the reflective symmetry of the trace over the color generators. Therefore, one would naively expect there to be $m(n-1)!/2$ independent integral coefficients, where $m = m_{box} + m_{tri} + m_{bub}$ is the number of cuts made per ordering of external momenta. In this section, we will show that the number of independent integral coefficients and tree amplitudes is actually smaller, since the BCJ relations can be recycled into the one-loop level by the unitarity method.

Since each d_i contains two adjacent loop momenta, the BCJ amplitude relations may be easily used if we fix the loop momenta to be the first two legs of the tree amplitude. Let us start by systematically considering possible box cuts of increasing complexity.

2.2.1 BCJ box integral coefficient identities

We start by considering the simplest box cuts. The first non-trivial example is a five-point one-loop amplitude, which contains only one-mass box cuts. After taking into account the cyclic and reflective symmetries of the partial amplitudes, one would expect $(n-1)!/2 = 12$ independent partial amplitudes. Furthermore, for each of these twelve amplitudes, there are

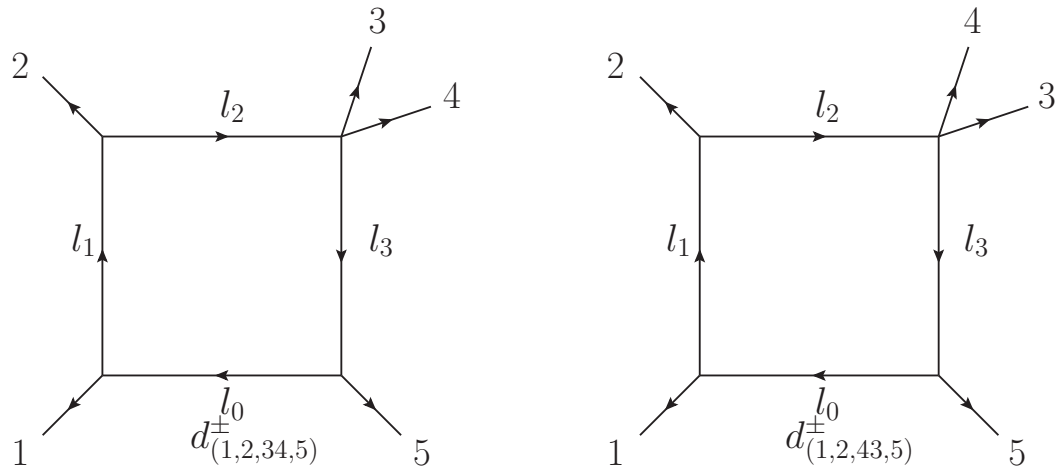

Figure 2.5: We consider two box cuts needed, which are identical up to a twisting of the K_3 leg. These two coefficients have the same loop solution, which allows for a tree level BCJ amplitude relation to be used to relate the two integral coefficients.

five box cuts, giving 60 coefficients to compute. We would like to demonstrate that after taking the BCJ relations into account, we can reduce the number of independent coefficients to 30.

Consider the following two integral coefficients $d^{\pm}_{(1,2,34,5)}$ and $d^{\pm}_{(1,2,43,5)}$, shown in Fig. 2.5. Not only do they have the same loop solution, but they share three tree amplitudes. Note that the total box coefficient is found by summing the two loop solutions, but we keep these two solutions separate to expose the tree-level BCJ amplitude relations. Let us take a closer inspection at the dissimilar tree amplitudes containing K_3

$$\begin{aligned} d^{\pm}_{3,(1,2,34,5)} &= A_4^{\text{tree}}(l_3^{\pm}, -l_2^{\pm}, 3, 4), \\ d^{\pm}_{3,(1,2,43,5)} &= A_4^{\text{tree}}(l_3^{\pm}, -l_2^{\pm}, 4, 3). \end{aligned} \tag{2.44}$$

Since the two amplitudes have the same loop momentum solution, we can use the four-point BCJ relation, Eq. (2.31), to relate the box coefficient. That is,

$$d^{\pm}_{1,2,43,5} = \frac{s_{l_3^{\pm}4}}{s_{-l_2^{\pm}4}} d^{\pm}_{1,2,34,5}. \tag{2.45}$$

We look to find all possible five-point box integral coefficient relations. After considering reflection symmetry as well as this new"twist symmetry" for the legs located on the tree, we find that there are 30 independent five-point coefficients instead of 60. Finding the form of the 30 integral coefficient relations at five points is as trivial as finding the correct four-point tree-level BCJ amplitude identity, so we will not review the one-mass boxes any further.

Next, consider six-point amplitudes. There are one-mass boxes and two-mass diagrams to consider. We start with the one-mass diagrams. In most cases, there will be multiple one-mass diagrams which have the same loop solution. Consider the following six coefficients: $d^{\pm}_{1,2,345,6}$, $d^{\pm}_{1,2,354,6}$, $d^{\pm}_{1,2,435,6}$, $d^{\pm}_{1,2,453,6}$, $d^{\pm}_{1,2,534,6}$, and $d^{\pm}_{1,2,543,6}$. It is clear that we can use the BCJ relations to remove the calculation of four coefficients. Using Eq. (2.31),

$$\begin{aligned}
d^{\pm}_{1,2,435,6} &= d^{\pm}_{1,2,345,6}\frac{s_{l_3^{\pm}4}+s_{45}}{s_{-l_2^{\pm}4}}+d^{\pm}_{1,2,354,6}\frac{s_{l_3^{\pm}4}}{s_{-l_2^{\pm}4}},\\
d^{\pm}_{1,2,453,6} &= -d^{\pm}_{1,2,345,6}\frac{s_{34}s_{l_3^{\pm}5}}{s_{-l_2^{\pm}4}s_{-l_2^{\pm}45}}-d^{\pm}_{1,2,354,6}\frac{s_{l_3^{\pm}4}(s_{-l_2^{\pm}45}+s_{35})}{s_{-l_2^{\pm}4}s_{-l_2^{\pm}45}},\\
d^{\pm}_{1,2,534,6} &= d^{\pm}_{1,2,354,6}\frac{s_{l_3^{\pm}5}+s_{45}}{s_{-l_2^{\pm}5}}+d^{\pm}_{1,2,345,6}\frac{s_{l_3^{\pm}5}}{s_{-l_2^{\pm}5}},\\
d^{\pm}_{1,2,543,6} &= -d^{\pm}_{1,2,354,6}\frac{s_{35}s_{l_3^{\pm}4}}{s_{-l_2^{\pm}5}s_{-l_2^{\pm}54}}-d^{\pm}_{1,2,345,6}\frac{s_{l_3^{\pm}5}(s_{-l_2^{\pm}54}+s_{34})}{s_{-l_2^{\pm}5}s_{-l_2^{\pm}54}}.
\end{aligned} \tag{2.46}$$

We see that at six-points, there are even more integral coefficient relations, since there are more cuts with the third leg of the tree amplitude fixed. For counting the number of independent box coefficients needed, it is important to note that not all of the six-point one-mass boxes have six coefficients with the same loop solution. In some cases, there will only be three independent coefficients with the same solution.

Note that at six points there are 360 one-mass coefficients, yet there are many fewer unique loop solutions. The BCJ relations relate a majority of the coefficients with the same loop momenta. We can see that if there are more than two six-point one-mass box coefficients with the same loop solution up to an overall minus sign to account for reflections, then those extra are dependent on two coefficients. In some cases, you may need to calculate a coefficient which is not needed, but this inconvenience decreases the number of coefficients calculated in the long run. For example, the one-loop solution has the following three coefficients:

$d^{\pm}_{4,5,612,3}$, $d^{\pm}_{4,5,126,3}$, and $d^{\pm}_{4,5,261,3}$. Notice how we can use $d^{\pm}_{4,5,612,3}$ and $d^{\pm}_{4,5,621,3}$ as independent basis coefficients, even though we do not need to calculate the second coefficient. It is beneficial, since we are still only calculating two instead of three.

Next, we consider the six-point two-mass-e coefficients. These are a bit more complicated, since there are potentially two tree amplitudes K_2 and K_3 which can be different for the same loop solution. Once again, we group all of the coefficients with the same loop coefficient. At most, we could have four coefficients which have the same loop solution. For example, consider the following coefficients: $d^{\pm}_{1,23,45,6}$, $d^{\pm}_{1,23,54,6}$, $d^{\pm}_{1,32,45,6}$, and $d^{\pm}_{1,32,54,6}$. It is clear that we can relate the second and third coefficient to the first, but the fourth has two twisted corners on K_2 and K_3. Expanding the fourth coefficient in terms of tree amplitudes makes the identity more apparent:

$$d^{\pm}_{1,32,54,6} = \frac{1}{2} A_3^{\text{tree}}(l_1^{\pm}, -l^{\pm}, 1) A_4^{\text{tree}}(l_2^{\pm}, -l_1^{\pm}, 3, 2) A_4^{\text{tree}}(l_3^{\pm}, -l_2^{\pm}, 5, 4) A_4^{\text{tree}}(l^{\pm}, -l_3^{\pm}, 6). \quad (2.47)$$

From expanding the coefficient in terms of tree amplitudes, we see that two four-point BCJ relations can be used to find this coefficient in terms of $d^{\pm}_{1,23,45,6}$. The three relations between the four coefficients mentioned above are

$$\begin{aligned} d^{\pm}_{1,23,54,6} &= d^{\pm}_{1,23,45,6} \frac{s_{l_3^{\pm}5}}{s_{-l_2^{\pm}5}}, \\ d^{\pm}_{1,32,45,6} &= d^{\pm}_{1,23,45,6} \frac{s_{l_2^{\pm}3}}{s_{-l_1^{\pm}3}}, \\ d^{\pm}_{1,32,54,6} &= d^{\pm}_{1,23,45,6} \frac{s_{l_3^{\pm}5} s_{l_2^{\pm}3}}{s_{-l_2^{\pm}5} s_{-l_1^{\pm}3}}. \end{aligned} \quad (2.48)$$

Therefore, we have demonstrated that even if multiple corners of a cut have different orderings, the BCJ relations can still be used multiple times, as long as the related coefficients have the same loop solution.

When continuing this analysis to higher-point amplitudes, we find that the simplification gets better as we increase n. The simplification occurs because there are more possible diagrams with the same loop solution. At seven-point, there are 12600 needed box coefficients, but only 1785 independent coefficients. For example, there are 24 permutations of K_3 for the coefficient $d^{\pm}_{1,2,3456,7}$, yet there are only six independent coefficients needed. We will not

write out these 18 relations, but it is clear that the BCJ amplitude relations could be used to reduce the number of coefficients. Also, at seven-point we introduce three-mass box coefficients, which could have up to eigth coefficients with the same loop solution. For example, consider twisting K_2, K_3, and K_4 on the coefficient $d^{\pm}_{1,23,45,67}$. These eight coefficients can all be related to one coefficient, which gives seven relations. Once again, we will not write them down, but it would be easy to generate with the BCJ relations. One would have to be a bit more careful with writing down the relations for the twelve coefficients corresponding to the loop solution contained in $d^{\pm}_{1,23,456,7}$. The K_3 term gives a dependence on two coefficients, while the K_2 would add an overall factor of inverse propagators from Eq. (2.31).

Interesting eight-point amplitudes to consider would be the four-mass and $d^{\pm}_{1,432,765,8}$, since that coefficient would depend on four coefficients. We will not go into deriving the identities, because it is fairly straightforward. Nothing new arises for higher-point boxes besides applying more complicated BCJ relations.

In Fig. 2.6, we plot the number of box coefficients needed before and after the BCJ integral coefficient relations have been taken into consideration. The log plot shows that as the number of external legs increases, the relations reduce a higher percentage of the coefficients. We see that by eight-points, the number of independent coefficients needed to calculate is roughly an order of magnitude less than what was naively expected.

Finally, we would like to present a formula to count the total number of independent coefficients, after applying the BCJ relations. The boxes are a bit complicated, as there is different counting for the one-mass, two-mass-e, two-mass-h, three-mass, and four-mass boxes. We found the following expression which gave the total number of independent coefficients $C(n)$ for $n \geq 4$.

$$C(n) = \sum_{i=1}^{\lfloor \frac{n-4}{4} \rfloor - 1} \sum_{j=1}^{\lfloor \frac{n-4}{3} \rfloor - 1} \sum_{k=1}^{\lfloor \frac{n-4}{2} \rfloor - 1} \frac{n!}{ijk(n-i-j-k)\text{sym}(i,j,k)}, \tag{2.49}$$

where $\lfloor x \rfloor$ is the floor function and sym is a symmetry factor which depends on whether i, j, k, and $n-i-j-k$, are the same or not. Note that i, j, k, and $n-i-j-k$ represent the number of external legs on each corner of the box. Naively, we would expect that there would be $n!$ for each cut topology, but we know that the BCJ relations allow for this new

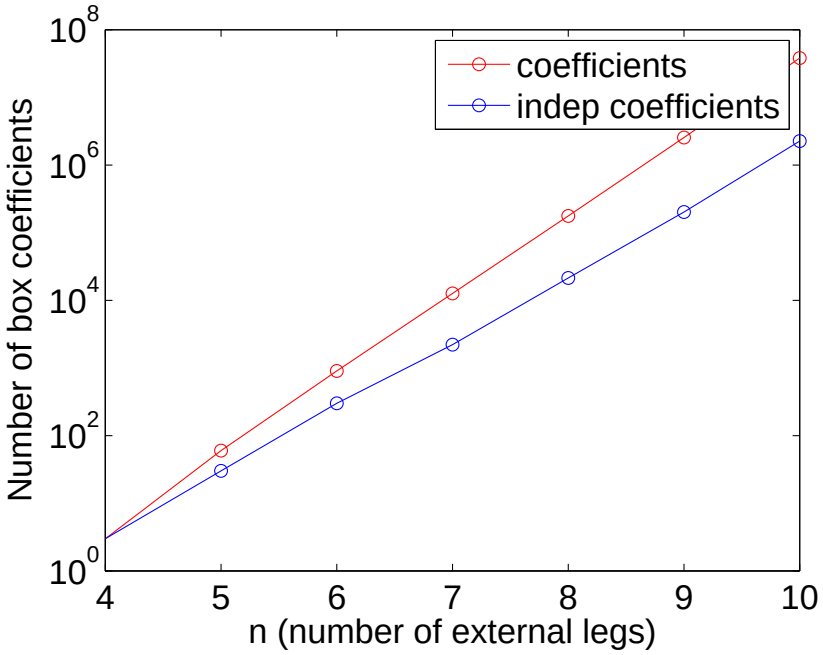

Figure 2.6: The number of box coefficients. The red line represents the number of independent coefficients before using the BCJ integral coefficient relations, and the blue line represents the number of independent coefficients needed after the relations are taken into consideration.

type of twist symmetry, which, up to symmetry factors, divides the number of diagrams by the number of legs on all corners. To get the counting exactly right, we introduced a symmetry factor sym,

$$\text{sym} = \begin{cases} 8 & : \text{ if } i = j = k = n - i - j - k \\ 2 & : \text{ if } i = j = k, \text{ or any other 3 equal} \\ 1 & : \text{ if } i = j \text{ and } k = n - i - j - k, \text{ or any other two pair equal} \\ 2/3 & : \text{ if } i = j, \text{ or any other two equal} \\ 1/3 & : \text{ else} \end{cases} \tag{2.50}$$

The symmetry factor is chosen to properly count the number of needed diagram as well as reflection symmetry. For example, consider a five-point box cut. There is only one type of diagram possible with one corner having two legs and three corners with one leg. There is only one diagram for this specification, yet there is a reflection symmetry, making s$ym = 2$. For other cases, there could be more diagrams needed, each with their own symmetry properties.

As we have shown, it is no surprise that the box coefficients should satisfy BCJ integral coefficient relations. Next, we investigate how similar identities can be found for the less trivial triangle coefficients.

2.2.2 BCJ triangle integral coefficient identities

Next, we study how the BCJ relations can be used to simplify triangle integral coefficients. Exactly how the BCJ relations will come into play is less clear, since the loop solutions contain the parameter t. In particular, the inverse propagators in the BCJ relations contain loop momenta, and therefore we will end up with expressions for dependent triangle coefficients in terms of the parameter t.

We start by considering two coefficients with the same loop solution, say $c^{\pm}_{(12,34,56)}$ and $c^{\pm}_{(12,34,65)}$. We would like to find a way to relate these coefficients by propagators, such that $c_{(12,34,56)} = \frac{s_{l5}}{s_{-l_2 5}} c_{(12,34,56)}$, but we need to be careful with the t dependence of the amplitude and the inverse propagators. The first natural guess would be to keep the t dependence in the inverse propagators and the coefficient and apply the proper expansion of t around

infinity, followed by extracting the t^0 term. It turns out that this precisely works, as we confirmed numerically. The coefficient identity is

$$c^{\pm}_{(12,34,65)}(t) = \frac{s_{l6}(t)}{s_{-l_26}(t)} c^{\pm}_{(12,34,56)}(t). \tag{2.51}$$

Finding this t-dependent coefficient, taking limit as t goes to infinity, and taking the t^0 term allows for the triangle coefficient to be found:

$$c^{\pm}_{(12,34,65)} = [\mathrm{Inf}_t c^{\pm}_{(12,34,65)}(t)]|_{t=0} \tag{2.52}$$

This shows that the triangle contributions to the bubbles should also satisfy this BCJ identity.

Now that we understand how to properly deal with the t parameter, generating triangle coefficient identities is essentially the same as the box coefficients. We group all of the coefficients with the same loop solution together, find the set of independent coefficients, and write down the analogous BCJ relations needed to find the dependent coefficients.

Now that we have demonstrated that the BCJ relations indeed hold for triangle coefficients with Forde's analytic approach [161], we would like to investigate how we can use them to speed up numerical calculations.

When considering if the BCJ relations speed up performance, there is a caveat since the triangle coefficient only needs the zeroth order term. However, finding $c_{(12,34,65)}$ with BCJ requires that we keep all of the coefficients in the expansion of t for $c_{(12,34,56)}$, since the factors of inverse propagators have t dependence and will change the zeroth order dependence of the undetermined triangle coefficient. Fortunately, all of these coefficients would be saved for the evaluation of bubble diagrams. Therefore, the only extra computational cost for determining $c_{(12,34,65)}$ involves finding the coefficients from expanding $\frac{s_{l5}(t)}{s_{l_25}(t)}$ with respect to t. Furthermore, it appears that all of the factors of inverse propagators in all of the BCJ relations, even for higher than four-points, will never have a t^n term for $n > 0$. Even if we did not extract out the boxes and numerically evaluated the coefficients in a Laurent expansion of t, we would only need to calculate the zeroth and first three negative powers of the inverse propagator terms. Thus, we have shown that the only extra computation needed the four coefficients for $\frac{s_{l5}(t)}{s_{l_25}(t)} = \mathcal{O}(\frac{1}{t^4}) + \sum_{i=-3}^{0} a_i t^i$, since $c_{(12,34,56)}$ only goes up to powers of t^3 for Forde's method.

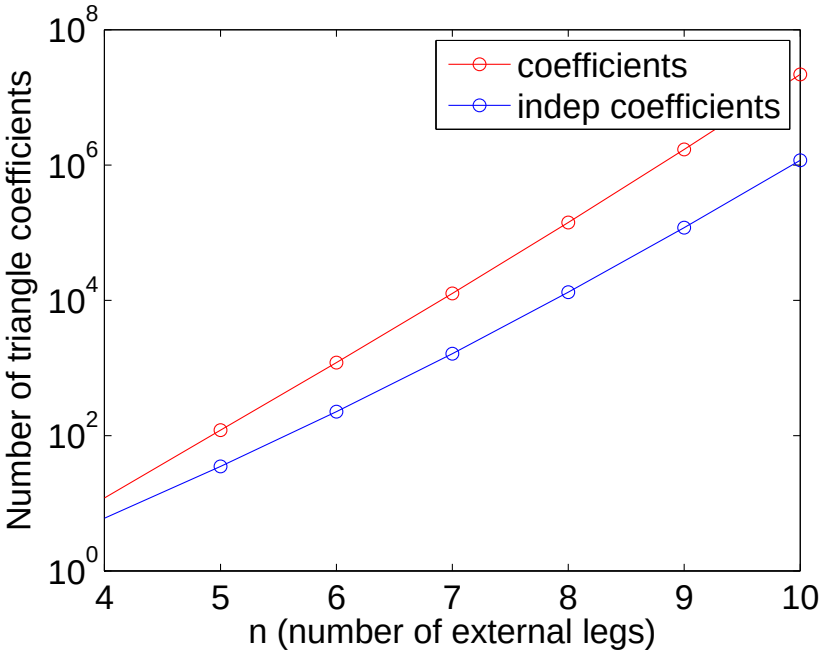

Figure 2.7: The number of triangle coefficients. The red line represents the number of independent coefficients before using the BCJ integral coefficient relations, and the blue line represents the number of independent coefficients needed after the relations are taken into consideration.

In Fig. 2.7, we plot the number of triangle coefficients needed before and after the BCJ integral coefficient relations are taken into account. We notice that the number of triangle coefficients is reduced even less than the boxes. This is due to the fact that less cuts puts more legs on a particular tree amplitude, which makes the BCJ relations more plentiful. We found that the absolute value of the Stirling number of the first kind S_n^3 gives the correct number of independent n-point coefficients. Next, we review the bubble integral coefficient identities.

2.2.3 BCJ bubble integral coefficient identities

We now look to see if the BCJ relations can be utilized with the bubbles. Typically, to calculate the bubble coefficient, one has to subtract out the triangle contributions to the bubble coefficient. However, since we already showed that the triangles follow the BCJ coefficient relations for all orders of t, we only need to show that the identity is valid for the bubble cut component of the bubble integral coefficient.

In particular, we analytically and numerically checked that the solution works for the $(41, 23)$ cut for the amplitude $A^{\text{one-loop}}(1^-, 2^-, 3^+, 4^+)$. For example, we would like to see how the coefficient $b_{(41,32)}$ of $A^{\text{one-loop}}(1^-, 3^+, 2^-, 4^+)$ could be found from $b_{(41,23)}$ using the BCJ relations,

$$b^{\pm}_{(12,43)}(y,t) = \frac{s_{l4}(t,y)}{s_{-l_14}(t,y)} b^{\pm}_{(12,34)}(t,y). \tag{2.53}$$

Note that to find the true bubble coefficient, we must properly remove the y and t dependence, such that

$$b^{\pm}_{(12,43)} = \left[\text{Inf}_t \left[\text{Inf}_y \frac{s_{l4}(t,y)}{s_{-l_14}(t,y)} b^{\pm}_{(12,34)}(t,y)\right]\right]\Bigg|_{t=0, y^i=Y_i}. \tag{2.54}$$

In Fig. 2.8, we plot the number of bubble coefficients needed before and after the BCJ integral coefficient relations are taken into consideration. As expected, the bubbles are simplified even more heavily than the triangles and boxes. Similar to the triangles, we can use the Stirling number of the first kind S_n^2 to count the number of independent coefficients, but this also includes one-mass coefficients. To find the numbers shown in Fig. 2.8, we subtracted $n(n-2)!$.

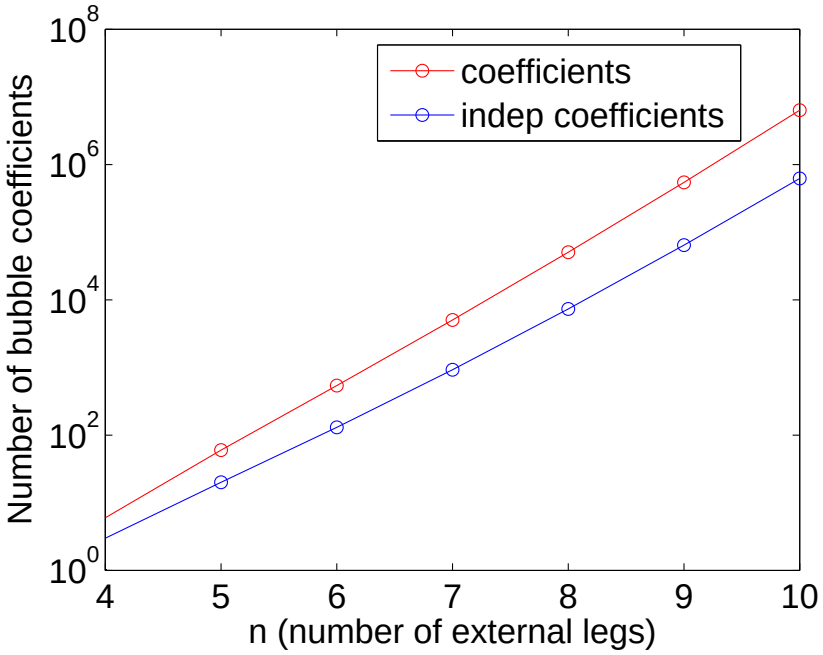

Figure 2.8: The number of bubble coefficients. We did not include one-mass coefficients, since the corresponding integrals integrate to zero.

We have clearly demonstrated that the tree-level BCJ amplitude relations can be used to create one-loop integral coefficient relations. However, we note that these BCJ integral coefficient relations are only useful for amplitudes with multiple identical particles, which often is the case for QCD jet processes. However, there will always be other particles interacting with these gluons, which would lessen the number of identities which are suggested by the figures shown throughout this section. These relations could be useful for improving the efficiency of QCD calculations or to check the stability of numerical code.

2.3 Examples of BCJ integral coefficient relations

2.3.1 Box integral coefficient relation example

Let us consider the box integral coefficients $d_{(1,2,34,5)}$ and $d_{(1,2,43,5)}$ and show explicitly that these coefficients satisfy the integral coefficient relation provided in this chapter. We start

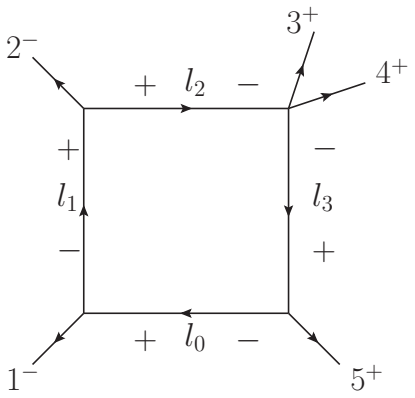

Figure 2.9: The one non-zero loop helicity configuration is shown above for the coefficient $d_{(1,2,34,5)}$.

by calculating the $d_{(1,2,34,5)}$ diagram explicitly, shown in Fig. 2.9. In principle, there are eight possible loop helicity configurations, but only one is non-zero for this specific cut. We can write down the coefficient by multiplying by the four tree amplitudes:

$$d_{(1,2,34,5)} = \frac{i\left\langle 1 l_1\right\rangle^3}{\left\langle l_1 - l\right\rangle\left\langle -l 1\right\rangle}\frac{-i\left[l_2 - l_1\right]^3}{\left[-l_1 2\right]\left[2 l_2\right]}\frac{i\left\langle l_3 - l_2\right\rangle^3}{\left\langle -l_2 3\right\rangle\left\langle 34\right\rangle\left\langle 4 l_3\right\rangle}\frac{-i\left[-l_3 5\right]^3}{\left[5 l\right]\left[l - l_3\right]} = \frac{\left\langle 1\right| l_1 l_2 l_3 \left|5\right]^3}{\left\langle 34\right\rangle\left\langle 1\right| l \left|5\right]\left\langle 3\right| l_2 \left|2\right]\left\langle 4\right| l_3 l l_1 \left|2\right]}, \tag{2.55}$$

where $l = l_0$ throughout. We can use the loop solution from Eq. (2.34) and find l to be

$$\begin{aligned} l^+ &= \frac{1}{2}\frac{[21]}{[25]}\left\langle 1\right| \gamma^\mu \left|5\right], \\ l^- &= \frac{1}{2}\frac{\langle 21\rangle}{\langle 25\rangle}\left\langle 5\right| \gamma^\mu \left|1\right]. \end{aligned} \tag{2.56}$$

Right away, it is clear that the positive solution gives zero, since $\langle 1 l^+\rangle = 0$. We continue by only considering the negative loop solution. We can make a choice for $\langle l^-|$ and $|l^-]$,

$$\left\langle l^-\right| = \left\langle 5\right|, \qquad \left|l^-\right] = \frac{\langle 21\rangle}{\langle 25\rangle}|1] \equiv \alpha|1], \tag{2.57}$$

which allows us to simplify the calculation in terms of external spinors.

Furthermore, we can use momentum conservation to express all other loop momenta in

terms of l:

$$\begin{aligned} d^-_{(1,2,34,5)} &= \frac{\langle 1|\, l\, |2]^3\, \langle 2|\, l\, |5]^3}{\langle 34\rangle\, \langle 1|\, l\, |5]\, \langle 3|\, l-1\, |2]\, \langle 45\rangle\, \langle 1|\, l\, |5]\, [12]} \\ &= \frac{\langle 15\rangle^3\, \alpha^3\, [12]^3\, \langle 25\rangle^3\, \alpha^3\, [15]^3}{\langle 34\rangle\, \langle 45\rangle\, (\langle 15\rangle\, \alpha\, [15])^2 (\langle 35\rangle\, \alpha\, [12] - \langle 31\rangle\, [12])\, [12]} \\ &= is_{51}s_{12}\frac{i\, \langle 12\rangle^3}{\langle 23\rangle\, \langle 34\rangle\, \langle 45\rangle\, \langle 51\rangle} = is_{51}s_{12}A_5^{\text{tree}}(1^-, 2^-, 3^+, 4^+, 5^+). \end{aligned} \tag{2.58}$$

In the last line, we used the Schouten identity to simplify the denominator. Similarly, we can immediately write down the equation for the box coefficient $c_{(1,2,43,5)}$ since p_3 and p_4 have the same helicity, which is given by

$$d^-_{(1,2,43,5)} = is_{51}s_{12}\frac{i\, \langle 12\rangle}{\langle 24\rangle\, \langle 43\rangle\, \langle 35\rangle\, \langle 51\rangle} = is_{51}s_{12}A_5^{\text{tree}}(1^-, 2^-, 4^+, 3^+, 5^+). \tag{2.59}$$

Next, we check that the coefficient cut relation $d^-_{(1,2,43,5)} = \frac{s_{l_3^- 4}}{s_{-l_2^- 4}} d^-_{(1,2,34,5)}$ holds. To start,

$$\begin{aligned} \frac{s_{l_3^- 4}}{s_{-l_2^- 4}} &= \frac{\langle 4|\, l_3\, |4]}{\langle 4|\, -l_2\, |4]} = \frac{\langle 4|\, l+5\, |4]}{\langle 4|\, 1+2-l\, |4]}, \\ \frac{s_{l_3^- 4}}{s_{-l_2^- 4}} &= \frac{-\frac{\langle 45\rangle}{\langle 25\rangle}(\langle 2|\, 1+5\, |4])}{\frac{[14]}{\langle 25\rangle}(\langle 45\rangle\, \langle 21\rangle - \langle 41\rangle\, \langle 25\rangle) - \langle 4|\, 2\, |4]} = -\frac{\langle 45\rangle\, \langle 23\rangle}{\langle 24\rangle\, \langle 35\rangle}. \end{aligned} \tag{2.60}$$

Schouten identities and momentum conservation are used throughout to simplify these expressions. We can see that this is the exact factor which is needed to find $d^-_{(1,2,43,5)}$ from $d^-_{(1,2,34,5)}$, since

$$\begin{aligned} d^+_{(1,2,43,5)} &= \frac{s_{l_3^+ 4}}{s_{-l_2^+ 4}} d^+_{(1,2,34,5)} = 0, \\ d^-_{(1,2,43,5)} &= \frac{s_{l_3^- 4}}{s_{-l_2^- 4}} d^-_{(1,2,34,5)} = is_{51}s_{12}\frac{i\, \langle 12\rangle}{\langle 24\rangle\, \langle 43\rangle\, \langle 35\rangle\, \langle 51\rangle}. \end{aligned} \tag{2.61}$$

As we have demonstrated, the BCJ integral coefficient identity holds for this five-point box cut example.

2.3.2 Triangle integral coefficient relation example

Next, we will show how the BCJ integral coefficient relation holds for a triangle cut. We will choose a four-point cut $c_{(1,23,4)}$ which has a zero triangle coefficient, but does have non-zero terms for powers of t greater than zero. These higher power terms contribute to the

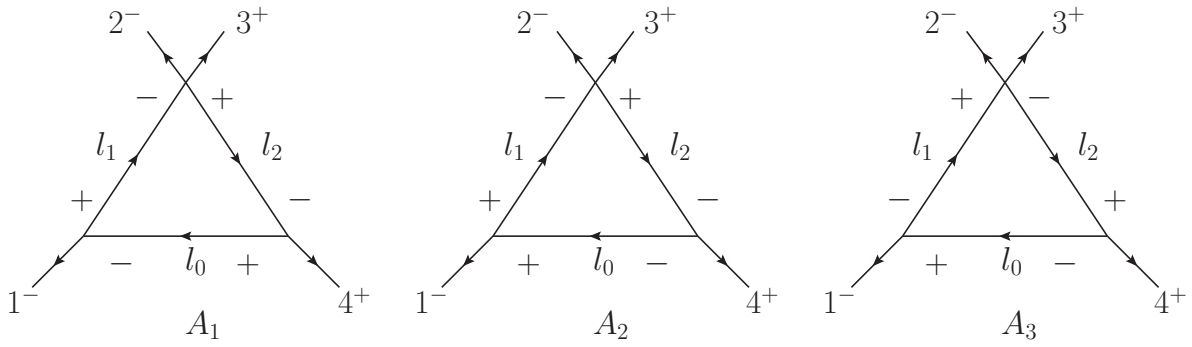

Figure 2.10: Diagrams needed for the coefficient $c_{(1,23,4)}$.

bubble coefficient, so we must confirm this in order to show that the BCJ integral coefficient relations work on the total bubble coefficient. In this example, the BCJ relations will be used to find a non-zero triangle integral coefficient from a zero triangle integral coefficient, which is possible since the inverse propagator ratio has t dependence.

We will calculate the triangle cut from the amplitude $A_4^{\text{one-loop}}(1^-, 2^-, 3^+, 4^+)$. There are three nonzero loop helicities which we must consider. We have the three diagrams, which we will label as A_1, A_2, and A_3 and are shown in Fig. 2.10, which when evaluated gives

$$\begin{aligned}
A_1 &= \frac{-i\,\langle l1\rangle^3}{\langle 1l_1\rangle\,\langle l_1 l\rangle}\frac{\langle l_1 2\rangle^3}{\langle 23\rangle\,\langle 3l_2\rangle\,\langle l_2 l_1\rangle}\frac{[4l]^3}{[ll_2]\,[l_2 4]},\\
A_2 &= \frac{-i\,[l_1 l]^3}{[l1]\,[1l_1]}\frac{\langle l_1 2\rangle^3}{\langle 23\rangle\,\langle 3l_2\rangle\,\langle l_2 l_1\rangle}\frac{\langle ll_2\rangle^3}{\langle l_2 4\rangle\,\langle 4l\rangle},\\
A_3 &= \frac{-i\,\langle 1l_1\rangle^3}{\langle l_1 l\rangle\,\langle l1\rangle}\frac{\langle 2l_2\rangle^4}{\langle 23\rangle\,\langle 3l_2\rangle\,\langle l_2 l_1\rangle\,\langle l_1 2\rangle}\frac{[l_2 4]^3}{[4l]\,[ll_2]}.
\end{aligned} \tag{2.62}$$

Choosing $K_1^{\flat,\mu} = p_1^\mu$ and $K_3^{\flat,\mu} = p_4^\mu$, we find that the following loop solution is

$$\begin{aligned}
\langle l^+| = t\,\langle 1|\,, \qquad & |l^+] = |4],\\
\left\langle l_1^+\right| = t\,\langle 1|\,, \qquad & |l_1^+] = |4] - \frac{1}{t}|1],\\
\left\langle l_2^+\right| = t\,\langle 1| + \langle 4|\,, \qquad & |l_2^+] = |4].
\end{aligned} \tag{2.63}$$

This leaves three non-zero contributions after considering the positive and negative loop

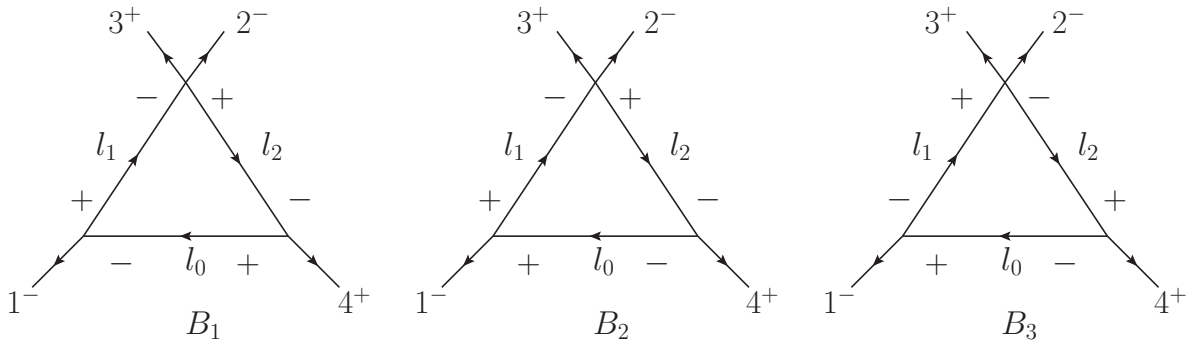

Figure 2.11: Diagrams needed for the coefficient $c_{(1,32,4)}$.

solutions,

$$\begin{aligned} A_2^+ &= \frac{i\,[41]\,\langle 12\rangle^3}{\langle 23\rangle\,(t\,\langle 31\rangle + \langle 34\rangle)}, \\ A_1^- &= \frac{-i(\langle 42\rangle - \frac{1}{t}\,\langle 12\rangle)^3 t^3\,[41]}{\langle 23\rangle\,\langle 34\rangle}, \\ A_3^- &= \frac{i\,\langle 24\rangle^4\,t^3\,[14]}{\langle 23\rangle\,\langle 34\rangle\,(\langle 42\rangle - \frac{1}{t}\,\langle 12\rangle)}. \end{aligned} \tag{2.64}$$

After expanding about $t = \infty$, we find that only the negative solution has non-zero contributions to the triangle and bubble coefficients. Next, we can calculate $c_{(1,23,4)}(t)$, which is the same as $c_{(1,23,4)}$ before picking the t^0 term after the expansion about infinity. We find

$$\begin{aligned} c^+_{(1,23,4)}(t) &= 0 + \mathcal{O}\left(\frac{1}{t}\right), \\ c^-_{(1,23,4)}(t) &= \frac{2i\,\langle 24\rangle\,[41]}{\langle 23\rangle\,\langle 34\rangle}(\langle 24\rangle^2\,t^3 + \langle 24\rangle\,\langle 12\rangle\,t^2 + 2\,\langle 12\rangle^2\,t) + \mathcal{O}\left(\frac{1}{t}\right). \end{aligned} \tag{2.65}$$

The fact that there is no zeroth order term shows that there is no triangle coefficient, yet the higher powers of t would feed into the bubble coefficient. Let us check the BCJ integral coefficient relation by first calculating the coefficient $c^{\pm}_{(1,32,4)}(t)$ and then confirming that the two coefficients satisfy the corresponding BCJ relation.

Once again, we can write down expressions for the three amplitudes, which we will refer to as B_1, B_2, and B_3 and are shown in Figure 2.11.

$$
\begin{aligned}
B_1 &= \frac{-i\,\langle l1\rangle^3}{\langle 1l_1\rangle\,\langle l_1 l\rangle}\frac{\langle 2l_1\rangle^4}{\langle 2l_2\rangle\,\langle l_2 l_1\rangle\,\langle l_1 3\rangle\,\langle 32\rangle}\frac{[4l]^3}{[ll_2]\,[l_2 4]},\\
B_2 &= \frac{-i\,[l_1 l]^3}{[l1]\,[1l_1]}\frac{\langle 2l_1\rangle^4}{\langle 2l_2\rangle\,\langle l_2 l_1\rangle\,\langle l_1 3\rangle\,\langle 32\rangle}\frac{\langle ll_2\rangle^3}{\langle l_2 4\rangle\,\langle 4l\rangle},\\
B_3 &= \frac{-i\,\langle 1l_1\rangle^3}{\langle l_1 l\rangle\,\langle l1\rangle}\frac{\langle 2l_2\rangle^3}{\langle l_2 l_1\rangle\,\langle l_1 3\rangle\,\langle 32\rangle}\frac{[l_2 4]^3}{[4l]\,[ll_2]}.
\end{aligned}
\tag{2.66}
$$

Similarly, there are three non-zero contributions to the triangle/bubble integral coefficient, which are shown below. We used the same loop solution as previously and find

$$
\begin{aligned}
B_2^+ &= \frac{i\,[41]\,\langle 12\rangle^4}{\langle 13\rangle\,\langle 32\rangle\,(t\,\langle 21\rangle + \langle 24\rangle)},\\
B_1^- &= \frac{-i\left(\langle 24\rangle - \frac{1}{t}\,\langle 21\rangle\right)^4 t^3\,[41]}{\langle 24\rangle\,\langle 32\rangle\left(\langle 43\rangle - \frac{1}{t}\,\langle 13\rangle\right)},\\
B_3^- &= \frac{it^3\,\langle 24\rangle^3\,[14]}{\langle 32\rangle\left(\langle 43\rangle - \frac{1}{t}\,\langle 13\rangle\right)}.
\end{aligned}
\tag{2.67}
$$

Once again, we find that the positive solution has no contribution to the bubble or triangle coefficient. The negative solution does have a non-zero triangle integral coefficient. Since the analytic expression for this amplitude is a bit lengthy, we will only report the zeroth order term, which corresponds to the triangle integral coefficient.

$$
\begin{aligned}
c^+_{(1,32,4)} &= 0,\\
c^-_{(1,32,4)} &= \frac{2is_{41}(\langle 13\rangle\,\langle 24\rangle\,\langle 14\rangle\,\langle 23\rangle + 2\,\langle 12\rangle^2\,\langle 34\rangle^2)}{\langle 34\rangle^4}.
\end{aligned}
\tag{2.68}
$$

Next, we show that we get the same result if we were to use the BCJ integral coefficient relations. The ratio of inverse propagators $\frac{s_{l_2 3}}{s_{-l_1 3}}$ for the positive and negative loop solution are

$$
\begin{aligned}
\frac{s_{l_2^+ 3}}{s_{-l_1^+ 3}} &= \frac{[43]\,(t\,\langle 13\rangle + \langle 43\rangle)}{\langle 13\rangle\,(t\,[34] - [31])},\\
\frac{s_{l_2^- 3}}{s_{-l_1^- 3}} &= \frac{\langle 34\rangle\,(t\,[31] + [34])}{[31]\,(t\,\langle 43\rangle - \langle 13\rangle)}.
\end{aligned}
\tag{2.69}
$$

We see that these two are complex conjugates of each other, if t is real. Next, we will multiply these by $b^{\pm}_{(1,23,4)}$, expand about t approaches infinity, and keep the zeroth order term. S@M

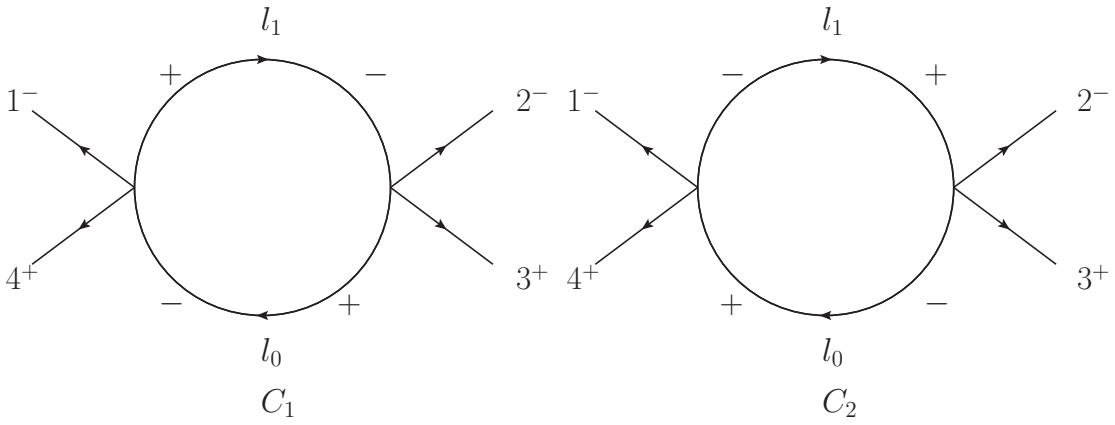

Figure 2.12: The non-zero helicity configurations for the coefficient $b_{(41,23)}$.

and Mathematica easily allow for this analytic expansion to be performed [155], which gives

$$\begin{aligned} c^+_{(1,32,4)} &= \mathrm{Inf}_t \left[\frac{s_{l_2^+ 3}(t)}{s_{-l_1^+ 3}(t)} c^+_{(1,23,4)}(t) \right] \Bigg|_{t=0} &&= 0, \\ c^-_{(1,32,4)} &= \mathrm{Inf}_t \left[\frac{s_{l_2^- 3}(t)}{s_{-l_1^- 3}(t)} c^-_{(1,23,4)}(t) \right] \Bigg|_{t=0} &&= \frac{2i s_{41} (\langle 13\rangle \langle 24\rangle \langle 14\rangle \langle 23\rangle + 2 \langle 12\rangle^2 \langle 34\rangle^2)}{\langle 34\rangle^4} \end{aligned} \tag{2.70}$$

After some factoring and application of the Schouten identity, one can get the BCJ integral coefficient relation to give the correct expression for the coefficient $c^{\pm}_{(1,32,4)}$. Furthermore, we numerically confirmed that the coefficients agree for all orders of t, not just for the t^0 term. This ensures that the triangle contributions to the bubbles will also satisfy the BCJ integral coefficient relations.

2.3.3 Bubble integral coefficient relation example

In this subsection, we present a calculation of a four-point bubble coefficient and show that it satisfies a BCJ integral coefficient relation. We start by considering the $b_{(41,23)}$ integral coefficient of the amplitude $A_4^{\text{one-loop}}(1^-, 2^-, 3^+, 4^+)$, which is shown in Figure 2.12.

We have two non-zero internal helicity configurations to consider, which we will refer to

as C_1 and C_2.

$$\begin{aligned} C_1 &= \frac{i\langle 1l\rangle^4}{\langle 1l_1\rangle\langle l_1 l\rangle\langle l4\rangle\langle 41\rangle}\frac{i\langle l_1 2\rangle^3}{\langle 23\rangle\langle 3l\rangle\langle ll_1\rangle}, \\ C_2 &= \frac{i\langle 1l_1\rangle^3}{\langle l_1 l\rangle\langle l4\rangle\langle 41\rangle}\frac{i\langle 2l\rangle^4}{\langle 23\rangle\langle 3l\rangle\langle ll_1\rangle\langle l_1 2\rangle}. \end{aligned} \tag{2.71}$$

Each also has two loop solutions, giving $C_1^{\pm}$ and $C_2^{\pm}$. We chose $\chi^\mu = p_1^\mu$, which makes $K_1^{\flat,\mu} = p_4^\mu$. The loop solutions are

$$\begin{aligned} \left\langle l^+\right| &= t\langle 4| + (1-y)\langle 1|, & |l^+] &= \frac{y}{t}|4] + |1], \\ \left\langle l_1^+\right| &= \langle 4| - \frac{y}{t}\langle 1|, & |l_1^+] &= (y-1)|4] + t|1]. \end{aligned} \tag{2.72}$$

Plugging these solutions in and simplifying, we find

$$\begin{aligned} C_1^+ &= \frac{t(t\langle 42\rangle - y\langle 12\rangle)^3}{\langle 23\rangle\langle 41\rangle(1-y)(t\langle 34\rangle + (1-y)\langle 31\rangle)}, \\ C_2^+ &= \frac{t(t\langle 24\rangle + (1-y)\langle 21\rangle)^4}{\langle 23\rangle\langle 41\rangle(1-y)(t\langle 34\rangle + (1-y)\langle 31\rangle)(t\langle 42\rangle - y\langle 12\rangle)}, \\ C_1^- &= \frac{\left(\frac{y}{t}\right)^4((y-1)\langle 42\rangle + t\langle 12\rangle)^3}{\langle 23\rangle\langle 41\rangle(y-1)\left(\frac{y}{t}\langle 34\rangle + \langle 31\rangle\right)}, \\ C_2^- &= \frac{(y-1)^3\left(\frac{y}{t}\langle 24\rangle + \langle 21\rangle\right)^4}{\langle 23\rangle\langle 41\rangle\left(\frac{y}{t}\langle 34\rangle + \langle 31\rangle\right)((y-1)\langle 42\rangle + t\langle 12\rangle)}. \end{aligned} \tag{2.73}$$

To calculate the bubble coefficient, one must typically subtract away the corresponding triangle contributions. However, we have already shown that the triangle contributions will cancel at all orders of t, not just the component contributing to the triangle coefficient. Therefore, to confirm that the BCJ integral coefficient relation holds for the bubble coefficient, we will just focus on the bubble cut contribution to the bubble coefficient.

We find the coefficient $b^+_{(41,23)}$ is zero by applying Eq. (2.43) to $C_1^+ + C_2^+$. For $b^-_{(41,23)}$, we get

$$b^-_{(41,23)} = \frac{2\langle 13\rangle^2\langle 24\rangle^2 - \langle 12\rangle\langle 13\rangle\langle 24\rangle\langle 34\rangle + 11\langle 12\rangle^2\langle 34\rangle^2}{3\langle 34\rangle^4}. \tag{2.74}$$

Next, we would like to calculate $b^{\pm}_{(41,32)}$ and see if it can be found from $b^{\pm}_{(41,23)}$. The former coefficient has four contributions $D_1^{\pm}$ and $D_2^{\pm}$, which is shown in Figure 2.13.

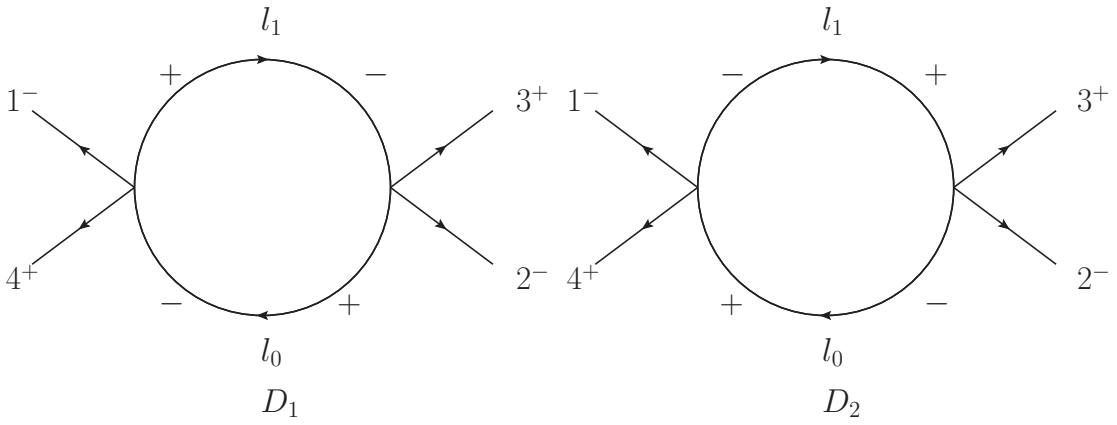

Figure 2.13: The non-zero helicity configurations for the coefficient $b_{(41,32)}$.

$$
\begin{aligned}
D_1 &= \frac{i\,\langle 1l\rangle^4}{\langle 1l_1\rangle\,\langle l_1 l\rangle\,\langle l4\rangle\,\langle 41\rangle}\frac{i\,\langle 2l_1\rangle^4}{\langle 2l\rangle\,\langle ll_1\rangle\,\langle l_1 3\rangle\,\langle 32\rangle}, \\
D_2 &= \frac{i\,\langle 1l_1\rangle^3}{\langle l_1 l\rangle\,\langle l4\rangle\,\langle 41\rangle}\frac{i\,\langle 2l\rangle^3}{\langle ll_1\rangle\,\langle l_1 3\rangle\,\langle 32\rangle}.
\end{aligned} \tag{2.75}
$$

We can use the same loop solution as before and evaluate $D_\pm^1$ and $D_\pm^2$ to find

$$
\begin{aligned}
D_1^+ &= \frac{t^4\left(\langle 24\rangle - \frac{y}{t}\langle 21\rangle\right)^4}{\langle 32\rangle\,\langle 41\rangle\,(1-y)(t\,\langle 24\rangle + (1-y)\,\langle 21\rangle)\left(\langle 43\rangle - \frac{y}{t}\langle 13\rangle\right)}, \\
D_2^+ &= \frac{(t\,\langle 24\rangle + (1-y)\,\langle 21\rangle)^3}{\langle 32\rangle\,\langle 41\rangle\,(1-y)\left(\langle 43\rangle - \frac{y}{t}\langle 13\rangle\right)}, \\
D_1^- &= \frac{\left(\frac{y}{t}\right)^4((y-1)\,\langle 24\rangle + t\,\langle 21\rangle)^4}{\langle 32\rangle\,\langle 41\rangle\,(y-1)\left(\frac{y}{t}\langle 24\rangle + \langle 21\rangle\right)((y-1)\,\langle 43\rangle + t\,\langle 13\rangle)}, \\
D_2^- &= \frac{(y-1)^3\left(\frac{y}{t}\langle 24\rangle + \langle 21\rangle\right)^3}{\langle 32\rangle\,\langle 41\rangle\,((y-1)\,\langle 43\rangle + t\,\langle 13\rangle)}.
\end{aligned} \tag{2.76}
$$

Finally, we can use Eq. (2.43) and find the contribution to the bubble coefficient $b^\pm_{(41,32)}$. It is no surprise that $b^+_{(41,32)}$ is zero, and we find

$$
b^-_{(41,32)} = \frac{-11\,\langle 13\rangle^2\,\langle 24\rangle^2 + 13\,\langle 12\rangle\,\langle 13\rangle\,\langle 24\rangle\,\langle 34\rangle - 14\,\langle 12\rangle^2\,\langle 34\rangle^2}{3\,\langle 34\rangle^4}. \tag{2.77}
$$

Next, we would like to calculate $b^\pm_{(41,32)}$ from $b^\pm_{(41,23)}$ by using the BCJ integral coefficient relation Eq. (2.54) and confirm that we get the correct result. First, we find the needed ratio

of inverse propagators, which are

$$\begin{aligned}\frac{s_{l^+3}}{s_{-l_1^+3}} &= -\frac{\left(t\left\langle 43\right\rangle+(1-y)\left\langle 13\right\rangle\right)\left(\frac{y}{t}\left[34\right]+\left[31\right]\right)}{\left(\left\langle 43\right\rangle-\frac{y}{t}\left\langle 13\right\rangle\right)\left((y-1)\left[34\right]+t\left[31\right]\right)},\\ \frac{s_{l^-3}}{s_{-l_1^-3}} &= -\frac{\left(\frac{y}{t}\left\langle 43\right\rangle+\left\langle 13\right\rangle\right)\left(t\left[34\right]+(1-y)\left[31\right]\right)}{\left((y-1)\left\langle 43\right\rangle+t\left\langle 13\right\rangle\right)\left(\left[34\right]-\frac{y}{t}\left[31\right]\right)}.\end{aligned} \tag{2.78}$$

We can apply the BCJ integral coefficient relation to confirm that we get the right result.

$$\begin{aligned}b^{\pm}_{(41,32)} &= \mathrm{Inf}_t\left[\mathrm{Inf}_y\left[\frac{s_{l^\pm 3}(t,y)}{s_{l_1^\pm 3}(t,y)}b^{\pm}_{(41,23)}(t,y)\right]\right]\Bigg|_{t=0,y^i=Y_i},\\ &= \frac{-11\left\langle 13\right\rangle^2\left\langle 24\right\rangle^2+13\left\langle 12\right\rangle\left\langle 13\right\rangle\left\langle 24\right\rangle\left\langle 34\right\rangle-14\left\langle 12\right\rangle^2\left\langle 34\right\rangle^2}{3\left\langle 34\right\rangle^4}.\end{aligned} \tag{2.79}$$

We confirmed that the two solutions agree numerically, thus showing that the BCJ integral coefficients work on bubble coefficients as well. Around the same time of this work, similar relations were utilized to find rational terms as well [164].

This chapter demonstrates that color-kinematics duality, which motivated tree-level amplitude relations, provides more structure to one-loop amplitudes via integral coefficient relations. While this work has only focused on Yang-Mills theory, in principle, these concepts could be carried over to scattering amplitudes in gravity via the double copy [30, 38, 39, 43, 51].

One-loop graviton scattering in general relativity is miraculously UV finite [165], yet adding matter causes unphysical divergences. Perhaps the divergences are due to the neglection of gravitational spin-spin interactions of quantized angular momentum via torsion in Einstein-Cartan theory. The double copy of the Yang-Mills boson in Riemannian geometry gives the graviton, axion, and dilaton. In 1974, Scherk and Schwarz showed that the Einstein-Hilbert action in Cartan geometry allows for spin-spin interactions between fermions via torsion, which when placed in Riemannian geometry results in the axion [166, 167]. Einstein-Cartan theory is a very natural extension of general relativity with semi-classical applications of quantized angular momentum [168].

While it has been argued that Einstein-Cartan theory treated as a quantum field theory provides a UV cutoff for matter via a Cartan radius [169, 170], scattering amplitudes have

only been computed in Einstein-Cartan theory at tree level [171]. Asymptotically safe quantum gravity as well as UV fixed points in theories with torsion and non-metricity have been investigated [172–174], as well as the short-scale differences caused by quantum gravity [175]. Finite entanglement entropy has been found in asymptotically safe quantum gravity [176]. A $U(1)$ gauge symmetry was found in the trace of the torsion tensor, suggesting some connetion to a gauge-gravity duality [177], which also allows for a $U(1) \times SU(2)$ symmetry to be found when considering the four-fermion interaction term [178, 179]. Dark matter, dark energy, and the hierarchy problem also may be addressed with Einstein-Cartan theory [180–183]. While it would be interesting to investigate the UV properties of quantum gravity with matter via generalizations of Einstein-Cartan theory that also encode the standard model, such a topic is outside the scope of this thesis.

CHAPTER 3

Radiation in Linearized Gravity and Electrodynamics

In this chapter, linearized gravity and the quadrupole moment method for gravitational waves are introduced. Interest in a radiative double copy motivates studying the connection between electromagnetic radiation and gravitational radiation in linearized gravity. By comparing with the quadrupole moment method, a generalization of the Lienard-Wiechert potential in electromagnetism is found in this section for relativistic gravitational sources. While such a formula would not be a valid approximation of general relativity for relativistic bound states, it could be applicable for gravitational wave production from relativistic scattering processes. While the simple classical solutions presented could be calculated with traditional methods, the hope is that a radiative double copy could help with more difficult calculations and provide new insight.

3.1 Gravitational Waves in Linearized Gravity

In 1893, Heaviside considered the possibility of gravitational waves in a linearized theory of gravity analogous to Maxwell's equations. With knowledge of the modern color-kinematics duality we can see an echo of some charge-mass duality between Maxwell's equations and Heaviside's theory of gravity. By 1905, Poincare proposed that gravitational waves would move at the speed of light. By 1915, Einstein developed his general theory of relativity, stating that all forms of stress, energy, and momentum curves the spacetime metric $g_{\mu\nu}$. Einstein's field equations are

$$R_{\mu\nu} - \frac{1}{2} g_{\mu\nu} R = G_{\mu\nu} = \frac{8\pi G}{c^4} T_{\mu\nu}, \tag{3.1}$$

where $R_{\mu\nu}$ is the Ricci tensor, $G_{\mu\nu}$ is the Einstein tensor, $T_{\mu\nu}$ is the stress-energy-momentum tensor, G is Newton's gravitational constant, and c is the speed of light. Around the same time, Hilbert developed a simple action, which gives Einstein's field equations when varied with respect to $g_{\mu\nu}$. The Einstein-Hilbert action is

$$S_{EH} = \int d^4x \mathcal{L}_{EH} = -\frac{c^3}{16\pi G} \int d^4x \sqrt{-\det(g_{\mu\nu})} R, \tag{3.2}$$

where $R = g^{\mu\nu} R_{\mu\nu}$ is the Ricci scalar. In 1916, Einstein demonstrated the transport of energy via gravitational waves. While claims of indirect experimental confirmation were made in the 1970's, it was not until 2015 that LIGO directly detected gravitational waves, which was publicly announced in February of 2016, coincidentally on the hundred-year anniversary of Einstein's discovery [184]. In this section, we look to linearize Einstein's field equations and study the associated gravitational wave equation.

Note that $g_\nu^{\ \mu} = \delta_\nu^{\ \mu}$, which means that $g_\mu^{\ \mu} = d$, where d is the number of dimensions. Throughout this chapter, we will work in $d = 4$ dimensions. As Einstein's field equations are a set of 16 nonlinear equations, calculating exact solutions is often quite cumbersome. As physicists often do, it helps to approximate the spacetime metric as the sum of a background metric and a weak gravitational field $\kappa h_{\mu\nu}$. We take the background metric to be the Minkowski metric, giving

$$g_{\mu\nu} = \eta_{\mu\nu} + \kappa h_{\mu\nu}, \tag{3.3}$$

where use the convention that $\kappa = \sqrt{\frac{32\pi G}{c^3}}$. The Minkowski metric is chosen to be

$$\eta_{\mu\nu} = \eta^{\mu\nu} = \text{diag}(-1, 1, 1, 1), \tag{3.4}$$

Our assumption is that $|\kappa h_{\mu\nu}| \ll 1$, which allows us to neglect all terms after leading order in κh. With this assumption, we find that the inverse metric is

$$g^{\mu\nu} = \eta^{\mu\nu} - \kappa h^{\mu\nu} + \mathcal{O}(\kappa^2), \tag{3.5}$$

where $h^{\mu\nu} \equiv \eta^{\mu\alpha}\eta^{\nu\beta} h_{\alpha\beta}$ and linearized gravity ignores metric contributions of the order κ^2 and higher. Since $\eta_{\mu\nu}$ is a constant tensor, we can now develop a theory of linearized gravity, which treats $h_{\mu\nu}$ as the dynamical field. The linear theory has a simpler set of field equations,

and all indices can be raised and lowered with the constant Minkowski metric. The linearized gravity action is

$$S_{LG} = \int d^4x \left(\frac{1}{2}\partial^\alpha h^{\mu\nu}\partial_\alpha h_{\mu\nu} - \partial_\mu h^{\mu\alpha}\partial^\nu h_{\nu\alpha} + \partial^\mu h_{\mu\nu}\partial^\nu h - \frac{1}{2}\partial_\mu h \partial^\mu h \right), \tag{3.6}$$

where we see that κ was conveniently chosen such that it drops out of the linearized gravity action. A short calculation shows that Eq. (3.6) is equivalent to

$$S_{LG} = \int d^4x \left(\frac{1}{2}\partial^\alpha \bar{h}^{\mu\nu}\partial_\alpha \bar{h}_{\mu\nu} - \frac{1}{4}\partial_\mu \bar{h}\partial^\mu \bar{h} \right). \tag{3.7}$$

As a brief side note, physicists will often write down the Lagrangian

$$S_{GF} = \int d^4x \left(\frac{1}{2}\partial^\alpha h^{\mu\nu}\partial_\alpha h_{\mu\nu} - \frac{1}{4}\partial_\mu h \partial^\mu h \right). \tag{3.8}$$

A field redefinition of $h_{\mu\nu} \to \bar{h}_{\mu\nu}$ can be made to find this Lagrangian. Since there is additional gauge freedom, many prefer to work in the transverse-traceless gauge defined later. If the metric is traceless, then $\bar{h}_{\mu\nu} = h_{\mu\nu}$, which makes the two Lagrangians equivalent in this gauge. This demonstrates that one does not necessarily need to gauge fix at the Lagrangian level to get the above action.

Varying the linearized gravity Lagrangian in Eq. (3.6) gives the equation of motion in vacuum

$$\partial^\alpha \partial_\alpha \bar{h}^{\mu\nu} - \partial^\mu \partial_\alpha \bar{h}^{\alpha\nu} - \partial^\nu \partial_\alpha \bar{h}^{\alpha\mu} + \eta^{\mu\nu}\partial_\alpha \partial_\beta \bar{h}^{\alpha\beta} = 0, \tag{3.9}$$

where $\bar{h}_{\mu\nu} = h_{\mu\nu} - \frac{1}{2}\eta_{\mu\nu}h$ is the trace-reversed metric. Alternatively, the trace-reversed metric in linearized gravity is given by $g^{\mu\nu}\sqrt{|\det(g)|} = \eta^{\mu\nu} - \kappa\bar{h}^{\mu\nu}$.

No gauge fixing was used yet to find the above equation of motion. By applying the harmonic, de Donder, Hilbert, Lorenz, Lorentz, or Fock gauge $\partial_\mu \bar{h}^{\mu\nu} = 0$, we remove the longitudinal degrees of freedom and find

$$\partial^\alpha \partial_\alpha \bar{h}^{\mu\nu} = 0, \tag{3.10}$$

which is just the linearized wave equation in vacuum. A simple route to getting the equation of motion in the presence of sources is to linearize Einstein's field equations, giving

$$\kappa\partial^\alpha \partial_\alpha \bar{h}_{\mu\nu} = -\frac{16\pi G}{c^4}T_{\mu\nu}, \tag{3.11}$$

where once again, we have restricted our metric to the harmonic gauge. There is still much gauge freedom left over, as a propagating gravitational wave only has two independent degrees of freedom. Due to diffeomorphism invariance or the coordinate independence of general relativity, a gauge transformation of $h_{\mu\nu}$ will not change any physical degrees of freedom. When $x'^{\mu} = x^{\mu} + \xi^{\mu}$, we have

$$\begin{aligned} \kappa h'_{\mu\nu} &= \kappa h_{\mu\nu} - \partial_{\mu}\xi_{\nu} - \partial_{\nu}\xi_{\mu}, \\ \kappa \bar{h}'_{\mu\nu} &= \kappa \bar{h}_{\mu\nu} - \partial_{\mu}\xi_{\nu} - \partial_{\nu}\xi_{\mu} + \eta_{\mu\nu}\partial^{\alpha}\xi_{\alpha}. \end{aligned} \tag{3.12}$$

The gauge transformed metric can remain in the harmonic gauge, provided that $\partial^{\alpha}\partial_{\alpha}\xi^{\mu} = 0$.

The general solution to the equation of motion can be found using a retarded Green function, which gives

$$\kappa \bar{h}_{\mu\nu}(t, \vec{x}) = \frac{4G}{c^4} \int d^3x' \frac{T_{\mu\nu}(t_{\text{ret}}, \vec{x}')}{|\vec{x} - \vec{x}'|}, \tag{3.13}$$

where $t_{\text{ret}} = t - |\vec{x} - \vec{x}'|/c$ is the retarded time. Next, we focus on the wave solutions emitted by arbitrary sources $T_{\mu\nu}$ in linearized gravity via the quadrupole moment method.

3.1.1 Radiation and the Quadrupole Moment Tensor

To introduce gravitational waves, we start by noting that they are solutions of the vacuum, found from Eq. (3.10). Since $\partial^{\alpha}\partial_{\alpha}\bar{h}_{\mu\nu} = 0$, this suggests that plane waves $e^{\pm ik_{\alpha}x^{\alpha}}$ times a constant polarization tensor $\epsilon_{\mu\nu}$ may work. Plugging the ansatz $\kappa\bar{h}_{\mu\nu} = \epsilon_{\mu\nu}e^{ik_{\alpha}x^{\alpha}} + \epsilon^{*}_{\mu\nu}e^{-ik_{\alpha}x^{\alpha}}$ gives

$$k_{\mu}k^{\mu} = 0, \tag{3.14}$$

and the harmonic gauge condition gives

$$k^{\mu}\epsilon_{\mu\nu} = 0. \tag{3.15}$$

Since the polarization tensor is symmetric, we have potentially ten independent components. The harmonic gauge condition above removes four, leaving potentially six independent components. We still have additional gauge freedom. By choosing $\xi^{\mu}(x) = \zeta^{\mu}e^{ik_{\alpha}x^{\alpha}} - \zeta^{\mu *}e^{-ik_{\alpha}x^{\alpha}}$, we find

$$\epsilon'_{\mu\nu} = \epsilon_{\mu\nu} - ik_{\mu}\zeta_{\nu} - ik_{\nu}\zeta_{\mu} + \eta_{\mu\nu}ik^{\alpha}\zeta_{\alpha}, \tag{3.16}$$

which leaves us with only two independent degrees of freedom in the polarization tensor. From a particle physics perspective, we know that the spin-2 graviton is massless. While a massive spin-2 particle would have five degrees of freedom, the massless graviton has only two degrees of freedom, and so does a massless photon.

Since there are only two physical degrees of freedom, it helps to choose a gauge that makes this simplicity more apparent. The transverse-traceless gauge does exactly that. Since it is traceless, $\bar{h}_{\mu\nu} = h_{\mu\nu}$. Without any loss of generality, we will assume that the plane wave is travelling in the z direction. Considering a single plane wave, the transverse-traceless gauge gives

$$\kappa \bar{h}^{TT}_{\mu\nu} = e^{ik_\alpha x^\alpha} \begin{pmatrix} 0 & 0 & 0 & 0 \\ 0 & \epsilon_{xx} & \epsilon_{xy} & 0 \\ 0 & \epsilon_{xy} & -\epsilon_{xx} & 0 \\ 0 & 0 & 0 & 0 \end{pmatrix}. \tag{3.17}$$

To put a metric in the transverse-traceless gauge from the harmonic gauge, one can utilize the spatial projection operator $P_{lm} = \delta_{lm} - n_l n_m$, where $n_l = x^l/r$, such that

$$\bar{h}^{TT}_{jk} = P_{jl}\bar{h}_{lm}P_{mk} - \frac{1}{2}P_{jk}(P_{lm}\bar{h}_{lm}). \tag{3.18}$$

Similar to light, gravitational waves can be linearly or circularly polarized. The linear polarizations of gravity are called "plus" and "cross", due to how they affect a ring of massive test particles. While most texts would label these as $\epsilon^{\mu\nu}_+$ and $\epsilon^{\mu\nu}_\times$, we will denote them as $\epsilon^{\mu\nu}_p$ and $\epsilon^{\mu\nu}_c$, saving the + label for right-handed circularly polarized gravitational waves. The dimensionful linear-polarization tensors are proportional to unit tensors $\hat{\epsilon}^{\mu\nu}$, given by

$$\epsilon^{\mu\nu}_p = \epsilon_{xx}\hat{\epsilon}^{\mu\nu}_p = \epsilon_{xx} \begin{pmatrix} 0 & 0 & 0 & 0 \\ 0 & 1 & 0 & 0 \\ 0 & 0 & -1 & 0 \\ 0 & 0 & 0 & 0 \end{pmatrix}, \qquad \epsilon^{\mu\nu}_c = \epsilon_{xy} \begin{pmatrix} 0 & 0 & 0 & 0 \\ 0 & 0 & 1 & 0 \\ 0 & 1 & 0 & 0 \\ 0 & 0 & 0 & 0 \end{pmatrix}. \tag{3.19}$$

Similar to the polarization vectors of electromagnetism, we can define the circular-polarization tensors from the linear, giving $\hat{\epsilon}^{\mu\nu}_\pm = \frac{1}{\sqrt{2}}\left(\hat{\epsilon}^{\mu\nu}_p \pm i\hat{\epsilon}^{\mu\nu}_c\right)$. With each component displayed ex-

plicitly, we find

$$\epsilon_{\pm}^{\mu\nu} = \epsilon_{\pm}\hat{\epsilon}_{\pm}^{\mu\nu} = \frac{\epsilon_{\pm}}{\sqrt{2}} \begin{pmatrix} 0 & 0 & 0 & 0 \\ 0 & 1 & \pm i & 0 \\ 0 & \pm i & -1 & 0 \\ 0 & 0 & 0 & 0 \end{pmatrix}. \tag{3.20}$$

Now that we have established that gravitational waves are a solution to the linearized field equations in vacuum, it is time to see how sources can radiate these waves. A multipole expansion is used to take a nonrelativistic expansion. While the retarded time $t - |\vec{x} - \vec{x}'|/c$ is conceptually intuitive, it helps to expand $|\vec{x} - \vec{x}'|$, such that

$$\begin{aligned} |\vec{x} - \vec{x}'| &= r - \vec{x}' \cdot \hat{n} + \mathcal{O}\left(\frac{d^2}{r}\right), \\ \frac{1}{|\vec{x} - \vec{x}'|} &= \frac{1}{r} + \mathcal{O}\left(\frac{d}{r^2}\right), \end{aligned} \tag{3.21}$$

where $\vec{x} = r\hat{n}$ and d is the characteristic size of the near zone, which is the region where $\vec{x}'$ is integrated over. Since $T^{\mu\nu}(t - |\vec{x} - \vec{x}'|/c, \vec{x}')$ is needed in Eq. (3.13) yet we want to evaluate it in terms of the average retarded time $t - r/c$, a Taylor expansion in $\vec{x}' \cdot \hat{n}/c$ can be taken, which is small in comparison to r/c, giving

$$T^{\mu\nu}\left(t - \frac{r}{c} + \frac{\vec{x}' \cdot \hat{n}}{c}, \vec{x}'\right) = \sum_{n=0}^{\infty} \frac{1}{n!} \left(\frac{\vec{x}' \cdot \hat{n}}{c} \frac{d}{dt}\right)^n T^{\mu\nu}\left(t - \frac{r}{c}, \vec{x}'\right). \tag{3.22}$$

It helps to imagine Fourier modes such that the nth time derivative would correspond to n factors of $i\omega$, with $\omega\vec{x}' \cdot \hat{n}/c \ll 1$ for nonrelativistic sources. Since this unitless quantity appears in the Taylor expansion, we only need the lowest order term with $n = 0$ to obtain an accurate approximation.

As we will show, in order to find the gravitational waves in the transverse-traceless gauge, the quadrupole moment tensor will correspond to this lowest-order term, which is defined by

$$I^{jk}(t) = \int d^3x \frac{T^{00}(x)}{c^2} x^j x^k, \tag{3.23}$$

where Latin indices only run over the three spatial dimensions. Since the stress-energy-momentum tensor is locally conserved in linearized gravity, $\partial_\mu T^{\mu\nu} = 0$, we can derive the

identity

$$\ddot{I}^{jk} = \frac{d^2}{dt^2}\int d^3x x^j x^k \frac{T^{00}}{c^2} = -\int d^3x x^j x^k \frac{\partial^2}{c\partial t \partial x^a} T^{a0}(x) = 2\int d^3x T^{jk}(x). \tag{3.24}$$

If we restrict ourselves to the transverse-traceless gauge, $\bar{h}_{0\mu} = 0$ and

$$\kappa \bar{h}^{TT}_{jk} = \frac{2G}{c^4 r}\ddot{I}_{jk}(t_{\text{ret}}). \tag{3.25}$$

This formula finds gravitational radiation for nonrelativistic sources in linearized gravity from the quadrupole moment. Relativistic sources necessitate higher multipole moments, such as the octupole moment; however, relativistic bound systems also introduce nonlinear fields, which is outside the scope of this current chapter.

3.2 Generalizing the Lienard-Wiechert Potential

Next, we investigate if a linearized double copy can be found to relate gravitational radiation to electromagnetic radiation. A derivation of the Lienard-Wiechert potential of electrodynamics for arbitrary trajectories is given. While simply replacing the electric charge with the momentum of a particle does not result in gravitational radiation, a nontrivial connection is found between the sources of electrodynamics and linearized gravity. This allows for a generalized Lienard-Wiechert metric, which is found to at least hold for nonrelativistic point-particle masses.

As one might expect, the plane waves from electromagnetism are related to plane waves in linearized gravity. Electromagnetism also has unit polarization vectors, which can be linear or circular. For waves propagating in the z direction, we define the electromagnetic unit polarization vectors as

$$\begin{aligned}
\hat{\epsilon}^{\mu}_{x} &= (0,1,0,0), \\
\hat{\epsilon}^{\mu}_{y} &= (0,0,1,0), \\
\hat{\epsilon}^{\mu}_{\pm} &= \frac{1}{\sqrt{2}}\left(\hat{\epsilon}^{\mu}_{x} \pm i\hat{\epsilon}^{\mu}_{y}\right) = \frac{1}{\sqrt{2}}(0,1,\pm i,0).
\end{aligned} \tag{3.26}$$

Interestingly enough, we can form the unit polarization tensors of gravity from the polariza-

tion vectors above. For the plus and cross polarizations, we find

$$\begin{aligned}\hat{\epsilon}_p^{\mu\nu} &= \hat{\epsilon}_x^\mu \hat{\epsilon}_x^\nu - \hat{\epsilon}_y^\mu \hat{\epsilon}_y^\nu, \\ \hat{\epsilon}_c^{\mu\nu} &= \hat{\epsilon}_x^\mu \hat{\epsilon}_y^\nu + \hat{\epsilon}_y^\mu \hat{\epsilon}_x^\nu. \end{aligned} \tag{3.27}$$

While it has been known for quite some time that these electromagnetic polarization vectors can be used to find the gravitational polarization tensors, we assert that the circular polarization tensors of linearized gravity are a double copy of the circular polarization vectors of electromagnetism, which can be seen by

$$\hat{\epsilon}_\pm^{\mu\nu} = \sqrt{2}\hat{\epsilon}_\pm^\mu \hat{\epsilon}_\pm^\nu. \tag{3.28}$$

Once again, this relationship is well known, but within the language of the double copy, circularly-polarized gravitational plane waves are a double copy of circularly-polarized electromagnetic plane waves.

To start with electromagnetism, the Lorentz-Heaviside units will be most appropriate for giving a canonically normalized kinetic term without any bizarre factors of ϵ_0 or μ_0, which SI would have. In fact, Lorentz–Heaviside units can be thought of as natural units with the factors of c left in, such that both SI and Lorentz–Heaviside units have the same equations when taking $\epsilon_0 = \mu_0 = c = 1$. Also, we will choose the mostly-positive Minkowski metric to agree with above, which is not typical for electromagnetism. Starting with the free Maxwell action, we find

$$S_M = -\frac{1}{4}\int d^4x F_{\mu\nu}F^{\mu\nu}, \tag{3.29}$$

where $F_{\mu\nu} = \partial_\mu A_\nu - \partial_\nu A_\mu$ is the electromagnetic tensor, and A_μ is the electromagnetic potential.

The Euler-Lagrange equations derive the equations of motion, and continuing with no sources, the equation of motion is

$$\partial^\mu F_{\mu\nu} = \partial_\mu \partial^\mu A_\nu + \partial_\nu \partial^\mu A_\mu = 0. \tag{3.30}$$

Similar to gravity, electromagnetism has gauge freedom. The Lorenz gauge ($\partial^\mu A_\mu = 0$) is analogous to the harmonic gauge ($\partial^\mu \bar{h}_{\mu\nu} = 0$) in gravity, which both remove the longitudinal

degrees of freedom from the potentials. Adding the interaction term $-\frac{1}{c}J_\mu A^\mu$ and applying the Lorenz gauge in the presence of sources J_μ gives

$$\partial_\alpha \partial^\alpha A_\mu = -\frac{J_\mu}{c}, \tag{3.31}$$

where J_μ is the electromagnetic four-current, which describes the density and momentum of electrical charge, just as $T_{\mu\nu}$ describes the stress, density and momentum of mass and energy. Comparing the above equation of motion with Eq. (3.11), it seems fruitful to consider that the solutions of these two wave equations will be similar.

Furthermore, point particle sources located at x_i with either charges q_i or m_i for the electromagnetic current and stress-energy-momentum tensor are remarkably similar, given by

$$\begin{aligned} J^\mu(x) &= \sum_{i=1}^{N} q_i \int d\tau v_i^\mu \delta^{(4)}(x - x_i(\tau)), \\ T^{\mu\nu}_{\text{free}}(x) &= \sum_{i=1}^{N} m_i \int d\tau v_i^\mu v_i^\nu \delta^{(4)}(x - x_i(\tau)), \end{aligned} \tag{3.32}$$

where the four-velocity $v_i^\mu = \frac{\partial x_i^\mu}{\partial \tau}$ is the standard Lorentz-invariant four-vector and $\frac{dt}{d\tau} = \gamma$. While the Lienard-Wiechert potential utilizes this electromagnetic current as a source, it is clear that this stress-energy-momentum tensor for free point particles cannot give the full gravitational radiation, as it neglects inter-particle interactions that may lead to stress and strain. However, we will carry through with the derivation of the Lienard-Wiechert potential and see what is missing in gravity.

The appropriate Green function for the wave equations is given by

$$\begin{aligned} \Box G(\vec{x} - \vec{x}', t - t') &= -\delta^{(3)}(\vec{x} - \vec{x}')\delta(t - t'), \\ G(\vec{x} - \vec{x}', t - t') &= \frac{1}{4\pi|\vec{x} - \vec{x}'|}\delta\left(t - t' - \frac{|\vec{x} - \vec{x}'|}{c}\right). \end{aligned} \tag{3.33}$$

The Green function allows us to find the fields at positions and times far away from the sources, giving

$$\begin{aligned} A^\mu(x) &= \frac{1}{c}\int d^4x' G(x - x') J^\mu(x'), \\ \kappa \bar{h}^{\mu\nu}(x) &= \frac{16\pi G}{c^4}\int d^4x' G(x - x') T^{\mu\nu}(x'). \end{aligned} \tag{3.34}$$

Plugging in the Green function and source for a single particle gives

$$A^{\mu}(x) = q_i \int dt' \frac{\delta\left(t - t' - \frac{|\vec{x}-\vec{x}_i(t')|}{c}\right)}{4\pi c\gamma|\vec{x}-\vec{x}_i(t')|} v^{\mu}_{\alpha}. \tag{3.35}$$

Switching integration variables to $\tilde{t} \equiv t' - \frac{|\vec{x}-\vec{x}_i(t')|}{c}$ allows for a Jacobian factor $\frac{dt'}{d\tilde{t}}$ to be added, which is found to be

$$\begin{aligned} \frac{d\tilde{t}}{dt'} &= 1 - \frac{\frac{d\vec{x}_{\alpha}(t')}{dt'} \cdot (\vec{x} - \vec{x}_{\alpha}(t'))}{c|\vec{x} - \vec{x}_{\alpha}(t')|}, \\ \frac{dt'}{d\tilde{t}} &= \frac{1}{1 - \vec{\beta} \cdot \hat{n}}, \end{aligned} \tag{3.36}$$

where $\vec{\beta} \equiv \frac{d\vec{x}_{\alpha}(t')}{dt'}$ and $\hat{n} \equiv \frac{\vec{x}-\vec{x}_{\alpha}(t')}{|\vec{x}-\vec{x}_{\alpha}(t')|}$. This allows for a simple integration over $\delta(t-\tilde{t})$, giving

$$A^{\mu}(x) = \left.\frac{q_i \beta^{\mu}}{4\pi(1 - \vec{\beta} \cdot \hat{n})R}\right|_{t'=t_{ret}} = \left.\frac{q_i v^{\mu}_i}{4\pi v^{\rho}_i R_{\rho}}\right|_{t'=t_{ret}}, \tag{3.37}$$

where $\beta^{\mu} \equiv (1, \vec{\beta})$, $R \equiv |\vec{x} - \vec{x}_{\alpha}(t')|$, and $R^{\mu} \equiv x^{\mu} - x^{\mu}_i(t')$. Doing the same calculations for gravity gives an incomplete generalization of the Lienard-Wiechert potential,

$$\kappa \bar{h}^{\mu\nu} \neq \left.\frac{4Gm_i}{c^3} \frac{v^{\mu}_i v^{\nu}_i}{v^{\rho}_i R_{\rho}}\right|_{t'=t_{ret}}. \tag{3.38}$$

While this result is based off of the same derivation going back to the original days of Lienard and Wiechert, the gravitational generalization above does not address gravitational interactions that contribute stress and strain. This is expected, since $T^{\mu\nu}_{\text{free}}$ is technically only conserved if all of the particles are at the exact same location, which is only valid during the moment of a collision. Maggiore also points out that the gravitational potential energy must be included [94]. Since the equivalence principle states that gravity is indistinguishable from acceleration, one might expect that an effective energy-momentum tensor which includes the acceleration may help, as the four-acceleration represents worldline curvature.

For relativistic sources, Whitney has pointed out that the Lienard-Wiechert derivation is a correct solution, but does not adequately apply boundary conditions in a Lorentz-invariant fashion, as R^{ρ} is the distance between the observer and the time-retarded source, which is combined with the time-retarded proper-velocity [185]. As a result, the radiation found by the collision of many particles may give inconsistent results, which can create

unphysical infinities in the radiative fields. Note how similar issues originally occurred in gravitational wave analyses when utilizing the post-Newtonian approximation due to time-retardation issues. While the PN approximation completely neglects retardation effects, Whitney asserts that the common derivation of the Lienard-Wiechert potential does not deal with retardation in a Lorentz-invariant manner necessary for describing relativistic phenomena in full generality. While we will elaborate on Whitney's claim in the following subsection, we first will correct the above generalization, ignoring Whitney's claim.

Comparison with the quadrupole moment method will allow for a more general formula that builds off of Eq. (3.38). While our construction will only apply to point particles, it may allow for gravitational fields to be found within a larger class of gauge conditions, as the quadrupole moment method assumes a transverse-traceless gauge. To find the additional terms, the quadrupole moment method will be investigated for point particles, and this will allow for a Lorentz-invariant generalization. The quadrupole moment method is given by

$$\kappa\bar{h}^{jk} = \frac{2G}{c^4 r}\ddot{I}^{jk}(t_{\text{ret}}). \tag{3.39}$$

Solving for the quadrupole moment tensor gives

$$\kappa\bar{h}^{jk} = \frac{2G}{c^4 r}\sum_{i=1}^{N} m_i \frac{\partial^2}{\partial t^2}(x_i^j x_i^k) = \frac{2G}{c^4 r}\sum_{i=1}^{N} m_i (x_i^j a_i^k + 2v_i^j v_i^k + a_i^j x_i^k). \tag{3.40}$$

Generalizing the Lienard-Wiechert metric to include gravitational forces adds terms proportional to $m_i a_i^\mu$ gives

$$\kappa\bar{h}^{\mu\nu} = \sum_{i=1}^{N} \frac{4Gm_i}{c^3 v_i^\rho R_\rho}\left(\frac{1}{2}x_i^\mu a_i^\nu + v_i^\mu v_i^\nu + \frac{1}{2}a_i^\mu x_i^\nu\right), \tag{3.41}$$

where $a_i^\mu \equiv \frac{d^2 x_i^\mu}{d\tau^2}$ and Eq.(3.41) will be referred to as the generalized Lienard-Wiechert metric. Looking back at this result, it appears it was generated by the following tensor

$$\hat{T}^{\mu\nu}(x) = \sum_{i=1}^{N}\int d\tau \frac{d}{d\tau}\left(x_i^{(\mu}p_i^{\nu)}\right)\delta^{(4)}(x - x_i(\tau)). \tag{3.42}$$

Analogous to color-kinematics duality and the double copy, the substitution of momentum for electric charge is made ($p_i^\mu \to q_i$) to find J^μ in electrodynamics, giving

$$J^\mu(x) = \sum_{i=1}^{N}\int d\tau \frac{d}{d\tau}\left(x_i^\mu q_i\right)\delta^{(4)}(x - x_i(\tau)). \tag{3.43}$$

Assuming no particle creation/annihilation, $\frac{dq_i}{d\tau} = 0$, which gives J^μ as shown in Eq. (3.32). In this sense, the generalized Lienard-Wiechert metric for linearized gravity, Eq. (3.41), can be thought of as the double copy of the Lienard-Wiechert potentials of electrodynamics, Eq. (3.37). However, this analogy has some quantitative differences from what will be presented in Chapter 4, as the time derivative must be factored out in order to show this resemblance. Since we have only compared this result with the quadrupole moment, it is clear that the above formula only applies to nonrelativistic phenomena, as higher multipole contributions such as octupole radiation have been omitted.

3.2.1 Limitations of the Nonperturbative Lienard-Wiechert Potentials

While the perturbative multipole expansion is quite rigorous in treating radiation from charged macroscopic media in motion, the Lienard-Wiechert potential is for point particles and is apparently exactly correct in the relativistic limit. While this may be true, the argument eventually breaks down when considering a collection of many particles, especially if the interactions become strong. The Lienard-Wiechert potentials provide merit because it is a nonperturbative relativistic result. This subsection briefly exemplifies some possible limitations of the Lienard-Wiechert potentials. Fixing these limitations suggests a duality between retarded fields and instantaneous effects, which is then compared to aspects of D0-branes in M-theory, a nonperturbative formulation of quantum gravity.

To start, Whitney claims that the Lienard-Wiechert potentials do not satisfy proper boundary conditions at infinity for relativistic phenomena, as they do not use the proper time of the source [185, 186]. If Whitney's claim is valid, then the problem would be more experimentally relevant in gravity than electrodynamics. Whitney states that a Jacobian was missed in the current density,

$$J^\mu(x) = \sum_{i=1}^{N} q_i c \int ds_i^0 \delta^{(4)}(x - x_i(s_i^0)) v_i^\mu(s_i^0), \tag{3.44}$$

where $v_i^\mu = dx_i^\mu/ds_i^0$ and s_i^0 is the source's proper time. She claims that distribution theory

or generalized functions suggest that the following object would be Lorentz invariant [186],

$$d^{(4)}(s-(s_i^0,0)) = \delta^{(4)}(x - x_i(s_i^0)) \left| \frac{\partial x}{\partial s} \right|, \tag{3.45}$$

as the expression on the left-hand side is explicity in the rest frame of the source with proper time s_i^0. Taking into account this Jacobian, Whitney states that the following solution to Maxwell's equations is Lorentz-invariant and satisfies the appropriate boundary conditions for relativistic sources at infinity [185],

$$A^\mu(x) = \sum_{i=1}^{N} \frac{q_i v_i^\mu}{4\pi c R_i'}, \tag{3.46}$$

where $R_i' = \sqrt{R_\perp^2 + \gamma^2 R_\parallel}$ is a Lorentz-invariant distance found most easily in the rest frame of the ith particle, which came from the Jacobian, giving a factor of $\gamma(1-\vec{\beta}\cdot\hat{n})R/R_i'$ from the result given in most textbooks. Whitneys result also appears to be manifestly Lorentz invariant and appears to be more directly in terms of intertial frames of the sources. The analogous equation for linearized gravity is given by

$$\kappa \bar{h}^{\mu\nu} = \sum_{i=1}^{N} \frac{4Gm_i}{c^4 R_i'} \left(\frac{1}{2} x_i^\mu a_i^\nu + v_i^\mu v_i^\nu + \frac{1}{2} a_i^\mu x_i^\nu \right). \tag{3.47}$$

While the above equation would not be a valid approximation for relativistic bound sources in general relativity, it may be interesting to compare the difference between Eqs. (3.41) and (3.47) for radiation emitted from relativistic scattering processes.

Around 1987, Whitney wrote several articles pointing out related issues [186–189]. Interestingly enough, two independent authors later have suggested the same correction. Field claims to have shown that Lienard and Wiechert derived their formula from one of Heaviside's formula, which turns out to be inconsistent with Feynman's QED [190, 191]. In related work, Field concludes that notions of instantaneous fields are needed [192]. Chubykov and Smirnov-Rueda have also found similar inconsistencies with the Lienard-Wiechert potential, which they claim necessitates a dualistic action at a distance and field theoretic approach that is completely self-consistent with Maxwell's equations [193].

While Jackson and others have argued that Chubykalo's argument is completely nullified on the basis of the assumption that the Lienard-Wiechert potentials are not a solution to

Maxwell's equations [194, 195], Whitney has pointed out over a decade earlier that both methods are a solution to the differential equations, yet they have different boundary conditions. As such, Chubykalo misrepresented the issues of the Lienard-Wiechert potential and potentially made some mathematical errors, and Jackson is valid in refuting Chubykalo yet does not address Whitney's complaints, as Jackson only considres a single proper time τ, which is valid for a single particle. In fact, Aspden previously followed up on the work of Whitney and argued that instantaneous fields would be needed only if the electrodynamics of hadrons and leptons at close ranges are different [196]. Our perspective is not that instantaneous dynamics is needed, but perhaps a nonperturbative approach for multiple particles could be found from Whitney's result instead of the perturbative multipole expansion.

The distinction of instantaneous action at a distance vs time-retarded fields has been heavily discussed over the past two centuries. In 1947, Feynman and Wheeler recall how Gauss first envisioned action at a distance propagating at the speed now known as the speed of light precisely one hundred years prior [197]. They state that fully understanding radiation in the action-at-a-distance picture is what is holding back the unification of field theory and action at a distance, which may allow for a new duality in nature. Tetrode states that an absorber is needed in order to radiate energy, fields only arise from other sources, and these fields are represented by one-half of the retarded Lienard-Wiechert solution plus one-half of the advanced Lienard-Wiechert solution.

Gauss, Weber, and Ampere developed a theory of electrodynamics that is an action-at-a-distance theory that predated Maxwell and was sophisticated in its abilities to obtain relativistic-looking phenomena in powers of v/c that satisfies Newton's third law [198]. In fact, Ampere's law currently taught was not discovered by Ampere, but rather is the law of Grassmann; Ampere's law was contained in Weber electrodynamics. Nasilovski and Graneau have performed experiments, including the study of exploding wires and Ampere's hairpin experiment, both arguing for Ampere's original law. However, properly accounting for thermoelectric effects describe the discrepancies in the exploding wire experiments [199]. Jackson points out that while certain gauge choices can allow for instantaneous phenomena, they are not needed [194] for classical electrodynamics. Jackson states on page 671 of his text-

book [200] that "the radiation emitted by a charge particle in arbitrary, extreme relativistic motion is approximately the same as that emitted by a particle moving instantaneously along the arc of a circular path." Assis and Bueno were able to show an equivalence between Ampere's law and Grassmann's law and provide further resolution to how field theory and action at a distance can agree [201].

While Einstein struggled with notions of entanglement and action at a distance in quantum mechanics, a string theorist may find some solace in these notions. 11-dimensional M-theory is said to be described by a matrix model of D0-branes, which exist in one time dimension zero spatial dimensions. When the light-cone frame is taken, which takes a Lorentz boost in one of the spatial dimensions, nine Galilean-invariant transverse dimensions with SO(9) symmetry remain [202]. Galilean invariance also gives an instantaneous Green function, which may be useful for depicting nonlocal interactions of strongly-correlated systems.

Holography admits a gauge theory description that encodes gravity via noncommutative membranes [203–205]. Furthermore, closed strings contain tachyons, which are often thought to be troublesome. Time-advanced fields from the absorber pointed out by Wheeler and Feynman are claimed to be related to tachyons [206]. If spacetime is emergent, then the time-retarded fields contained within spacetime must also be emergent. Without making any connection to M-theory and the light-cone frame, Stefanovich has also suggested that action at a distance would help unite general relativity and quantum mechanics, the ultimate goal of string theory [207]. Since ultra-relativistic phenomena seemingly necessitate stronger fields, perhaps it is not coincidental that string theorists are also emerging on notions of action at a distance for the description of strongly-interacting systems.

Finally, to make connections back to theories of gravity in four dimensions, it is interesting to note that Newton-Cartan gravity in 4D gives Galilean symmetry [208–210], which can be recovered from 5D Einstein gravity theory by taking a Kaluza-Klein reduction along a null-like direction [211]. This reduction is related to a non-relativistic AdS/CFT model [212]. Such a reduction from 5D suggests that Newton-Cartan and 4D general relativity are both limiting cases of 5D de Sitter space. Perhaps certain gravitational phenomena may be modelled with Galilean or Lorentz symmetry, even though relativistic Lorentz symmetry is

most commonplace.

Our perspective is not to object to conventional notions of classical electrodynamics or relativity, but rather to point out that M-theory seems to provide a unified description of strongly correlated phenomena based on instantaneous Galilean symmetry, which captures aspects of classical action at a distance, except with noncommutative geometry allowing for spacetime uncertainty. If so, perhaps a dualistic picture of time-retardation of energy transfer via fields and instantaneous information transfer via action at a distance would allow for a semi-classical approach to nonperturbative gravitational wave emission from ultra-relativistic or strongly-interacting systems. Investigating the Lienard-Wiechert potential provides hope for bridging the gaps, as it is a nonperturbative solution applicable for relativistic phenomena. Friedlander has also utilized distribution theory to find a generalization of the Lienard-Wiechert potential on curved spacetime [213].

While it would be interesting to study the gravitational radiation from black holes in a semi-classical theory based upon noncommutative geometry and the dualistic field and action-at-a-distance principles previously mentioned that is self-consistent with Einstein's field equations and is a low-energy limit of the holographic principle from M-theory, such a direction is outside the scope of this thesis. Next, the gravitational radiation is calculated for a few simple examples by utilizing the generalized Lienard-Wiechert metric previously found in Eq. (3.41).

3.3 Simple Examples

3.3.1 Binary Inspiral with Equal Mass

Two particles with mass m are assumed to be in circular orbit with the following trajectories

$$\vec{x}_{\pm}(t) = \pm(a\cos(\omega t), a\sin(\omega t), 0), \tag{3.48}$$

where we will assume that the non-relativistic limit $\epsilon_\omega = \frac{a\omega}{c} \ll 1$ holds. The three- and four-velocities are found by taking the appropriate derivatives, giving

$$\begin{aligned} \vec{v}_\pm(t) &= \pm(-a\omega\sin(\omega t), a\omega\cos(\omega t), 0) = c\vec{\beta}_\pm, \\ v^\mu_\pm(t) &= \gamma c(1, \mp\epsilon_\omega\sin(\omega t), \pm\epsilon_\omega\cos(\omega t), 0) = \gamma c(1, \vec{\beta}_\pm), \end{aligned} \tag{3.49}$$

where the scalar quantity $\gamma = 1/\sqrt{1-\epsilon_\omega^2}$ is the same for both masses.

The calculation with the standard quadrupole moment method will be presented first. The quadrupole moment tensor for the two-particle circular orbit gives

$$I_{jk}(t) = \int d^3x_1 T^{00} x_1^j x_1^k = 2ma^2 \begin{pmatrix} \cos^2(\omega t) & \cos(\omega t)\sin(\omega t) & 0 \\ \cos(\omega t)\sin(\omega t) & \sin^2(\omega t) & 0 \\ 0 & 0 & 0 \end{pmatrix}. \tag{3.50}$$

Eq. (3.25) states that we can simply take two time derivatives and multiply by $\frac{2G}{c^4 r}$ to find the gravitational potential in a gauge where $\bar{h}_{\mu 0} = 0$, giving

$$\begin{aligned} \ddot{I}_{jk}(t) &= 2ma^2\omega^2 \begin{pmatrix} -2\cos(2\omega t) & -2\sin(2\omega t) & 0 \\ -2\sin(2\omega t) & 2\cos(2\omega t) & 0 \\ 0 & 0 & 0 \end{pmatrix} \\ \kappa\bar{h}_{jk} &= -\frac{8Gm\epsilon_\omega^2}{rc^2} \begin{pmatrix} \cos(2\omega t) & \sin(2\omega t) & 0 \\ \sin(2\omega t) & -\cos(2\omega t) & 0 \\ 0 & 0 & 0 \end{pmatrix}. \end{aligned} \tag{3.51}$$

Since $\bar{h}^{\mu 0} = 0$ and $\bar{h} = 0$, $h^{\mu\nu} = \bar{h}^{\mu\nu}$. For gravitational waves travelling in the z-direction, this result is in the transverse-traceless gauge.

Next, the generalized Lienard-Wiechert metric, Eq. (3.41), will be used to find the same result. While this formula is more complicated than the quadrupole moment method, its relation to relativistic electrodynamics is more clear, which will allow for a deeper understanding of radiative double copy methods that are applicable to the post-Minkowski method. Taking care with relativistic quantities allows for a gauge transformation to put the final result in the transverse-traceless gauge.

Since the two particles have slightly different locations, their retarded times $t_\pm = t - |\vec{r} - \vec{x}_\pm|/c$ are slightly different. To put these variables into the same coordinate system, the retarded time from the center of mass $t_{\rm com} = t - |\vec{r}|/c$ will be used. For highly relativistic processes, the Whitney metric and the Lienard-Wiechert metric would slightly disagree, but they both are equivalent in the non-relativistic limit, which will be assumed for now. The denominator of the Lienard-Wiechert metric is

$$v_\pm^\rho R_{\pm\rho} = \gamma c(1 - \vec{\beta} \cdot \hat{n}_\pm)R_\pm. \tag{3.52}$$

Upon inversion, applying the geometric expansion and taking the radiative limit $a \ll r$ gives

$$\frac{1}{v_\pm^\rho R_{\pm\rho}} = \frac{1}{\gamma c R_\pm} \sum_{k=0}^{\infty} \left(\vec{\beta}_\pm \cdot \hat{n}_\pm\right)^k = \frac{1}{\gamma c r} \sum_{k=0}^{\infty} \left(\vec{\beta}_\pm \cdot \hat{n}_\pm\right)^k + \mathcal{O}\left(\frac{a}{r^2}\right). \tag{3.53}$$

The Minkowski approximation keeps every term in this infinite sum, but the Newtonian approximation only needs to keep terms to second order, since $\vec{\beta}_\pm$ scales with ϵ_ω. To introduce more notation, $\vec{x} = r(n_x, n_y, n_z) = r\hat{n}$, where $1 = n_x^2 + n_y^2 + n_z^2$. In the radiative limit, the geometric expansion term is

$$\vec{\beta}_\pm \cdot \hat{n}_\pm = \vec{\beta}_\pm \cdot \left(\frac{\vec{x} - \vec{x}_\pm}{R_\pm}\right) = \vec{\beta}_\pm \cdot \hat{n} + \mathcal{O}\left(\frac{a}{r}\right) = \mp\epsilon_\omega(n_x \sin(\omega t_\pm) - n_y \cos(\omega t_\pm)). \tag{3.54}$$

Time retardation from multiple sources introduces $t_\pm$, which can be expanded via

$$\omega t_\pm = \omega\left(t - \frac{|\vec{r} - \vec{x}_\pm|}{c}\right) = \omega t_{\rm ave} \pm \epsilon_\omega(n_x \cos(\omega t_\pm) + n_y \sin(\omega t_\pm)), \tag{3.55}$$

which leads to the necessity of expansions of trigonometric functions in terms of $t_{\rm ave}$, where

$$\begin{aligned} \sin(\omega t_\pm) &= \sin(\omega t_{\rm ave}) \pm \epsilon_\omega(n_x \cos^2(\omega t_{\rm ave}) + n_y \sin(\omega t_{\rm ave})\cos(\omega t_{\rm ave}) + \mathcal{O}\left(\epsilon_\omega^2\right), \quad (3.56) \\ \cos(\omega t_\pm) &= \cos(\omega t_{\rm ave}) \mp \epsilon_\omega(n_x \sin(\omega t_{\rm ave})\cos(\omega t_{\rm ave}) + n_y \sin^2(\omega t_{\rm ave})) + \mathcal{O}\left(\epsilon_\omega^2\right). \end{aligned}$$

This allows for the geometric expansion term to be properly expanded,

$$\vec{\beta}_\pm \cdot \hat{n}_\pm = \mp\epsilon_\omega\left(n_x \sin(\omega t_{\rm ave}) - n_y \cos(\omega t_{\rm ave})\right) - \epsilon_\omega^2\left(n_x \cos(\omega t_{\rm ave}) + n_y \sin(\omega t_{\rm ave})\right)^2. \tag{3.57}$$

To lowest order in ϵ_ω, these complications are only needed to properly get the $\kappa\bar{h}^{00}$ scales as $\mathcal{O}(1)$, while $\kappa\bar{h}^{11}$ scales as $\mathcal{O}(\epsilon_\omega^2)$, since

$$\kappa\bar{h}^{\mu\nu} = \sum_{i=\pm}\left[\frac{2Gm}{\gamma c^4 r}(x_i^\mu a_i^\nu + 2v_i^\mu v_i^\nu + a_i^\mu x_i^\nu)\sum_{k=0}^{\infty}(\vec{\beta}_i \cdot \hat{n}_i)^k\right]. \tag{3.58}$$

As such, $\bar{h}^{11}$ only needs the $k = 0$ terms to lowest order, while $\bar{h}^{00}$ needs terms up to $k = 2$. Introducing the shorthand notation of $c_n \equiv \cos(n\omega t_{\text{ave}})$ and $s_n \equiv \sin(n\omega t_{\text{ave}})$, the radiative field to lowest nontrivial order in ϵ_ω is found by dropping the simple $1/r$ term in $\kappa\bar{h}^{00}$ corresponding to the Newtonian potential,

$$\kappa\bar{h}^{\mu\nu} = \frac{8Gm\gamma}{c^2 r}\epsilon_\omega^2 \begin{pmatrix} -(n_x^2 - n_y^2)c_2 - 2n_x n_y s_2 & -\frac{1}{2}(n_x(1+c_2) + n_y s_2) & -\frac{1}{2}(n_x s_2 + n_y(1-c_2)) & 0 \\ -\frac{1}{2}(n_x(1+c_2) + n_y s_2) & -c_2 & -s_2 & 0 \\ -\frac{1}{2}(n_x s_2 + n_y(1-c_2)) & -s_2 & c_2 & 0 \\ 0 & 0 & 0 & 0 \end{pmatrix}. \tag{3.59}$$

Since this result is in the harmonic gauge, the projector in Eq. (3.18) can be used to find the final result in the transverse-traceless gauge with respect to the z-axis, giving

$$\kappa\bar{h}_{ij}^{TT} = -\frac{8Gm\gamma}{c^2 r}\epsilon_\omega^2 \begin{pmatrix} c_2 & s_2 & 0 \\ s_2 & -c_2 & 0 \\ 0 & 0 & 0 \end{pmatrix}. \tag{3.60}$$

We find that along the z-axis, circularly-polarized gravitational waves are found. By construction, this generalization of the Lienard-Wiechert potential agrees precisely with the quadrupole moment method.

3.3.2 Two-Mass Oscillating Spring System (Weber Bar)

Consider two point particles denoted by trajectories $\vec{x}_+(t)$ and $\vec{x}_-(t)$ with mass m connected by a spring, which are a distance l_0 away from each other, on average. We will assume that they are oscillating at a frequency ω with an amplitude of oscillation A. Since the energy of the emitted gravitational waves is extremely small, we will assume that the amplitude and frequency remain constant over time, similar to the previous example. The position of the particles as a function of time is given by

$$\vec{x}_\pm(t) = \pm\left(\frac{l_0}{2} + A\cos(\omega t)\right)\hat{x}. \tag{3.61}$$

Once again, we will assume that the velocities are nonrelativistic. The velocities and accelerations are given by

$$\begin{aligned}\vec{v}_{\pm}(t) &= \mp A\omega \sin(\omega t)\hat{x},\\ \vec{a}_{\pm}(t) &= \mp A\omega^2 \cos(\omega t)\hat{x}.\end{aligned} \tag{3.62}$$

As we anticipate a simple result in the transverse-traceless gauge, we only look to evaluate the purely spatial components of Eq. (3.41). In the nonrelativistic limit, the denominator $c^3 v_i^\rho R_\rho$ is adequately approximated by $c^4 r$, and the only finite component of $\bar{h}^{ij}$ is

$$\begin{aligned}\kappa\bar{h}^{11} &= \frac{4Gm}{c^4 r}\left(-Al_0\omega^2\cos(\omega t) - 2A^2\omega^2\cos^2(\omega t) + 2A^2\omega^2\sin^2(\omega t)\right)\Big|_{t=t_{\rm ave}},\\ \kappa\bar{h}^{11} &= -\frac{4Gm\omega^2 A}{c^4 r}\left(l_0\cos(\omega t) + 2A\cos(2\omega t)\right)\Big|_{t=t_{\rm ave}},\end{aligned} \tag{3.63}$$

where $t_{\rm ave}$ is an averaged retarded time taken from the center-of-mass of the source. Finally, this term can be projected into the transverse-traceless gauge with respect to the z-axis via Eq. (3.18), such that

$$\bar{h}^{TT}_{jk} = \frac{-2Gm\omega^2}{c^4 r}(2A^2\cos(2\omega t_{\rm ave}) + Al_0\cos(\omega t_{\rm ave}))\begin{pmatrix}1 & 0 & 0\\ 0 & -1 & 0\\ 0 & 0 & 0\end{pmatrix}. \tag{3.64}$$

We find that the gravitational waves are linearly polarized in the "plus" orientation. Note that this result has radiation with modes of frequency ω and 2ω.

This chapter has demonstrated that there is a connection between electrodynamics and linearized gravity for radiating point particles via the Lienard-Wiechert potential and its appropriate generalization. Qualitatively analogous to color-kinematics duality, a simplified charge-momentum duality was found to connect the two theories. This motivated the introduction of an interacting energy-momentum tensor, which generalizes the commonplace free-particle energy-momentum tensor. The next chapter is dedicated to the study of the radiative double copy for nonlinear theories of gravitation, based off of a slightly different color-kinematics duality.

CHAPTER 4

The Radiative Double Copy for Nonlinear Gravity Theories

This chapter contains a review of the author's publication on the radiative double copy for Einstein-Yang-Mills theory [214]. To start, the diagrammatic formalism from Goldberger and Ridgway [92] is elaborated to allow for radiative Feynman diagrams at lowest order in Section 4.2. Similar to how ghosts were utilized to remove dilatons in Ref. [139], an ansatz for scalar radiation analogous to ghosts are also introduced to remove the dilaton in Section 4.2.2, confirming that the two formalisms allow for dilaton removal. Sections 4.3 and 4.4 conclude with combining concepts in Refs. [92, 134] to compute gravitational radiation for Einstein-Yang-Mills theory via the radiative double copy.

4.1 Introduction

The Lagrangians and equations of motion for gauge and gravity theories appear to be rather different. Nevertheless, there are intriguing double-copy connections between their solutions. This includes the Kawai-Lewellen-Tye (KLT) tree-level relations between gauge and gravity amplitudes in string theory [1] and the Bern-Carrasco-Johansson (BCJ) double-copy relations between diagrams in quantum field theory [30]. The BCJ double-copy relations are based on color-kinematics duality, which gives particularly simple constructions of gravity amplitudes starting from gauge-theory amplitudes.

At tree level the BCJ amplitude relations are proven [31, 32, 35, 36, 215]. Numerous calculations at higher loops provide evidence for the loop-level double-copy conjecture [38, 39, 43, 51] and progress has been made to understand analogous monodromy relations,

extending KLT relations to loop level [56, 57, 60, 61, 64, 216]. Einstein-Yang-Mills scattering amplitudes [69, 80, 217, 218] can also be found via the double copy [66, 78, 79] using the Cachazo-He-Yuan (CHY) formalism [219]. Biadjoint scalar fields can be used to find solutions in Yang-Mills [130], and solutions in a Yang-Mills-biadjoint-scalar theory have been shown to give scattering amplitudes in Einstein-Yang-Mills [72–74].

With the recent experimental detection of gravitational waves by LIGO [184], precision calculational tools for gravitational wave emission are essential. Exploiting color-kinematics duality to relate radiation solutions between Yang-Mills and general relativity is attractive because general relativity is difficult to solve and the double copy has been shown to work for a wide variety of gravity theories [46, 220, 221]. The connection between radiation solutions of gauge theory and gravity has been described recently [90, 91, 125, 126, 131, 133, 139]. The first example of using the radiative double copy to find nonlinear terms in general relativity utilized perturbative Yang-Mills solutions [92]. Similarly a biadjoint scalar field can be used to find Yang-Mills radiation [134].

This chapter builds off the radiative double copy for general relativity found by Goldberger and Ridgway [92] to find gravitational radiation in Einstein-Yang-Mills theory. By comparing the differential equations of the sources and fields in gauge theory and gravity, radiative diagrams are used to represent specific algebraic terms. Solutions in gravity can be found from Yang-Mills theory, and the diagrams with three-point vertices can be computed by stitching lower-order solutions together. At leading order, the trace-reversed metric [222], $\bar{h}^{\mu\nu}$, is a natural double copy of the Yang-Mills potential $A^{\mu a}$ [223]. Motivation for a perturbative double copy can be seen at the Lagrangian level, as the linearized gravity Lagrangian is quite similar to the QED Lagrangian, a linearized version of the Yang-Mills Lagrangian. Similarly, these two theories both have an analogous linearized wave equation. Remarkably, radiation solutions of nonlinear gauge and gravity theories are related, at least when iterated perturbatively. A double copy of Yang-Mills-adjoint-scalar theory is also briefly mentioned, which can recover radiation solutions in Einstein-Maxwell theory.

While this paper focuses on classical solutions that could be calculated with more traditional methods [103, 105, 115, 116, 121–123, 224–226], the hope is that the radiative double

copy could help with difficult calculations that may be more cumbersome to do in general relativity alone. As more experimental data for gravitational radiation is collected, new methods for calculating complicated radiation processes are encouraged.

Section (4.2) focuses on deriving classical Yang-Mills radiation, gravitational radiation in general relativity with and without a dilaton coupled to matter, and how the radiative double copy can be used to recover these results from Yang-Mills solutions. Section (4.3) calculates radiation in Yang-Mills-biadjoint-scalar theory. Section (4.4) calculates radiation in Einstein-Yang-Mills theory and the double copy is confirmed by direct calculation. Section (A.2) calculates details of the gravitational contribution to the energy momentum pseudotensor and Section (A.3) gives radiative Feynman rules for simple diagrams with three-point vertices.

4.2 Radiative Double Copy of Yang-Mills and General Relativity

In this section, the non-Abelian Yang-Mills radiation field $A^{\mu a}$ is derived for N colliding point particles. Similarly, the gravitational radiation field $\bar{h}^{\mu\nu}$ is found in general relativity for the same initial conditions. Following Ref. [92], replacement rules are used to find gravitational radiation from Yang-Mills via a radiative double copy. We conclude with some brief remarks on replacement rules for ghost fields to remove the dilaton exchange in the radiative double copy, which is similar to what was found in Ref. [139].

4.2.1 Radiation in Yang-Mills

The Yang-Mills Lagrangian,

$$\mathcal{L} = -\frac{1}{4}F^a_{\mu\nu}F^{\mu\nu a} - gJ^{\mu a}A^a_\mu, \tag{4.1}$$

is in terms of the non-Abelian field strength,

$$F^a_{\mu\nu}(x) = \partial_\mu A^a_\nu(x) - \partial_\nu A^a_\mu(x) - gf^{abc}A^b_\mu(x)A^c_\nu(x), \tag{4.2}$$

where the the mostly minus metric will be used, such that

$$\eta^{\mu\nu} = \mathrm{diag}(1, -1, -1, -1). \tag{4.3}$$

The covariant derivative is defined as

$$D_\mu A^a_\nu(x) = \partial_\mu A^a_\nu(x) - g f^{abc} A^b_\mu(x) A^c_\nu(x). \tag{4.4}$$

Using the covariant derivative, the equations of motion for the non-Abelian field sourced by a current $J^{\mu a}$ are

$$D_\mu F^{\mu\nu a}(x) = J^{\nu a}(x). \tag{4.5}$$

We look to calculate the radiation created from the collision of N charged particles, which is sourced by the current

$$J^{\mu a}(x) = g \sum_{\alpha=1}^{N} \int d\tau v^\mu_\alpha(\tau) c^a_\alpha(\tau) \delta^d(x - x_\alpha(\tau)), \tag{4.6}$$

where α is a particle number label, $v^\mu_\alpha(\tau) = \frac{dx^\mu_\alpha(\tau)}{d\tau}$ is the velocity, and $c^a_\alpha(\tau)$ is the associated adjoint color charge [227]. The vector source is covariantly conserved, such that $D_\mu J^{\mu a} = 0$. In order to solve the equations of motion for the source above, it helps to choose the Lorenz gauge $\partial_\mu A^{\mu a} = 0$. It also is convenient to define a pseudovector $\hat{J}^{\mu a} = J^{\mu a} + j^{\mu a}$ which is locally conserved and is the source for a simple wave equation, such that

$$\Box A^{\mu a} = \hat{J}^{\mu a}, \qquad \partial_\mu \hat{J}^{\mu a} = 0. \tag{4.7}$$

In the Lorenz gauge, the gauge-dependent pseudovector is found by manipulating Eq. (4.5) to give

$$j^{\mu a} = g f^{abc} A^b_\nu (\partial^\nu A^{\mu c} + F^{\nu \mu c}), \tag{4.8}$$

where $\hat{J}^{\mu a} = J^{\mu a} + j^{\mu a}$ is the entire pseudovector, and $j^{\mu a}$ contains the contributions above from the non-Abelian field.

Next, the initial conditions of the particles at $\tau \to -\infty$ are chosen to be $x^\mu_\alpha(\tau) = b^\mu_\alpha + v^\mu_\alpha \tau$, where $b^\mu_{\alpha\beta} = b^\mu_\alpha - b^\mu_\beta$ is an impact parameter, and v^μ_α is the initial velocity, taken to be a constant. At arbitrary times near and after the collision,

$$x^\mu_\alpha(\tau) = b^\mu_\alpha + v^\mu_\alpha \tau + z^\mu_\alpha(\tau), \tag{4.9}$$

where $z^\mu_\alpha(\tau)$ is the deflection to the trajectory due to the fields created by the other particles. Since the deflections introduce acceleration into the trajectories, they produce a radiation

field. In the weak-field limit, the sources are assumed to be nonrelativistic such that they predominately have four-velocities in the time direction and $v_\alpha^2 \approx 1$. Similarly, the color charges are given by

$$c_\alpha^a(\tau) = c_\alpha^a + \bar{c}_\alpha^a(\tau), \tag{4.10}$$

where c_α^a is the initial charge, and $\bar{c}_\alpha^a(\tau)$ is the deflection of the charge due to the interacting fields.

The classical equations of motion for momenta and charges in a Dirac-Yang-Mills system can be found from Hamilton's equations [228]. The internal spin of the Dirac fermions will be neglected, as this would introduce new effective matter interactions [229, 230]. Fortunately, the equations of motion found for Dirac fermions also are valid for Klein-Gordon scalars without spin. The following equations can be used to solve for $z_\alpha^\mu(\tau)$ and $c_\alpha^a(\tau)$, which are

$$\begin{aligned} m_\alpha \frac{d^2 z_\alpha^\mu(\tau)}{d\tau^2} &= g c_\alpha^a(\tau) F^{\mu\nu a}(x_\alpha(\tau)) v_{\alpha\nu}(\tau), \\ \frac{dc_\alpha^a(\tau)}{d\tau} &= g f^{abc} v_\alpha^\mu(\tau) A_\mu^b(x_\alpha(\tau)) c_\alpha^c(\tau). \end{aligned} \tag{4.11}$$

The radiation field is solved iteratively by finding the lowest-order field, correcting the sources, and finding the radiation field created by these corrections and interactions between the lowest-order field. First, the lowest-order sources are specified in momentum space,

$$\begin{aligned} \hat{J}^{\mu a}(k)|_{\mathcal{O}(g^1)} &= \int d^d x e^{ik\cdot x} \hat{J}(x)|_{\mathcal{O}(g^1)} = \int d^d x e^{ik\cdot x} g \sum_{\alpha=1}^N \int d\tau c_\alpha^a v_\alpha^\mu \delta^d(x - x_\alpha(\tau)) \\ &= g \sum_{\alpha=1}^N \int d\tau e^{ik\cdot(b_\alpha + v_\alpha \tau)} c_\alpha^a v_\alpha^\mu = g \sum_{\alpha=1}^N e^{ik\cdot b_\alpha} (2\pi)\delta(k\cdot v_\alpha) c_\alpha^a v_\alpha^\mu, \end{aligned} \tag{4.12}$$

which can be utilized to find the fields to lowest order, giving

$$\begin{aligned} A^{\mu a}(x)|_{\mathcal{O}(g^1)} &= \Box^{-1} \hat{J}^{\mu a}(x)|_{\mathcal{O}(g^1)} = \int_l \frac{-1}{l^2} e^{-il\cdot x} \hat{J}^{\mu a}(l)|_{\mathcal{O}(g^1)} \\ &= -g \sum_{\alpha=1}^N \int_l (2\pi)\delta(l\cdot v_\alpha) \frac{e^{-il\cdot(x - b_\alpha)}}{l^2} v_\alpha^\mu c_\alpha^a, \end{aligned} \tag{4.13}$$

where $\int_l \equiv \int \frac{d^d l}{(2\pi)^d}$ and l is chosen as a momentum variable for the lowest-order fields, as k will be reserved for the momentum of the radiation field. These fields above do not give radiation, since the sources are from charges that are moving at constant velocity.

The lowest-order field can be used to find the deflections of the sources, given by

$$m_\alpha \frac{d^2 z_\alpha^\mu(\tau)}{d\tau^2}\bigg|_{\mathcal{O}(g^2)} = g c_\alpha^a \left(\partial^\mu A^{\nu a}(x_\alpha(\tau))|_{\mathcal{O}(g^1)} - \partial^\nu A^{\mu a}(x_\alpha(\tau))|_{\mathcal{O}(g^1)}\right) v_{\alpha\nu}. \tag{4.14}$$

The derivative of the lowest-order field acting on the particle associated with m_α is

$$\partial^\mu A^{\nu a}(x)|_{\mathcal{O}(g^1)} = -g \sum_{\beta\neq\alpha} \int_l (2\pi)\delta(l\cdot v_\beta)(-il^\mu)\frac{e^{-il\cdot(x-b_\beta)}}{l^2} v_\beta^\nu c_\beta^a. \tag{4.15}$$

Plugging in the derivative of the lowest-order field from above gives

$$m_\alpha \frac{d^2 z_\alpha^\mu(\tau)}{d\tau^2}\bigg|_{\mathcal{O}(g^2)} = ig^2 \sum_{\beta\neq\alpha} c_\alpha^a c_\beta^a \int_l (2\pi)\delta(l\cdot v_\beta)\frac{e^{-il\cdot(b_{\alpha\beta}+v_\alpha\tau)}}{l^2}\left[(v_\alpha\cdot v_\beta)l^\mu - (v_\alpha\cdot l)v_\beta^\mu\right]. \tag{4.16}$$

Similarly for the color charges, their first correction to second order in g is given by

$$\frac{d\bar{c}_\alpha^a(\tau)}{d\tau}\bigg|_{\mathcal{O}(g^2)} = g f^{abc} v_\alpha^\mu A_\mu^b(x_\alpha(\tau))|_{\mathcal{O}(g^1)} c_\alpha^c. \tag{4.17}$$

Once again, plugging in the lowest-order field gives

$$\frac{d\bar{c}_\alpha^a(\tau)}{d\tau}\bigg|_{\mathcal{O}(g^2)} = -g^2 \sum_{\beta\neq\alpha} f^{abc} c_\beta^b c_\alpha^c (v_\alpha\cdot v_\beta)\int_l (2\pi)\delta(l\cdot v_\beta)\frac{e^{-il\cdot(b_{\alpha\beta}+v_\alpha\tau)}}{l^2}. \tag{4.18}$$

Now that the lowest-order field and the charge/momentum deflections have been found, the pseudovector $\hat{J}^{\mu a}$ can be found to next order, which sources the radiation field. The pseudovector may be found algebraically and is also represented diagrammatically in Fig. (4.1). Diagrams (1a) and (1b) are associated with $J^{\mu a}$, and diagram (1c) is associated with $j^{\mu a}$, such that the three diagrams add to give $\hat{J}^{\mu a}$. The matter propagators in the first two diagrams should not have the typical rules associated with Feynman diagrams seen in scattering amplitudes, as a worldline propagator associated with τ and not x^μ would be needed to deal with the radiation emitted along the entire trajectory.[1] Scattering amplitudes do not have this complication, as particle emission is studied at a localized point in time, rather than a continuous radiative field emission.

In this section, the radiation is found algebraically. In Section (A.3), the diagrammatic approach is used to calculate (1c) by stitching two lowest-order field solutions with the three-point vertex, which agrees precisely with the algebraic result found below.

[1]The author became aware of this through discussions with Jed Thompson.

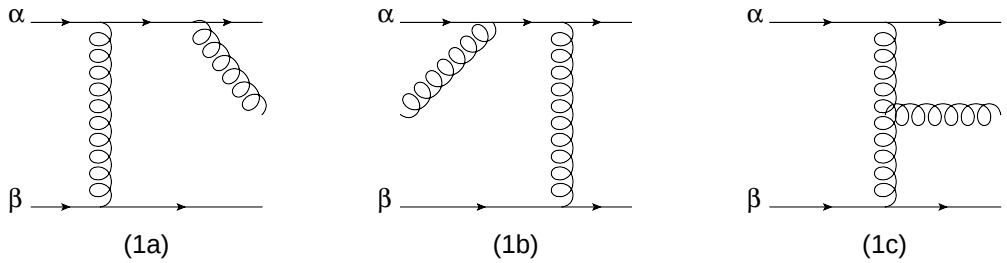

Figure 4.1: Schematic radiative diagrams are shown above. Diagrams (1a) and (1b) correspond to $J^{\mu a}$, the radiation from the deflection of the sources. Diagram (1c) corresponds to $j^{\mu a}$, the radiation from the nonlinear gluon interactions. The three radiative diagrams sum to give $\hat{J}^{\mu a}$, the total pseudovector source for radiation. Solid lines represent scalar matter fields and curly lines represent Yang-Mills fields.

Expanding Eq. (4.6) gives $J^{\mu a}$ to next order. Taking the Fourier transform and integrating over the delta function gives

$$J^{\mu a}(k) = g \sum_{\alpha=1}^{N} \int d\tau e^{ik\cdot(b_\alpha + v_\alpha \tau + z_\alpha(\tau))} \left(v_\alpha^\mu + \frac{dz_\alpha^\mu(\tau)}{d\tau} \right) (c_\alpha^a + \bar{c}_\alpha^a(\tau)) \,. \tag{4.19}$$

Expanding to next-to-leading order will be to first order in the deflections z_α^μ and $\bar{c}_\alpha^a$, giving

$$J^{\mu a}(k) = g \sum_{\alpha=1}^{N} \int d\tau e^{ik\cdot(b_\alpha + v_\alpha \tau)} \left((1 + ik\cdot z_\alpha(\tau)) v_\alpha^\mu c_\alpha^a + v_\alpha^\mu \bar{c}_\alpha^a(\tau) + \frac{dz_\alpha^\mu(\tau)}{d\tau} c_\alpha^a + \mathcal{O}(g^4) \right). \tag{4.20}$$

The following next-order terms are sources for radiation, giving

$$J^{\mu a}(k)|_{\mathcal{O}(g^3)} = g \sum_{\alpha=1}^{N} \int d\tau e^{ik\cdot(b_\alpha + v_\alpha \tau)} \left(ik\cdot z_\alpha(\tau) v_\alpha^\mu c_\alpha^a + v_\alpha^\mu \bar{c}_\alpha^a(\tau) + \frac{dz_\alpha^\mu(\tau)}{d\tau} c_\alpha^a \right), \tag{4.21}$$

where the source for radiation omits the lowest-order term proportional to $v_\alpha^\mu c_\alpha^a$.

To define which terms correspond to diagrams (1a) and (1b), respectively, it helps to think about expanding $f(\tau) \equiv e^{ik\cdot z_\alpha(\tau)}$ and $g(\tau) \equiv v_\alpha^\mu(\tau) c_\alpha^a(\tau)$ separately, such that $f_0 = 1$, $f_1(\tau) = ik\cdot z_\alpha(\tau)$, $g_0 = v_\alpha^\mu c_\alpha^a$, and $g_1(\tau) = \frac{dz_\alpha(\tau)}{d\tau} c_\alpha^a + v_\alpha^\mu \bar{c}_\alpha^a(\tau)$. To lowest order, two terms $f_0 g_1(\tau)$ and $f_1(\tau) g_0$ are needed. The interpretation is that sources containing $f_0 g_1(\tau)$ refer to radiation that was emitted after the force interaction between particles α and β, and sources proportional to $f_1(\tau) g_0$ refer to radiation that was emitted before the force

interaction occurred, such that they can be separated into two diagrams given by

$$\begin{aligned}(1a)^{\mu a} &\equiv g\sum_{\alpha=1}^{N}\int d\tau e^{ik\cdot(b_\alpha+v_\alpha\tau)}\left(v_\alpha^\mu \bar{c}_\alpha^a(\tau)+\frac{dz_\alpha^\mu(\tau)}{d\tau}c_\alpha^a\right),\\ (1b)^{\mu a} &\equiv g\sum_{\alpha=1}^{N}\int d\tau e^{ik\cdot(b_\alpha+v_\alpha\tau)}\left(ik\cdot z_\alpha(\tau)v_\alpha^\mu c_\alpha^a\right).\end{aligned} \tag{4.22}$$

These diagrams have sensible uncontracted indices, as (1a) contains radiation resulting from shifts $\frac{dz_\alpha^\mu}{d\tau}$ and $\bar{c}_\alpha^a$, while (1b) emits a gauge boson before correcting the position and therefore should be proportional to $v_\alpha^\mu c_\alpha^a$. The first two diagrams will be used as a heuristic guide, and investigation of the worldline propagator will be postponed to later work.

Integrating Eqs. (4.16) and (4.18) results in dividing by $-ik\cdot v_\alpha$, since the source integrates over τ and sets $l_\beta\cdot v_\alpha = k\cdot v_\alpha$. To more easily combine these results with diagram (1c), an extra integral over l_α with a momentum conserving delta function is added and $l\to l_\beta$, such that $k^\mu = l_\alpha^\mu + l_\beta^\mu$ and

$$\begin{aligned}J^{\mu a}(k)|_{\mathcal{O}(g^3)} &= g^3\sum_{\substack{\alpha=1\\ \beta\neq\alpha}}^{N}\int_{l_\alpha,l_\beta}\mu_{\alpha,\beta}(k)\frac{l_\alpha^2}{k\cdot v_\alpha}\Big[if^{abc}c_\alpha^b c_\beta^c(v_\alpha\cdot v_\beta)v_\alpha^\mu\\ &\quad+\frac{c_\alpha^b c_\beta^b}{m_\alpha}c_\alpha^a\left\{-v_\alpha\cdot v_\beta\left(l_\beta^\mu-\frac{k\cdot l_\beta}{k\cdot v_\alpha}v_\alpha^\mu\right)+k\cdot v_\alpha v_\beta^\mu-k\cdot v_\beta v_\alpha^\mu\right\}\Big],\end{aligned} \tag{4.23}$$

where $\mu_{\alpha,\beta}(k)$ will be used frequently and is given by

$$\mu_{\alpha,\beta}(k)=\left[(2\pi)\delta(v_\alpha\cdot l_\alpha)\frac{e^{il_\alpha\cdot b_\alpha}}{l_\alpha^2}\right]\left[(2\pi)\delta(v_\beta\cdot l_\beta)\frac{e^{il_\beta\cdot b_\beta}}{l_\beta^2}\right](2\pi)^d\delta^d(k-l_\alpha-l_\beta). \tag{4.24}$$

Next, contributions to diagram (1c) are found from $j^{\mu a}$ in Eq. (4.8), giving

$$\begin{aligned}j^{\mu a}(k) &= gf^{abc}\int d^dx e^{ik\cdot x}A_\nu^b(x)\left(\partial^\nu A^{\mu c}(x)-F^{\mu\nu c}(x)\right)\\ j^{\mu a}(k)|_{\mathcal{O}(g^3)} &= gf^{abc}\int d^dx e^{ik\cdot x}A_\nu^b(x)|_{\mathcal{O}(g^1)}\left(2\partial^\nu A^{\mu c}(x)|_{\mathcal{O}(g^1)}-\partial^\mu A^{\nu c}(x)|_{\mathcal{O}(g^1)}\right),\end{aligned} \tag{4.25}$$

Plugging in the lowest-order field solution gives

$$j^{\mu a}(k)_{\mathcal{O}(g^3)} = g^3\sum_{\substack{\alpha=1\\ \beta\neq\alpha}}^{N}if^{abc}c_\alpha^b c_\beta^c\int_{l_\alpha,l_\beta}\mu_{\alpha,\beta}(k)\left[2k\cdot v_\beta v_\alpha^\mu - v_\alpha\cdot v_\beta l_\alpha^\mu\right], \tag{4.26}$$

where the dummy indices α and β were switched to obtain this result.

The pseudovector $\hat{J}^{\mu a}(k)$ can be found by summing $J^{\mu a}$ and $j^{\mu a}$, giving

$$\begin{aligned}\hat{J}^{\mu a}(k)|_{\mathcal{O}(g^3)} &= g^3 \sum_{\substack{\alpha=1 \\ \beta\neq\alpha}}^{N} \int_{l_\alpha, l_\beta} \mu_{\alpha,\beta}(k) \left[i f^{abc} c_\alpha^b c_\beta^c \left\{ 2(k\cdot v_\beta) v_\alpha^\mu + (v_\alpha \cdot v_\beta) \left(\frac{l_\alpha^2}{k\cdot v_\alpha} v_\alpha^\mu - l_\alpha^\mu \right) \right\} \right. \\ &\quad \left. + \frac{c_\alpha^b c_\beta^b}{m_\alpha} \frac{l_\alpha^2 c_\alpha^a}{k\cdot v_\alpha} \left\{ v_\alpha \cdot v_\beta \left(\frac{k\cdot l_\beta}{k\cdot v_\alpha} v_\alpha^\mu - l_\beta^\mu \right) + k\cdot v_\alpha v_\beta^\mu - k\cdot v_\beta v_\alpha^\mu \right\} \right]. \end{aligned} \tag{4.27}$$

To find the radiation field $A^{\mu a}_{\text{rad}}$ from the source $\hat{J}^{\mu a}$ [200],

$$A^{\mu a}_{\text{rad}}(x) = \frac{1}{4\pi r} \int \frac{d\omega}{2\pi} e^{-i\omega t} \hat{J}^{\mu a}(k), \tag{4.28}$$

where $k^\mu = \omega(1, \vec{x}/r)$.

4.2.2 Radiation in General Relativity with a Dilaton

Next, we find the radiation field $\bar{h}^{\mu\nu}$ in general relativity with matter coupled to a dilaton, which will be shown later to agree with the radiative double copy [92]. The action is given by

$$S = \int d^d x \left[-\frac{2}{\kappa^2} \sqrt{-g} R + \frac{2}{\kappa^2} (d-2) \sqrt{-g} g^{\mu\nu} \partial_\mu \phi \partial_\nu \phi \right] - m \int d\tau e^\phi, \tag{4.29}$$

where ϕ is the dilaton field and $d\tau = \sqrt{g_{\mu\nu} dx^\mu dx^\nu}$. This action also leaves out the coupling of $T^{\mu\nu}$ with the gravitational field. Since Einstein's field equations,

$$R^{\mu\nu} - \frac{1}{2} g^{\mu\nu} R = 8\pi G T^{\mu\nu}, \tag{4.30}$$

naturally contain the energy-momentum tensor, the Einstein-dilaton field equations can be found by varying the action in Eq. (4.29), giving

$$8\pi G T^{\mu\nu} = R^{\mu\nu} - \frac{1}{2} g^{\mu\nu} R - (d-2) \left(\partial^\mu \phi \partial^\nu \phi - \frac{1}{2} g^{\mu\nu} g^{\rho\sigma} \partial_\rho \phi \partial_\sigma \phi \right). \tag{4.31}$$

For a classical particle in the absence of gravity, the energy-momentum tensor $T^{\mu\nu}$ is

$$T^{\mu\nu}(x) = \sum_{\alpha=1}^{N} m_\alpha \int d\tau v_\alpha^\mu(\tau) v_\alpha^\nu(\tau) \delta^d(x - x_\alpha(\tau)), \tag{4.32}$$

where this tensor is only locally conserved when all of the particles collide precisely at a point.

To study gravitational interactions, a locally conserved pseudotensor is often introduced. According to Dirac's interpretation, $\sqrt{|g|}T^{\mu\nu}$ is the density and flux of energy and momentum for matter in general relativity [231] such that in the presence of gravity,

$$\sqrt{|g|}T^{\mu\nu}(x) = \sum_{\alpha=1}^{N} m_\alpha \int d\tau v_\alpha^\mu(\tau) v_\alpha^\nu(\tau) \delta^d(x - x_\alpha(\tau)). \tag{4.33}$$

A locally conserved energy-momentum pseudotensor $\hat{T}^{\mu\nu}$ will be introduced to include contributions from the gravitational field. A weak-field approximation is taken by introducing $h^{\mu\nu}$ as

$$\begin{aligned} g_{\mu\nu} &= \eta_{\mu\nu} + \kappa h_{\mu\nu}, \\ g^{\mu\nu} &= \eta^{\mu\nu} - \kappa h^{\mu\nu} + \kappa^2 h^{\mu\rho} h_\rho^\nu + \ldots, \\ |g| &\equiv -\det(g_{\mu\nu}) = 1 + \kappa h - \frac{\kappa^2}{2}(h^{\mu\nu} h_{\mu\nu} - h^2) + \ldots, \end{aligned} \tag{4.34}$$

where the radiation can be calculated perturbatively in powers of κ and $h \equiv h_\rho^\rho$. To lowest order, the weak-field approximation gives a linearized wave equation, except the D'Alembertian operator does not simply act on $h_{\mu\nu}$. Textbook presentations of gravitational waves often focus on linearized gravity [222], which introduces the trace-reversed metric,

$$\bar{h}_{\mu\nu} \equiv h_{\mu\nu} - \frac{1}{2}\eta_{\mu\nu} h, \tag{4.35}$$

and find that $\Box \bar{h}^{\mu\nu} = -\frac{\kappa}{2} T^{\mu\nu}$. However, this equation is only an approximation of general relativity and does not pick up the nonlinear aspects. Post-Newtonian approximation methods [103, 138] often use a harmonic gravitational field or harmonic metric

$$\kappa \hat{h}^{\mu\nu} \equiv \eta^{\mu\nu} - \sqrt{|g|} g^{\mu\nu}, \tag{4.36}$$

which is subject to the harmonic gauge condition $\partial_\mu \hat{h}^{\mu\nu} = 0$. In terms of relating $\hat{h}^{\mu\nu}$ and $\bar{h}^{\mu\nu}$,

$$\kappa \hat{h}^{\mu\nu} = \eta^{\mu\nu} - \sqrt{|g|}\left(\eta^{\mu\nu} - \kappa h^{\mu\nu} + \mathcal{O}(h^2)\right) = \left(1 - \sqrt{|g|}\right)\eta^{\mu\nu} + \sqrt{|g|}\kappa h^{\mu\nu} + \mathcal{O}(h^2), \tag{4.37}$$

and the lowest-order term in $\hat{h}^{\mu\nu}$ is given by $\bar{h}^{\mu\nu}$. If an effective energy-momentum pseudotensor $\hat{T}^{\mu\nu}$ was found to contain contributions from matter and gravitational fields, then

the following equation of motion can be solved iteratively within the context of the post-Newtonian approximation

$$\Box \bar{h}^{\mu\nu} = -\frac{\kappa}{2}\hat{T}^{\mu\nu}. \tag{4.38}$$

Due to the harmonic gauge condition, it is essential that the pseudotensor satisfies $\partial_\mu \hat{T}^{\mu\nu} = 0$. The gravitational contributions to the pseudotensor $t^{\mu\nu}$ will be found from expanding Einstein's field equations. This slightly differs from the common pseudotensor used by Landau and Lifshitz [103, 222, 232] and is closer to ones used previously by Einstein and Dirac. The properly conserved pseudotensor is given by

$$\hat{T}^{\mu\nu} = T^{\mu\nu} + t^{\mu\nu} \equiv \sqrt{|g|}T^{\mu\nu} + \hat{t}^{\mu\nu}, \tag{4.39}$$

where $\hat{t}^{\mu\nu}$ is conveniently defined to absorb $(1 - \sqrt{|g|})T^{\mu\nu}$. In this section, the algebraic method of perturbing Einstein's field equations and iteratively solving for the radiation field is presented, leaving some technical details of the calculation of $\hat{t}^{\mu\nu}$ to Section (A.2). Since the three-point graviton vertex is derived from the Lagrangian of the full theory, diagrams can encode how to find higher order field contributions from linearized field solutions. In Section (A.3), radiative Feynman rules are provided for the three-point vertices. The Christoffel symbol $\Gamma^\rho{}_{\mu\nu}$ and the Ricci tensor $R_{\mu\nu}$ are given by

$$\begin{aligned} \Gamma^\rho{}_{\mu\nu} &= \frac{1}{2}g^{\rho\sigma}(g_{\sigma\nu,\mu} + g_{\sigma\mu,\nu} - g_{\mu\nu,\sigma}), \\ R_{\mu\nu} &= \Gamma^\rho{}_{\mu\nu,\rho} - \Gamma^\rho{}_{\mu\rho,\nu} + \Gamma^\rho{}_{\sigma\rho}\Gamma^\sigma{}_{\mu\nu} - \Gamma^\rho{}_{\sigma\nu}\Gamma^\sigma{}_{\mu\rho}. \end{aligned} \tag{4.40}$$

After expanding the metric perturbatively in κ and applying the gauge condition $\partial^\mu h_{\mu\nu} = \frac{1}{2}\eta_{\mu\nu}h^{,\mu}$,

$$\Gamma^\rho{}_{\mu\nu} = \frac{\kappa}{2}\left(h^\rho_{\nu,\mu} + h^\rho_{\mu,\nu} - h_{\mu\nu,}{}^\rho - \kappa h^{\rho\sigma}(h_{\sigma\nu,\mu} + h_{\sigma\mu,\nu} - h_{\mu\nu,\sigma})\right) + \mathcal{O}(\kappa^3), \tag{4.41}$$

$$\begin{aligned} R_{\mu\nu} = &-\frac{\kappa}{2}\Box h_{\mu\nu} + \frac{\kappa^2}{2}\left[h^{\rho\sigma}(h_{\mu\nu,\rho\sigma} + h_{\rho\sigma,\mu\nu} - h_{\sigma\nu,\mu\rho} - h_{\mu\rho,\sigma\nu})\right. \\ &\left. + h_{\mu\rho,\sigma}h^{\rho,\sigma}_\nu - h_{\mu\rho,\sigma}h^{\sigma,\rho}_\nu + \frac{1}{2}h_{\rho\sigma,\mu}h^{\rho\sigma,}{}_\nu\right] + \mathcal{O}(\kappa^3). \end{aligned} \tag{4.42}$$

This gives the Ricci scalar R,

$$R = (\eta^{\mu\nu} - \kappa h^{\mu\nu})R_{\mu\nu} = -\frac{\kappa}{2}\Box h + \kappa^2\left(h^{\rho\sigma}\Box h_{\rho\sigma} + \frac{3}{4}h^{\rho\sigma,\mu}h_{\rho\sigma,\mu} - \frac{1}{2}h^{\mu\rho,\sigma}h_{\mu\sigma,\rho}\right) + \mathcal{O}(\kappa^3), \tag{4.43}$$

Plugging these results into the Einstein-dilaton field equations, Eq. (4.31), gives

$$\begin{aligned}\left(\frac{\kappa}{2}\right)^2 T_{\mu\nu} &= -\frac{\kappa}{2}\Box\bar{h}_{\mu\nu} + \frac{\kappa^2}{2}\Big[\, h^{\rho\sigma}(h_{\mu\nu,\rho\sigma} + h_{\rho\sigma,\mu\nu} - h_{\sigma\nu,\mu\rho} - h_{\mu\rho,\sigma\nu}) \\ &\quad + h_{\mu\rho,\sigma}h_{\nu}^{\rho,\sigma} - h_{\mu\rho,\sigma}h_{\nu}^{\sigma,\rho} + \frac{1}{2}h_{\rho\sigma,\mu}h^{\rho\sigma,}{}_{\nu} + \frac{1}{2}h_{\mu\nu}\Box h \\ &\quad - \eta_{\mu\nu}\left(h^{\rho\sigma}\Box h_{\rho\sigma} + \frac{3}{4}h^{\rho\sigma,\lambda}h_{\rho\sigma,\lambda} - \frac{1}{2}h^{\lambda\rho,\sigma}h_{\lambda\sigma,\rho}\right)\Big] \\ &\quad - (d-2)\left(\partial_\mu\phi\partial_\nu\phi - \frac{1}{2}\eta_{\mu\nu}\partial_\rho\phi\partial^\rho\phi + \frac{\kappa}{2}\left(\eta_{\mu\nu}h^{\rho\sigma}\partial_\rho\phi\partial_\sigma\phi - h_{\mu\nu}\partial_\rho\phi\partial^\rho\phi\right)\right) + \mathcal{O}(\kappa^3),\end{aligned} \tag{4.44}$$

where all indices have been contracted with the flat spacetime metric $\eta_{\rho\sigma}$. Some care is needed, since $T^{\mu\nu}$ and $T_{\mu\nu}$ still are raised and lowered with the full metric $g_{\mu\nu}$. In order to derive the correct pseudotensor $\hat{T}^{\mu\nu}$ in a way that is compatible with these index contraction conventions, it helps to find $G^{\mu\nu} = R^{\mu\nu} - \frac{1}{2}g^{\mu\nu}R$ rather than $G_{\mu\nu}$. The lower order term corresponds to $-\frac{\kappa}{2}\Box\bar{h}^{\mu\nu}$, and the rest acts as a piece of the contribution to $t^{\mu\nu}$. Raising the indices of $T^{\mu\nu}$ with $g^{\mu\nu}$ and expanding $g^{\mu\nu}$ to include extra terms in $h^{\mu\nu}$ and splitting the $\mathcal{O}(\kappa^2)$ terms between $t^{\mu\nu}|_{\Delta h}$ and $t^{\mu\nu}|_{\Delta\phi}$ gives

$$\begin{aligned}t^{\mu\nu}|_{\Delta h} &= 2h_{\rho\sigma}\left(h^{\mu\rho,\nu\sigma} + h^{\nu\sigma,\mu\rho} - h^{\mu\nu,\rho\sigma} - h^{\rho\sigma,\mu\nu}\right) + h^{\mu\nu}\Box h - 2h^{\mu\rho}\Box h_{\rho}^{\nu} - 2h^{\nu\rho}\Box h_{\rho}^{\mu} \\ &\quad - 2h^{\mu\rho,\sigma}\left(h_{\rho,\sigma}^{\nu} - h_{\sigma,\rho}^{\nu}\right) - h^{\rho\sigma,\mu}h_{\rho\sigma,}{}^{\nu} + \eta^{\mu\nu}\left[2h^{\rho\sigma}\Box h_{\rho\sigma} + h_{\rho\sigma,\lambda}\left(\frac{3}{2}h^{\rho\sigma,\lambda} - h^{\rho\lambda,\sigma}\right)\right], \\ t^{\mu\nu}|_{\Delta\phi} &= (d-2)\left(\frac{2}{\kappa}\right)^2\left(\partial^\mu\phi\partial^\nu\phi - \frac{1}{2}\eta^{\mu\nu}\partial_\rho\phi\partial^\rho\phi\right),\end{aligned} \tag{4.45}$$

where

$$\left(\frac{\kappa}{2}\right)^2 T^{\mu\nu} = -\frac{\kappa}{2}\left(\Box\bar{h}^{\mu\nu} + \frac{\kappa}{2}t^{\mu\nu}\right). \tag{4.46}$$

The pseudotensor $\hat{T}_{\mu\nu}$ can be defined by bringing all terms of order κ^2 to the other side of the equation, with the harmonic gauge condition $\partial_\mu\bar{h}^{\mu\nu} = 0$ and Eq. (4.38) satisfied.

The radiative Feynman diagrams separate $\hat{T}^{\mu\nu}$ into six pieces. Similar to the Yang-Mills calculation, $\hat{T}^{\mu\nu} = \sqrt{|g|}T^{\mu\nu} + \hat{t}^{\mu\nu}$, where $\hat{t}^{\mu\nu}$ contains all of the nonlinear field content. The graviton and dilaton both contribute to each, $\sqrt{|g|}T^{\mu\nu} = \sqrt{|g|}T^{\mu\nu}|_{\Delta h} + \sqrt{|g|}T^{\mu\nu}|_{\Delta\phi}$ and $\hat{t}^{\mu\nu} = \hat{t}^{\mu\nu}|_{\Delta h} + \hat{t}^{\mu\nu}|_{\Delta\phi}$. Diagrams (2a), (2b), (2c), (2d), (2e), and (2f) are shown in Fig. (4.2).

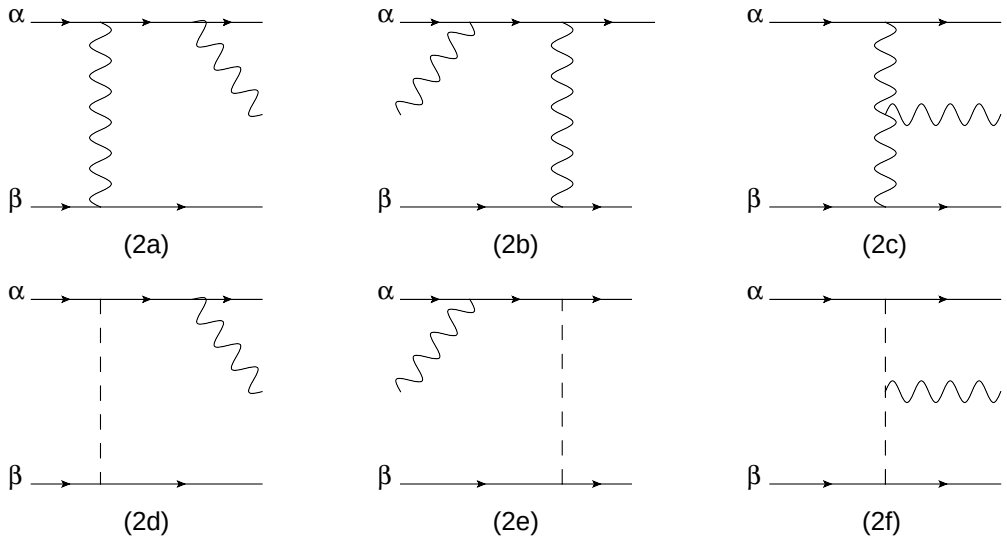

Figure 4.2: (2a) and (2b) correspond to $\sqrt{|g|}T^{\mu\nu}|_{\Delta h}$, (2c) corresponds to $\hat{t}^{\mu\nu}|_{\Delta h}$, (2d) and (2e) correspond to $\sqrt{|g|}T^{\mu\nu}|_{\Delta\phi}$, and (2f) corresponds to $\hat{t}^{\mu\nu}|_{\Delta\phi}$. The sum over all six gives the radiation pseudotensor source $\hat{T}^{\mu\nu}$. Wavy lines represent gravitational fields and dashed lines represent dilaton fields.

Algebraically, the first three diagrams for the pure gravity contributions are

$$\begin{aligned}(2\mathrm{a})^{\mu\nu} + (2b)^{\mu\nu} &= \sqrt{|g|}T^{\mu\nu}|_{\Delta h}, \\ (2\mathrm{c})^{\mu\nu} &= \hat{t}^{\mu\nu}|_{\Delta h} \equiv t^{\mu\nu}|_{\Delta h} + \left(1 - \sqrt{|g|}\right) T^{\mu\nu}|_{\Delta h},\end{aligned} \tag{4.47}$$

while the diagrams with internal dilatons algebraically represent

$$\begin{aligned}(2\mathrm{d})^{\mu\nu} + (2\mathrm{e})^{\mu\nu} &= \sqrt{|g|}T^{\mu\nu}|_{\Delta\phi}, \\ (2\mathrm{f})^{\mu\nu} &= \hat{t}^{\mu\nu}|_{\Delta\phi} \equiv t^{\mu\nu}_{\Delta\phi},\end{aligned} \tag{4.48}$$

where the definition of diagrams (2a), (2b), (2d), and (2e) individually are given by expressions similar to Eq. (4.22), except replacing $c^a_\alpha(\tau)$ with $v^\nu_\alpha(\tau)$ and g with m_α. Furthermore, since $\left(1 - \sqrt{|g|}\right)$ is purely gravitational, $\hat{t}^{\mu\nu}|_{\Delta\phi} \equiv t^{\mu\nu}|_{\Delta\phi}$.

Similar to the previous section, the position of the particle is given by

$$x^\mu_\alpha(\tau) = b^\mu_\alpha + v^\mu_\alpha \tau + z^\mu_\alpha(\tau), \tag{4.49}$$

where now $z^\mu_\alpha(\tau)$ is the correction due to the graviton and dilaton. The Christoffel symbol

can be used to find the force on each particle, giving

$$m_\alpha \frac{d^2 z_\alpha^\mu(\tau)}{d\tau^2}\bigg|_{\Delta h} = -\Gamma^\mu{}_{\nu\rho} m_\alpha v_\alpha^\nu v_\alpha^\rho. \tag{4.50}$$

The equation of motion utilized for the dilaton is

$$m_\alpha \frac{d^2 z_\alpha^\mu(\tau)}{d\tau^2}\bigg|_{\Delta \phi} = m_\alpha v_{\alpha\nu} \partial^\mu \phi v_\alpha^\nu. \tag{4.51}$$

While this equation differs slightly from Ref. [92], both of our total pseudotensors agree and are the physical object that satisfies the gauge-invariant Ward identity. With the equations of motions for the deflections, the four diagrams associated with $\sqrt{|g|}T^{\mu\nu}$ are proportional to

$$\begin{aligned}
(2a)^{\mu\nu}(k) &= \sum_{\alpha=1}^{N} m_\alpha \int d\tau e^{ik\cdot(b_\alpha + v_\alpha \tau)} \left(\frac{dz_\alpha^\mu}{d\tau}\bigg|_{\Delta h} v_\alpha^\nu + v_\alpha^\mu \frac{dz_\alpha^\nu(\tau)}{d\tau}\bigg|_{\Delta h} \right), \\
(2b)^{\mu\nu}(k) &= \sum_{\alpha=1}^{N} m_\alpha \int d\tau e^{ik\cdot(b_\alpha + v_\alpha \tau)} ik\cdot z_\alpha(\tau)|_{\Delta h} v_\alpha^\mu v_\alpha^\nu, \\
(2d)^{\mu\nu}(k) &= \sum_{\alpha=1}^{N} m_\alpha \int d\tau e^{ik\cdot(b_\alpha + v_\alpha \tau)} \left(\frac{dz_\alpha^\mu(\tau)}{d\tau}\bigg|_{\Delta \phi} v_\alpha^\nu + v_\alpha^\mu \frac{dz_\alpha^\nu(\tau)}{d\tau}\bigg|_{\Delta \phi} \right), \\
(2e)^{\mu\nu}(k) &= \sum_{\alpha=1}^{N} m_\alpha \int d\tau e^{ik\cdot(b_\alpha + v_\alpha \tau)} ik\cdot z_\alpha(\tau)|_{\Delta \phi} v_\alpha^\mu v_\alpha^\nu.
\end{aligned} \tag{4.52}$$

However, for the purposes of confirming the validity of the radiative double copy to leading order, it is simple enough to calculate $\sqrt{|g|}T^{\mu\nu}$ as a whole algebraically.

Continuing with the algebraic derivation, the lowest-order solutions can be found, which give the deflections and the radiation field iteratively. These are found from the lowest order of the energy-momentum tensor,

$$\hat{T}^{\mu\nu}(k)|_{\mathcal{O}(\kappa^0)} = \sum_{\alpha=1}^{N} m_\alpha e^{ik\cdot b_\alpha} (2\pi)\delta(k\cdot v_\alpha) v_\alpha^\mu v_\alpha^\nu. \tag{4.53}$$

This source can be used to find the fields $h^{\mu\nu}$ and ϕ to lowest order, giving

$$\begin{aligned}
h^{\mu\nu}(x)|_{\mathcal{O}(\kappa^2)} &= \frac{\kappa}{2} \sum_{\alpha=1}^{N} m_\alpha \int_l (2\pi)\delta(v_\alpha \cdot l) \frac{e^{-il\cdot(x-b_\alpha)}}{l^2} \left(v_\alpha^\mu v_\alpha^\nu - \frac{\eta^{\mu\nu}}{d-2} \right), \\
\phi(x)|_{\mathcal{O}(\kappa^2)} &= \frac{1}{(d-2)} \left(\frac{\kappa}{2}\right)^2 \sum_{\alpha=1}^{N} m_\alpha \int_l (2\pi)\delta(l\cdot v_\alpha) \frac{e^{-il\cdot(x-b_\alpha)}}{l^2}.
\end{aligned} \tag{4.54}$$

Plugging the lowest-order field solutions into the deflections gives

$$\begin{aligned}
\left.\frac{d^2 z_\alpha^\mu(\tau)}{d\tau^2}\right|_{\Delta h} &= i\left(\frac{\kappa}{2}\right)^2 \sum_{\beta\neq\alpha} m_\beta \int_{l_\beta} (2\pi)\delta(l_\beta\cdot v_\beta)\frac{e^{-il_\beta\cdot(x-b_\beta)}}{l_\beta^2} \\
&\quad\times\left[2(v_\alpha\cdot v_\beta)k\cdot v_\alpha v_\beta^\mu - \frac{2k\cdot v_\alpha}{d-2}v_\alpha^\mu - \left((v_\alpha\cdot v_\beta)^2 - \frac{1}{d-2}\right)l_\beta^\mu\right], \\
\left.\frac{d^2 z_\alpha^\mu(\tau)}{d\tau^2}\right|_{\Delta\phi} &= \frac{-i}{d-2}\left(\frac{\kappa}{2}\right)^2 \sum_{\beta\neq\alpha} m_\beta \int_{l_\beta} (2\pi)\delta(l_\beta\cdot v_\beta)\frac{e^{-il_\beta\cdot(x-b_\beta)}}{l_\beta^2} l_\beta^\mu. \qquad (4.55)
\end{aligned}$$

The corrections to the position are useful for finding $\sqrt{|g|}T^{\mu\nu}(k)|_{\mathcal{O}(\kappa^2)}$,

$$\begin{aligned}
\sqrt{|g|}T^{\mu\nu}(k) &= \sum_{\alpha=1}^N m_\alpha \int d\tau e^{ik\cdot(b_\alpha+v_\alpha\tau+z_\alpha(\tau))}\left(v_\alpha^\mu + \frac{dz_\alpha^\mu(\tau)}{d\tau}\right)\left(v_\alpha^\nu + \frac{dz_\alpha^\nu(\tau)}{d\tau}\right), \\
\sqrt{|g|}T^{\mu\nu}(k)|_{\mathcal{O}(\kappa^2)} &= \sum_{\alpha=1}^N m_\alpha \int d\tau e^{ik\cdot(b_\alpha+v_\alpha\tau)}\left[ik\cdot z_\alpha v_\alpha^\mu v_\alpha^\nu + \frac{dz_\alpha^\mu}{d\tau}v_\alpha^\nu + v_\alpha^\mu\frac{dz_\alpha^\nu}{d\tau}\right]. \qquad (4.56)
\end{aligned}$$

Separating the gravity and dilaton contributions gives

$$\begin{aligned}
\sqrt{|g|}T^{\mu\nu}(k)|_{\Delta h} &= \left(\frac{\kappa}{2}\right)^2 \sum_{\alpha\neq\beta} m_\alpha m_\beta \int_{l_\alpha,l_\beta} \mu_{\alpha,\beta}(k) l_\alpha^2 \\
&\quad\times\left[v_\alpha^\mu v_\alpha^\nu\left(2v_\alpha\cdot v_\beta\frac{k\cdot v_\beta}{k\cdot v_\alpha} + \frac{2}{d-2} - \frac{l_\beta\cdot k}{(k\cdot v_\alpha)^2}\left((v_\alpha\cdot v_\beta)^2 - \frac{1}{d-2}\right)\right)\right. \\
&\quad\left. - 2v_\alpha\cdot v_\beta(v_\alpha^\mu v_\beta^\nu + v_\alpha^\nu v_\beta^\mu) + \frac{1}{k\cdot v_\alpha}\left((v_\alpha\cdot v_\beta)^2 - \frac{1}{d-2}\right)(v_\alpha^\mu l_\beta^\nu + v_\alpha^\nu l_\beta^\mu)\right], \\
\sqrt{|g|}T^{\mu\nu}(k)|_{\Delta\phi} &= \frac{1}{d-2}\left(\frac{\kappa}{2}\right)^2 \sum_{\alpha\neq\beta} m_\alpha m_\beta \int_{l_\alpha,l_\beta} \mu_{\alpha,\beta}(k) l_\alpha^2 \\
&\quad\times\left[-v_\alpha^\mu v_\alpha^\nu\left(\frac{l_\beta\cdot k}{(k\cdot v_\alpha)^2}\right) + \frac{1}{k\cdot v_\alpha}(v_\alpha^\mu l_\beta^\nu + v_\alpha^\nu l_\beta^\mu)\right]. \qquad (4.57)
\end{aligned}$$

Adding the two contributions,

$$\begin{aligned}
\sqrt{|g|}T^{\mu\nu}|_{\mathcal{O}(g^2)} &= -\left(\frac{\kappa}{2}\right)^2 \sum_{\substack{\alpha=1\\\beta\neq\alpha}}^N m_\alpha m_\beta \int_{l_\alpha,l_\beta} \mu_{\alpha,\beta}(k) l_\alpha^2 \\
&\quad\times\left[v_\alpha^\mu v_\alpha^\nu\left(\frac{(v_\alpha\cdot v_\beta)^2}{(k\cdot v_\alpha)^2}k\cdot l_\beta - 2v_\alpha\cdot v_\beta\frac{k\cdot v_\beta}{k\cdot v_\alpha} - \frac{2}{(d-2)}\right)\right. \\
&\quad\left. + 2v_\alpha\cdot v_\beta(v_\alpha^\mu v_\beta^\nu + v_\alpha^\nu v_\beta^\mu) - (v_\alpha^\mu l_\beta^\nu + v_\alpha^\nu l_\beta^\mu)\frac{(v_\alpha\cdot v_\beta)^2}{k\cdot v_\alpha}\right]. \qquad (4.58)
\end{aligned}$$

Next, the pseudotensor contribution from fields $\hat{t}^{\mu\nu}$ is calculated from the lowest-order field solutions, as they will multiply and contract together to give higher order corrections.

Starting with $\hat{t}^{\mu\nu}|_{\Delta h}$, the diagram is calculated algebraically in Section (A.2) and also by the radiative Feynman rules outlined in Section (A.3), which found

$$\begin{aligned}\hat{t}^{\mu\nu}(k)|_{\Delta h} &= \left(\frac{\kappa}{2}\right)^2 \sum_{\substack{\alpha=1\\ \beta\neq\alpha}}^{N} m_\alpha m_\beta \int_{l_\alpha, l_\beta} \mu_{\alpha,\beta}(k) \left[2v_\alpha^\mu v_\alpha^\nu \left((k\cdot v_\beta)^2 - \frac{l_\alpha^2}{d-2} \right) \right. \\ &+ \left(v_\alpha^\mu v_\beta^\nu + v_\alpha^\nu v_\beta^\mu\right)\left(l_\alpha^2 v_\alpha\cdot v_\beta - k\cdot v_\alpha k\cdot v_\beta\right) - 2\left(v_\alpha^\mu l_\alpha^\nu + v_\alpha^\nu l_\alpha^\mu\right)\left(v_\alpha\cdot v_\beta k\cdot v_\beta\right) \\ &\left. + l_\alpha^\mu l_\alpha^\mu \left((v_\alpha\cdot v_\beta)^2 - \frac{1}{d-2} \right) + \eta^{\mu\nu}\left(k\cdot v_\alpha k\cdot v_\beta v_\alpha\cdot v_\beta - \frac{l_\alpha^2}{2}\left((v_\alpha\cdot v_\beta)^2 - \frac{1}{d-2} \right) \right) \right].\end{aligned} \tag{4.59}$$

Similarly, the radiative Feynman rules for diagram (2f) agree with the algebraic expression for Eq. (4.48), giving

$$t^{\mu\nu}(k)|_{\Delta\phi} = \frac{1}{(d-2)}\left(\frac{\kappa}{2}\right)^2 \sum_{\substack{\alpha=1\\ \beta\neq\alpha}}^{N} m_\alpha m_\beta \int_{l_\alpha, l_\beta} \mu_{\alpha,\beta}(k) \left[-l_\alpha^\mu l_\beta^\nu + \eta^{\mu\nu}\frac{l_\alpha\cdot l_\beta}{2} \right]. \tag{4.60}$$

Summing the diagrams gives the energy-momentum pseudotensor source for radiation,

$$\begin{aligned}\hat{T}^{\mu\nu} &= \left(\frac{\kappa}{2}\right)^2 \sum_{\substack{\alpha=1\\ \beta\neq\alpha}}^{N} m_\alpha m_\beta \int_{l_\alpha, l_\beta} \mu_{\alpha,\beta}(k) \left[v_\alpha^\mu v_\alpha^\nu \left(2(k\cdot v_\beta)^2 + 2k\cdot v_\beta \frac{l_\alpha^2 v_\alpha\cdot v_\beta}{k\cdot v_\alpha} - \frac{l_\alpha^2 (v_\alpha\cdot v_\beta)^2 k\cdot l_\beta}{(k\cdot v_\alpha)^2} \right) \right. \\ &- \left(v_\alpha^\mu v_\beta^\nu + v_\alpha^\nu v_\beta^\mu\right)\left(l_\alpha^2 v_\alpha\cdot v_\beta + k\cdot v_\alpha k\cdot v_\beta\right) - \left(v_\alpha^\mu l_\alpha^\nu + v_\alpha^\nu l_\alpha^\mu\right)(v_\alpha\cdot v_\beta)\left(\frac{l_\alpha^2 v_\alpha\cdot v_\beta}{k\cdot v_\alpha} + 2k\cdot v_\beta \right) \\ &\left. + l_\alpha^\mu l_\alpha^\nu (v_\alpha\cdot v_\beta)^2 + \eta^{\mu\nu}(v_\alpha\cdot v_\beta)\left(\frac{l_\alpha^2 v_\alpha\cdot v_\beta}{2} + k\cdot v_\alpha k\cdot v_\beta \right) \right].\end{aligned} \tag{4.61}$$

In order to find the radiation field from the source,

$$\bar{h}^{\mu\nu}_{\rm rad}(x) = \frac{-1}{4\pi r}\left(\frac{\kappa}{2}\right)\int \frac{d\omega}{2\pi} e^{-i\omega t}\hat{T}^{\mu\nu}(k), \tag{4.62}$$

where $k^\mu = \omega(1, \vec{x}/r)$. This result agrees with Ref. [92]. Note that the gravitational polarization tensor $\epsilon_{\mu\nu}$ can be contracted with $h^{\mu\nu} = \bar{h}^{\mu\nu} - \frac{1}{d-2}\eta^{\mu\nu}\bar{h}$. This allows further equivalent manipulations, since the harmonic gauge forces $k_\mu \epsilon^{\mu\nu} = \frac{1}{2}k^\nu \epsilon^\sigma_\sigma$ in the radiative limit. Next, we show that taking the double copy of Yang-Mills agrees with this result above.

4.2.3 The Radiative Double Copy

Radiation in general relativity coupled to a dilaton can be acquired by applying the radiative double copy to the Yang-Mills results found previously. The double-copy replacement rules

are

$$\begin{aligned} c_\alpha^a &\to p_\alpha^\nu, \\ g &\to \frac{1}{2m_{\rm Pl}^{(d-2)/2}} = \frac{\kappa}{2}, \\ if^{a_1a_2a_3} &\to -\frac{1}{2}(\eta^{\nu_1\nu_3}(q_1-q_3)^{\nu_2} + \eta^{\nu_1\nu_2}(q_2-q_1)^{\nu_3} + \eta^{\nu_2\nu_3}(q_3-q_2)^{\nu_1}), \\ \hat{J}^{\mu a}(k) &\to \hat{T}^{\mu\nu}(k), \end{aligned} \tag{4.63}$$

where the momenta $q_1 + q_2 + q_3 = 0$. Similar to the Ward identity $k_\mu \hat{J}^{\mu a} = 0$, we can shift $\hat{T}^{\mu\nu}$ by terms proportional to either k^μ or k^ν, such that $k_\mu \hat{T}^{\mu\nu} = k_\nu \hat{T}^{\mu\nu} = 0$, which shifts the gauge-dependent pseudotensor into the harmonic gauge.

The double copy relates field components of two Yang-Mills fields $A^{\mu a}$ to the symmetric gravitational field $h^{\mu\nu}$, an antisymmetric tensor field $B^{\mu\nu}$, and a scalar/dilaton ϕ. To find the gravitational field from $\hat{T}^{\mu\nu}$, it helps to put it in a form that is manifestly symmetric. While it is straightforward to find the gravitational radiation, the only setback is to recognize that this will include gravitational radiation that was produced by diagrams with internal dilaton lines.

Applying the double-copy replacement rules gives

$$\begin{aligned} \hat{T}^{\mu\nu}(k) &= \sum_{\substack{\alpha=1 \\ \beta\neq\alpha}}^{N} \frac{m_\alpha m_\beta}{8m_{\rm Pl}^{3(d-2)/2}} \int_{l_\alpha, l_\beta} \mu_{\alpha,\beta}(k) \\ &\quad \times \left[v_\alpha \cdot v_\beta \frac{l_\alpha^2 v_\alpha^\nu}{k\cdot v_\alpha} \left\{ v_\alpha \cdot v_\beta \left(\frac{k\cdot l_\beta}{k\cdot v_\alpha} v_\alpha^\mu - l_\beta^\mu \right) + k\cdot v_\alpha v_\beta^\mu - k\cdot v_\beta v_\alpha^\mu \right\} \right. \\ &\quad - \frac{1}{2}\left(2k\cdot v_\beta v_\alpha^\nu - 2k\cdot v_\alpha v_\beta^\nu + v_\alpha\cdot v_\beta (l_\beta - l_\alpha)^\nu\right) \\ &\quad \left. \times \left\{ 2k\cdot v_\beta v_\alpha^\mu + v_\alpha \cdot v_\beta \left(\frac{l_\alpha^2}{k\cdot v_\alpha} v_\alpha^\mu - l_\alpha^\mu \right) \right\} \right]. \end{aligned} \tag{4.64}$$

As this answer does not quite satisfy the analogous Ward identity, this result must shifted by terms proportional to k^μ or k^ν. This shift results in sending $l_\beta^\mu \to (l_\beta - l_\alpha)^\mu/2$ in the

above expression, giving

$$\begin{aligned}\hat{T}^{\mu\nu}(k) &= \sum_{\substack{\alpha=1\\ \beta\neq\alpha}}^{N} \frac{m_\alpha m_\beta}{8 m_{\rm Pl}^{3(d-2)/2}} \int_{l_\alpha, l_\beta} \mu_{\alpha,\beta}(k) \\ &\quad \times \left[v_\alpha \cdot v_\beta \frac{l_\alpha^2 v_\alpha^\nu}{k\cdot v_\alpha} \left\{ v_\alpha \cdot v_\beta \left(\frac{k\cdot l_\beta}{k\cdot v_\alpha} v_\alpha^\mu - \frac{1}{2}(l_\beta - l_\alpha)^\mu \right) + k\cdot v_\alpha v_\beta^\mu - k\cdot v_\beta v_\alpha^\mu \right\} \right. \\ &\quad - \frac{1}{2}\left(2k\cdot v_\beta v_\alpha^\nu - 2k\cdot v_\alpha v_\beta^\nu + v_\alpha\cdot v_\beta (l_\beta - l_\alpha)^\nu\right) \\ &\quad \left. \times \left\{ 2k\cdot v_\beta v_\alpha^\mu + v_\alpha \cdot v_\beta \left(\frac{l_\alpha^2}{k\cdot v_\alpha} v_\alpha^\mu - l_\alpha^\mu \right) \right\} \right]. \end{aligned} \tag{4.65}$$

Further simplification and symmetrization in μ and ν gives

$$\begin{aligned}\hat{T}^{\mu\nu}(k) &= \sum_{\substack{\alpha=1\\ \beta\neq\alpha}}^{N} \frac{m_\alpha m_\beta}{8 m_{\rm Pl}^{3(d-2)/2}} \int_{l_\alpha, l_\beta} \mu_{\alpha,\beta}(k) \\ &\quad \times \left[v_\alpha^\mu v_\alpha^\nu \left(\left(\frac{v_\alpha\cdot v_\beta}{k\cdot v_\alpha} \right)^2 l_\alpha^2 k\cdot l_\beta - 2\frac{v_\alpha\cdot v_\beta}{k\cdot v_\alpha} l_\alpha^2 k\cdot v_\beta - 2(k\cdot v_\beta)^2 \right) \right. \\ &\quad + \left(v_\alpha^\mu v_\beta^\nu + v_\alpha^\nu v_\beta^\mu\right)\left(k\cdot v_\alpha k\cdot v_\beta + v_\alpha\cdot v_\beta l_\alpha^2\right) + \frac{1}{2} l_\alpha^\mu (l_\beta - l_\alpha)^\nu (v_\alpha\cdot v_\beta)^2 \\ &\quad \left. - \left(v_\alpha^\mu (l_\beta - l_\alpha)^\nu + v_\alpha^\nu (l_\beta - l_\alpha)^\mu\right)\left(v_\alpha\cdot v_\beta k\cdot v_\beta + \frac{1}{2}\frac{(v_\alpha\cdot v_\beta)^2}{k\cdot v_\alpha} l_\alpha^2 \right) \right]. \end{aligned} \tag{4.66}$$

It is straightforward to show that this correctly satisfies $k_\mu \hat{T}^{\mu\nu} = k_\nu \hat{T}^{\mu\nu} = 0$ after considering that terms antisymmetric in α and β will cancel. The radiative double copy can find the same result as Eq. (4.61), once considering that the gauge condition allows for various equivalent representations of the gravitational source $\hat{T}^{\mu\nu}$. Due to the fact that $k^\mu = l_\alpha^\mu + l_\beta^\mu$ and the harmonic gauge condition gives $k_\mu \epsilon^{\mu\nu} = \frac{1}{2} k^\nu \epsilon_\sigma^\sigma$, the sources and fields may allow for substitutions such as $v_\alpha^\mu k^\nu \to \frac{1}{2}\eta^{\mu\nu} k\cdot v_\alpha$. Such transformations do not change the physical content of the gravitational radiation, which can be used on Eq. (4.61) to agree with the result above.

4.2.4 Double Copy of Ghost Fields to Remove the Dilaton

A non-Abelian scalar field can be added to the Yang-Mills radiation field construction, and Ref. [139] found that ghost fields can be used to remove the dilaton. With the appropriate replacement rules, we show that analogous ghost fields can be used in the double copy to

remove the dilaton in gravity theories. A ghost contribution to the Lagrangian would be given by

$$\mathcal{L}_{ghost} = -(d-2)\partial_\mu \bar{C}^a D^\mu C^a, \tag{4.67}$$

where the $(d-2)$ normalization was chosen to agree with the dilaton normalization on the gravitational side. While we will not derive a solution to the ghost-field equation of motion, we find an ansatz for a solution that when utilizing the Feynman rules for ghost fields, removes the dilaton in the radiative double copy procedure.

For typical scattering processes, ghosts are needed for loop corrections involving fermions, so it might be surprising that ghosts could be used at all for classical radiation. However, the classical radiation formulas integrate over l_α and l_β, which are not associated with loop quantum corrections, but will take a similar interpretation to loop integrals in scattering amplitudes due to the worldline parametrization. An ansatz for the ghost field solution is given by

$$C^a(x) = \frac{-g}{\sqrt{d-2}} \sum_{\alpha=1}^{N} c^a_{l_\alpha} \int_{l_\alpha} (2\pi)\delta(l_\alpha \cdot v_\alpha) \frac{e^{-il_\alpha \cdot (x-b_\alpha)}}{l_\alpha^2}, \tag{4.68}$$

where the color charge c_{l_α} must be used instead of the matter color charge c^a_α. The primary motivation of this solution is that simple replacement rules can be found to properly remove the dilaton at leading order.

The ghost field contribution to gluon radiation comes in two pieces associated with different diagrams. The first is from ghosts ability to cause apparent deflection from the sources v^μ_α and c^a_α. Assuming a shift in z^μ_α and c^a_α by C^a gives

$$\begin{aligned} \left.\frac{d^2 z^\mu_\alpha(\tau)}{d\tau^2}\right|_{\Delta C} &= \frac{1}{\sqrt{d-2}} c^a_{C_\alpha} \partial^\mu C^a, \\ \left.\frac{d\bar{c}^a_\alpha(\tau)}{d\tau}\right|_{\Delta C} &= \frac{f^{abc}}{\sqrt{d-2}} c^b_{C_\alpha} C^c, \end{aligned} \tag{4.69}$$

where $c^a_{C_\alpha}$ is a color charge that will have a double-copy replacement rule specified below. These shifts create corrections to $J^{\mu a}$, which is in general given by

$$J^{\mu a}|_{\Delta C} = g \int d\tau e^{ik\cdot(b_\alpha + v_\alpha \tau)} \left(ik \cdot z_\alpha|_{\Delta C} v^\mu_\alpha c^a_\alpha + \left.\frac{dz^\mu_\alpha}{d\tau}\right|_{\Delta C} c^a_\alpha + v^\mu_\alpha \bar{c}^a_\alpha|_{\Delta C} \right). \tag{4.70}$$

After plugging in for the shifts associated with the ghosts, we find

$$J^{\mu a}(k)|_{\Delta C} = \frac{-g^2}{d-2}\sum_{\alpha,\beta}\int_{l_\alpha,l_\beta}\mu_{\alpha,\beta}(k)l_\alpha^2\left[\frac{k\cdot l_\beta c^b_{C_\alpha}c^b_{l_\beta}}{(k\cdot v_\alpha)^2}v^\mu_\alpha c^a_\alpha + \frac{1}{k\cdot v_\alpha}\left(v^\mu_\alpha if^{abc}c^b_{C_\alpha}c^c_{l_\beta} - l^\mu_\beta c^a_\alpha c^b_{C_\alpha}c^b_{l_\beta}\right)\right]. \tag{4.71}$$

There is also a ghost-antighost-vector boson interaction, which has a three-point vertex given by

$$V^{\mu,abc}_{ghost} = -igf^{abc}p^\mu. \tag{4.72}$$

The potential field for a trivial ghost emission source can be used to stitch two copies together, corresponding to particles α and β, respectively. The gluonic radiation current contribution $j^{\mu a} = \hat{J}^{\mu a} - J^{\mu a}$ specifically for ghosts is

$$j^{\mu a}|_{\Delta C} = \frac{ig^2}{d-2}\sum_{\alpha\neq\beta}f^{abc}\int_{l_\alpha,l_\beta}\mu_{\alpha,\beta}(k)c^b_{C_\alpha}c^c_{l_\beta}l^\mu_\alpha. \tag{4.73}$$

Adding these two contributions together gives

$$\begin{aligned}\hat{J}^{\mu a}(k)|_{\Delta C} &= \frac{g^2}{d-2}\sum_{\alpha\neq\beta}\int_{l_\alpha,l_\beta}\mu_{\alpha,\beta}(k)\\ &\quad\times\left[l^2_\alpha\frac{c^b_{C_\alpha}c^b_{l_\beta}}{k\cdot v_\alpha}\left(\frac{k\cdot l_\alpha}{k\cdot v_\alpha}v^\mu_\alpha c^a_\alpha + l^\mu_\beta c^a_\alpha\right) - if^{abc}c^b_{C_\alpha}c^c_{l_\beta}\left(\frac{l^2_\alpha v^\mu_\alpha}{k\cdot v_\alpha} - l^\mu_\alpha\right)\right].\end{aligned} \tag{4.74}$$

Under the double-copy procedure for the ghost, the replacement rule for f^{abc} becomes linearized to a single term instead of three, since the resulting field will be a scalar dilaton. To this order, all terms are proportion For the ghost-dilaton correspondence, the following replacement rules were found to apply:

$$\begin{aligned} c^a_{l_\alpha} &\to l^\nu_\alpha,\\ if^{abc} &\to -\frac{1}{2}\left(\eta^{\nu_2\nu_3}(q_3-q_2)^{\nu_1}\right),\\ c^a_{C_\alpha} &\to C^\nu_\alpha = -\frac{l^\nu_\beta}{l^2_\beta},\end{aligned} \tag{4.75}$$

which can be used to find

$$\begin{aligned}\hat{T}^{\mu\nu}(k)|_{\Delta C} &= \frac{1}{d-2}\left(\frac{\kappa}{2}\right)^2\sum_{\alpha\neq\beta}m_\alpha m_\beta\int_{l_\alpha,l_\beta}\mu_{\alpha,\beta}(k)\left[l^2_\alpha\frac{C_\alpha\cdot l_\beta k\cdot l_\alpha}{(k\cdot v_\alpha)^2}v^\mu_\alpha v^\nu_\alpha + l^2_\alpha\frac{C_\alpha\cdot l_\beta}{k\cdot v_\alpha}l^\mu_\beta v^\nu_\alpha\right.\\ &\quad\left.+\frac{1}{2}\left(\eta_{\rho\sigma}(l_\beta-l_\alpha)^\nu\right)\left(l^2_\alpha\frac{C^\rho_\alpha l^\sigma_\beta}{k\cdot v_\alpha}v^\mu_\alpha - C^\rho_\alpha l^\sigma_\beta l^\mu_\alpha\right)\right],\end{aligned} \tag{4.76}$$

where in our substitution, we chose $q_1 = -k$, $q_2 = l_\alpha$ and $q_3 = l_\beta$. By sending $l_\beta^\mu \to (l_\beta - l_\alpha)^\mu/2$ to preserve the Ward identity, we find

$$\begin{aligned}\hat{T}^{\mu\nu}(k)|_{\Delta C} &= \frac{1}{d-2}\left(\frac{\kappa}{2}\right)^2 \sum_{\alpha\neq\beta} m_\alpha m_\beta \int_{l_\alpha, l_\beta} \mu_{\alpha,\beta}(k) C_\alpha \cdot l_\beta \\ &\times \left[l_\alpha^2 \frac{k\cdot l_\alpha}{(k\cdot v_\alpha)^2} v_\alpha^\mu v_\alpha^\nu + \frac{l_\alpha^2}{2}\frac{1}{k\cdot v_\alpha}(l_\beta - l_\alpha)^\mu v_\alpha^\nu + \frac{1}{2}(l_\beta - l_\alpha)^\nu \left(l_\alpha^2 \frac{1}{k\cdot v_\alpha} v_\alpha^\mu - l_\alpha^\mu \right) \right].\end{aligned} \tag{4.77}$$

Simplifying further gives

$$\begin{aligned}\hat{T}^{\mu\nu}(k)|_{\Delta C} &= \frac{1}{d-2}\left(\frac{\kappa}{2}\right)^2 \sum_{\alpha\neq\beta} m_\alpha m_\beta \int_{l_\alpha, l_\beta} \mu_{\alpha,\beta}(k) C_\alpha \cdot l_\beta \\ &\times \left[l_\alpha^2 \frac{k\cdot l_\alpha}{(k\cdot v_\alpha)^2} v_\alpha^\mu v_\alpha^\nu - \frac{l_\alpha^2}{k\cdot v_\alpha}(v_\alpha^\mu l_\alpha^\nu + v_\alpha^\nu l_\alpha^\mu) + \frac{l_\alpha^2}{2}\eta^{\mu\nu} + l_\alpha^\mu l_\alpha^\nu \right].\end{aligned} \tag{4.78}$$

Setting $C_\alpha \cdot l_\beta = -1$ gives the exact contribution that cancels out the dilaton contribution to gravitational radiation. As pointed out by Ref. [139], it is unclear if this construction will work at higher orders, but the dilaton can at least be removed with ghosts at this order. This section demonstrates that ghosts also can be used to remove the dilaton in the formalism of Goldberger and Ridgway [92].

4.3 Radiation in Yang-Mills-Biadjoint-Scalar Theory

In the context of scattering amplitudes, the double-copy method has been used to calculate Einstein-Yang-Mills theory by double copying Yang-Mills with a Yang-Mills-biadjoint-scalar theory. Just as the Yang-Mills field A_μ^a is related to $h_{\mu\nu}$, a biadjoint scalar with trivalent interactions $\Phi^{\tilde{a}a}$ is related to a Yang-Mills field $A_\nu^{\tilde{a}}$, where a and $\tilde{a}$ are indices for two different gauge groups.

In this section, the non-Abelian radiation field for Yang-Mills-biadjoint-scalar field theory is computed and the radiative double copy is used to find gravitational radiation solutions in Einstein-Yang-Mills theory. In the next section, the gravitational radiation emitted in Einstein-Yang-Mills theory is calculated directly and shown to agree with this section, providing more evidence that color-kinematics duality is useful for understanding the relation between gauge theories and gravity for classical radiation problems in addition to scattering amplitudes in effective quantum field theories.

4.3.1 Equations of Motion and Initial Conditions

To start, the Lagrangian associated with the Yang-Mills-biadjoint-scalar theory is

$$\mathcal{L} = -\frac{1}{4}F^a_{\mu\nu}F^{\mu\nu a} + \frac{1}{2}D_\mu\Phi^{\tilde{a}a}D^\mu\Phi^{\tilde{a}a} - \frac{y}{3}f^{abc}f^{\tilde{a}\tilde{b}\tilde{c}}\Phi^{\tilde{a}a}\Phi^{\tilde{b}b}\Phi^{\tilde{c}c} - gJ^{\mu a}A^a_\mu - yJ^{\tilde{a}a}\Phi^{\tilde{a}a}, \tag{4.79}$$

where f^{abc} and $f^{\tilde{a}\tilde{b}\tilde{c}}$ refer to structure constants of different groups, the biadjoint scalar $\Phi^{\tilde{a}a}$ has an index associated with each gauge group, and $y = -ig\tilde{g}/2$ relates the conventions of Ref. [72] with the conventions of Refs. [130, 134]. In principle, there could be an $\mathcal{O}(\Phi^4)$ term in the Lagrangian, but this would have a different dimensional coupling and will not be needed. The non-Abelian field strength is given by Eq. (4.2) and the covariant derivative is given by

$$D_\mu\Phi^{\tilde{a}a}(x) = \partial_\mu\Phi^{\tilde{a}a}(x) - gf^{abc}A^b_\mu(x)\Phi^{\tilde{a}c}(x). \tag{4.80}$$

The equations of motion in vacuum is found by applying the Euler-Lagrange equations. For the vector boson,

$$D_\mu F^{\mu\nu a}(x) - gf^{abc}\Phi^{\tilde{a}b}(x)D^\nu\Phi^{\tilde{a}c}(x) = 0, \tag{4.81}$$

and for the biadjoint scalar,

$$\partial_\mu D^\mu\Phi^{\tilde{a}a}(x) - gf^{abc}A^b_\mu(x)D^\mu\Phi^{\tilde{a}c}(x) - yf^{abc}f^{\tilde{a}\tilde{b}\tilde{c}}\Phi^{\tilde{b}b}(x)\Phi^{\tilde{c}c}(x) = 0, \tag{4.82}$$

where f^{abc} and $f^{\tilde{a}\tilde{b}\tilde{c}}$ are structure constants in two different gauge groups. To study radiation, an adjoint vector source $J^{\nu a}(x)$ and a biadjoint scalar source $J^{\tilde{a}a}(x)$ can be added. For the vector boson, we have

$$D_\mu F^{\mu\nu a}(x) - gf^{abc}\Phi^{\tilde{a}b}(x)D^\nu\Phi^{\tilde{a}c}(x) = J^{\nu a}(x). \tag{4.83}$$

The equation of motion for the biadjoint scalar field in the presence of a source $J^{\tilde{a}a}(x)$ is

$$\partial_\mu D^\mu\Phi^{\tilde{a}a}(x) - gf^{abc}A^b_\mu(x)D^\mu\Phi^{\tilde{a}c}(x) - yf^{abc}f^{\tilde{a}\tilde{b}\tilde{c}}\Phi^{\tilde{b}b}(x)\Phi^{\tilde{c}c}(x) = J^{\tilde{a}a}(x). \tag{4.84}$$

The biadjoint source $J^{\tilde{a}a}(x)$ for N particles is

$$J^{\tilde{a}a}(x) = y\sum_{\alpha=1}^{N}\int d\tau c^{\tilde{a}}_\alpha(\tau)c^a_\alpha(\tau)\delta^d(x - x_\alpha(\tau)), \tag{4.85}$$

where it is assumed that the particles of mass m_α travel along the trajectories given by $x^\mu_\alpha(\tau)$ and the color charges $c^{\tilde{a}}_\alpha$ and c^a_α are in two different gauge groups. Similarly, the vector field is sourced by

$$J^{\mu a}(x) = g\sum_{\alpha=1}^{N}\int d\tau c^a_\alpha(\tau)v^\mu_\alpha(\tau)\delta^d(x - x_\alpha(\tau)), \tag{4.86}$$

where $v^\mu_\alpha = \frac{dx^\mu_\alpha}{d\tau}$. The vector source is covariantly conserved, such that $D_\mu J^{\mu a} = 0$.

The Lorenz gauge is taken by setting $\partial_\mu A^{\mu a} = 0$. In order to simplify these equations, the explicit dependence on the covariant derivatives is removed and gauge dependent sources $\hat{J}^{\mu a}$ and $\tilde{J}^{\tilde{a}a}$ are defined such that $\Box A^{\mu a}(x) = \hat{J}^{\mu a}(x)$ and $\Box\Phi^{\tilde{a}a} = \hat{J}^{\tilde{a}a}$, where $\Box \equiv \partial_\nu\partial^\nu$. With these definitions, the pseudo-vector source is

$$\hat{J}^{\mu a} = J^{\mu a} + gf^{abc}\left[A^b_\nu(\partial^\nu A^{\mu c} + F^{\nu\mu c}) + \Phi^{\tilde{a}b}D^\mu\Phi^{\tilde{a}c}\right], \tag{4.87}$$

where the pseudo-vector is locally conserved, $\partial_\mu\hat{J}^{\mu a} = 0$. The pseudo-scalar source is given by

$$\hat{J}^{\tilde{a}a} = J^{\tilde{a}a} + gf^{abc}\left[A^b_\mu\left(\partial^\mu\Phi^{\tilde{a}c} + D^\mu\Phi^{\tilde{a}c}\right) + \Phi^{\tilde{b}b}\left(\frac{y}{g}f^{\tilde{a}\tilde{b}\tilde{c}}\Phi^{\tilde{c}c} + gf^{cde}\Phi^{\tilde{b}d}\Phi^{\tilde{a}e}\right)\right]. \tag{4.88}$$

Specifying the initial conditions, the position of each particle is

$$x^\mu_\alpha(\tau) = b^\mu_\alpha + v^\mu_\alpha\tau + z^\mu_\alpha(\tau) + \tilde{z}^\mu_\alpha(\tau), \tag{4.89}$$

where $z^\mu_\alpha(\tau)$ is the correction to the trajectory due to the adjoint vector field and $\tilde{z}^\mu_\alpha$ is the correction to the trajectory due to the biadjoint scalar field. Similarly, the charges are given by

$$\begin{aligned} c^a_\alpha(\tau) &= c^a_\alpha + \bar{c}^a_\alpha(\tau) + \tilde{c}^a_\alpha(\tau), \\ c^{\tilde{a}}_\alpha(\tau) &= c^{\tilde{a}}_\alpha + \tilde{c}^{\tilde{a}}_\alpha(\tau), \end{aligned} \tag{4.90}$$

where c^a_α and $c^{\tilde{a}}_\alpha$ are the initial charges, $\bar{c}^a_\alpha(\tau)$ is the correction due to the adjoint vector field, and $\tilde{c}^a_\alpha(\tau)$ and $\tilde{c}^{\tilde{a}}_\alpha(\tau)$ are the corrections due to the biadjoint scalar field.

The additional deflections needed for Yang-Mills-biadjoint-scalar theory are $\tilde{z}^\mu_\alpha$, $\tilde{c}^a_\alpha$, and $\tilde{c}^{\tilde{c}}_\alpha$. Following Ref. [134], the time evolution of the momentum is

$$\frac{dp^\mu_\alpha(\tau)}{d\tau} = gc^a_\alpha(\tau)F^{\mu\nu a}(x_\alpha(\tau))v_{\alpha\nu}(\tau) - y\partial^\mu\Phi^{\tilde{a}a}(x_\alpha(\tau))c^a_\alpha(\tau)c^{\tilde{a}}_\alpha(\tau), \tag{4.91}$$

and the time evolution of the charges is

$$\begin{aligned}\frac{dc^a_\alpha(\tau)}{d\tau} &= gf^{abc}v^\mu_\alpha(\tau)A^b_\mu(x_\alpha(\tau))c^c_\alpha(\tau) - yf^{abc}\Phi^{\tilde{b}b}(x_\alpha(\tau))c^{\tilde{b}}_\alpha(\tau)c^c_\alpha(\tau),\\ \frac{dc^{\tilde{a}}_\alpha(\tau)}{d\tau} &= -yf^{\tilde{a}\tilde{b}\tilde{c}}\Phi^{\tilde{b}b}(x_\alpha(\tau))c^b_\alpha(\tau)c^{\tilde{c}}_\alpha(\tau).\end{aligned} \tag{4.92}$$

These summarize all of the equations needed to iteratively solve for radiation in Yang-Mills-biadjoint-scalar theory.

4.3.2 Solutions of the Radiation Fields

The radiation field source for Yang-Mills is given by Eq. (4.27), so all that is needed are the biadjoint scalar contributions. The pseudoscalar current in momentum space is

$$\hat{J}^{\tilde{a}a}(k)|_{\mathcal{O}(y^1)} = y\sum_{\alpha=1}^{N} e^{ik\cdot b_\alpha}(2\pi)\delta(k\cdot v_\alpha)c^{\tilde{a}}_\alpha c^a_\alpha, \tag{4.93}$$

which can be utilized to find the scalar field to lowest order, giving

$$\Phi^{\tilde{a}a}(x)|_{\mathcal{O}(y^1)} = -y\sum_{\alpha=1}^{N}\int_l (2\pi)\delta(l\cdot v_\alpha)\frac{e^{-il\cdot(x-b_\alpha)}}{l^2}c^{\tilde{a}}_\alpha c^a_\alpha. \tag{4.94}$$

The lowest-order fields can be used to find the deflections of the sources, given by

$$\begin{aligned} m_\alpha\frac{d^2z^\mu_\alpha(\tau)}{d\tau^2}\bigg|_{\Delta A} &= gc^a_\alpha\left(\partial^\mu A^{\nu a}(x_\alpha(\tau))|_{\mathcal{O}(g^1)} - \partial^\nu A^{\mu a}(x_\alpha(\tau))|_{\mathcal{O}(g^1)}\right)v_{\alpha\nu},\\ m_\alpha\frac{d^2\tilde{z}^\mu_\alpha(\tau)}{d\tau^2}\bigg|_{\Delta\Phi} &= -y\partial^\mu\Phi^{\tilde{b}b}(x_\alpha(\tau))|_{\mathcal{O}(y^1)}c^{\tilde{b}}_\alpha c^b_\alpha.\end{aligned} \tag{4.95}$$

The derivatives of the lowest-order fields acting on the particle associated with m_α are

$$\begin{aligned}\partial^\mu A^{\nu a}(x)|_{\mathcal{O}(g^1)} &= -g\sum_{\beta\neq\alpha}\int_l(2\pi)\delta(l\cdot v_\beta)(-il^\mu)\frac{e^{-il\cdot(x-b_\beta)}}{l^2}v^\nu_\beta c^a_\beta,\\ \partial^\mu\Phi^{\tilde{b}b}(x)|_{\mathcal{O}(y^1)} &= -y\sum_{\beta\neq\alpha}\int_l(2\pi)\delta(l\cdot v_\beta)(-il^\mu)\frac{e^{-il\cdot(x-b_\beta)}}{l^2}c^{\tilde{b}}_\beta c^b_\beta.\end{aligned} \tag{4.96}$$

Plugging in the derivatives of the lowest-order fields from above gives

$$\begin{aligned} m_\alpha\frac{d^2z^\mu_\alpha(\tau)}{d\tau^2}\bigg|_{\mathcal{O}(g^2)} &= ig^2\sum_{\beta\neq\alpha}(c^a_\alpha c^a_\beta)\int_l(2\pi)\delta(l\cdot v_\beta)\frac{e^{-il\cdot(b_{\alpha\beta}+v_\alpha\tau)}}{l^2}\left[(v_\alpha\cdot v_\beta)l^\mu - (v_\alpha\cdot l)v^\mu_\beta\right],\\ m_\alpha\frac{d^2\tilde{z}^\mu_\alpha(\tau)}{d\tau^2}\bigg|_{\mathcal{O}(y^2)} &= -iy^2\sum_{\beta\neq\alpha}(c^a_\alpha c^a_\beta)c^{\tilde{a}}_\alpha c^{\tilde{a}}_\beta\int_l(2\pi)\delta(l\cdot v_\beta)\frac{e^{-il\cdot(b_{\alpha\beta}+v_\alpha\tau)}}{l^2}l^\mu.\end{aligned} \tag{4.97}$$

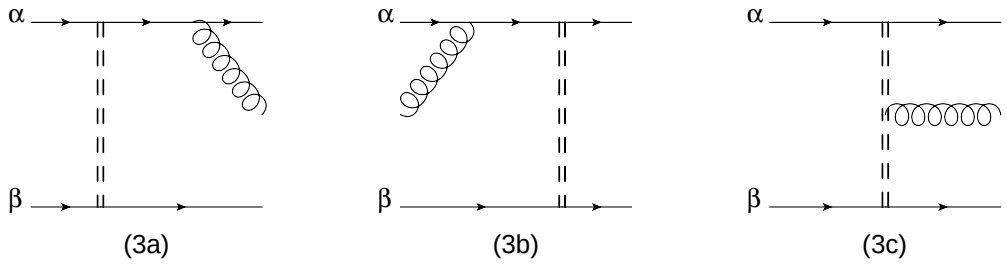

Figure 4.3: The diagrams (3a) and (3b) represent $J^{\mu a}|_{\Delta\Phi}$ and (3c) represents $j^{\mu a}|_{\Delta\Phi}$. Doubly-dashed lines represent biadjoint scalars and curly lines are used for Yang-Mills fields.

Note that writing the color charge contraction as $c_\alpha \cdot c_\beta$ would be ambiguous with our notation. The first correction of the color charges to second order in g is given by

$$\begin{aligned}
\left.\frac{d\bar{c}^a_\alpha(\tau)}{d\tau}\right|_{\mathcal{O}(g^2)} &= g f^{abc} v^\mu_\alpha A^b_\mu(x_\alpha(\tau))|_{\mathcal{O}(g^1)} c^c_\alpha, \\
\left.\frac{d\tilde{c}^a_\alpha(\tau)}{d\tau}\right|_{\mathcal{O}(y^2)} &= -y f^{abc} \Phi^{\tilde{b}b}(x_\alpha(\tau))|_{\mathcal{O}(y)} c^{\tilde{b}}_\alpha c^c_\alpha, \\
\left.\frac{d\tilde{c}^{\tilde{a}}_\alpha(\tau)}{d\tau}\right|_{\mathcal{O}(y^2)} &= -y f^{\tilde{a}\tilde{b}\tilde{c}} \Phi^{\tilde{b}b}(x_\alpha(\tau))|_{\mathcal{O}(y)} c^b_\alpha c^{\tilde{c}}_\alpha.
\end{aligned} \tag{4.98}$$

Once again, plugging in the lowest-order fields gives

$$\begin{aligned}
\left.\frac{d\bar{c}^a_\alpha(\tau)}{d\tau}\right|_{\mathcal{O}(g^2)} &= -g^2 \sum_{\beta\neq\alpha} f^{abc} c^b_\beta c^c_\alpha (v_\alpha \cdot v_\beta) \int_l (2\pi)\delta(l\cdot v_\beta) \frac{e^{-il\cdot(b_{\alpha\beta}+v_\alpha\tau)}}{l^2}, \\
\left.\frac{d\tilde{c}^a_\alpha(\tau)}{d\tau}\right|_{\mathcal{O}(y^2)} &= y^2 \sum_{\beta\neq\alpha} f^{abc} c^b_\beta c^c_\alpha c^{\tilde{b}}_\alpha c^{\tilde{b}}_\beta \int_l (2\pi)\delta(l\cdot v_\beta) \frac{e^{-il\cdot(b_{\alpha\beta}+v_\alpha\tau)}}{l^2}, \\
\left.\frac{d\tilde{c}^{\tilde{a}}_\alpha(\tau)}{d\tau}\right|_{\mathcal{O}(y^2)} &= y^2 \sum_{\beta\neq\alpha} f^{\tilde{a}\tilde{b}\tilde{c}} c^{\tilde{b}}_\beta c^{\tilde{c}}_\alpha c^b_\alpha c^b_\beta \int_l (2\pi)\delta(l\cdot v_\beta) \frac{e^{-il\cdot(b_{\alpha\beta}+v_\alpha\tau)}}{l^2}.
\end{aligned} \tag{4.99}$$

To find the gluon radiation, three additional diagrams shown in Fig. (4.3) are added to the three pure Yang-Mills diagrams shown in Fig. (4.1). In principle, there are also diagrams for biadjoint scalar radiation, but they double copy to give Yang-Mills radiation in Einstein-Yang-Mills theory, not gravitational radiation. Diagrams (1a)–(3c) represent $\hat{J}^{\mu a}$ and satisfy the Ward identity $k_\mu \hat{J}^{\mu a}(k) = 0$. Since Yang-Mills radiation without the biadjoint scalar is gauge invariant, (1d) + (1e) + (1f) also satisfies the Ward identity and is orthogonal to k^μ.

Expanding Eqs. (4.85)-(4.86) perturbatively by adding in the deflections due to the lowest-order fields, taking the Fourier transform, and integrating over the delta function

gives

$$J^{\mu a}(k) = g\sum_{\alpha=1}^{N}\int d\tau e^{ik\cdot x_\alpha(\tau)}\left(v_\alpha^\mu + \frac{dz_\alpha^\mu(\tau)}{d\tau} + \frac{d\tilde{z}_\alpha^\mu(\tau)}{d\tau}\right)\left(c_\alpha^a + \bar{c}_\alpha^a(\tau) + \tilde{c}_\alpha^a(\tau)\right), \tag{4.100}$$

Expanding these results gives

$$\begin{aligned} J^{\mu a}(k) \;\approx\; & g\sum_{\alpha=1}^{N}\int d\tau e^{ik\cdot(b_\alpha+v_\alpha\tau)}\left[(1+ik\cdot\tilde{z}_\alpha)\left((1+ik\cdot z_\alpha)c_\alpha^a v_\alpha^\mu + \left(\bar{c}_\alpha^a v_\alpha^\mu + c_\alpha^a\frac{dz_\alpha^\mu}{d\tau}\right)\right)\right. \\ & \left. + (1+ik\cdot z_\alpha)\left(\tilde{c}_\alpha^a v_\alpha^\mu + c_\alpha^a\frac{d\tilde{z}_\alpha^\mu}{d\tau}\right) + \frac{d\tilde{z}_\alpha^\mu}{d\tau}\bar{c}_\alpha^a + \frac{dz_\alpha^\mu}{d\tau}\tilde{c}_\alpha^a\right], \end{aligned} \tag{4.101}$$

where explicit τ dependence has been suppressed and terms to order g^3y^2 are included. The $\mathcal{O}(g^3)$ term was computed previously, and $J^{\mu a}|_{\mathcal{O}(gy^2)}$ gives

$$J^{\mu a}(k)|_{\mathcal{O}(gy^2)} = g\sum_{\alpha=1}^{N}\int d\tau e^{ik\cdot(b_\alpha+v_\alpha\tau)}\left[ik\cdot\tilde{z}_\alpha(\tau)c_\alpha^a v_\alpha^\mu + \tilde{c}_\alpha^a(\tau)v_\alpha^\mu + c_\alpha^a\frac{d\tilde{z}_\alpha^\mu(\tau)}{d\tau}\right]. \tag{4.102}$$

Integrating Eqs. (4.97) and (4.99) helps solve for $J^{\mu a}|_{\Delta\Phi}$ to lowest order, giving

$$J^{\mu a}(k)|_{\mathcal{O}(gy^2)} = gy^2\sum_{\substack{\alpha=1\\ \beta\neq\alpha}}^{N} c_\alpha^{\tilde{a}}c_\beta^{\tilde{a}}\int_{l_\alpha,l_\beta}\mu_{\alpha,\beta}(k)\frac{l_\alpha^2}{k\cdot v_\alpha}\left[\frac{c_\alpha^b c_\beta^b}{m_\alpha}c_\alpha^a\left(l_\beta^\mu - \frac{k\cdot l_\beta}{k\cdot v_\alpha}v_\alpha^\mu\right) - if^{abc}c_\alpha^b c_\beta^c v_\alpha^\mu\right]. \tag{4.103}$$

One more diagram (3c) is needed to obtain the non-Abelian radiation source for Yang-Mills-biadjoint-scalar theory, which is given by $j^{\mu a}|_{\Delta\Phi}$ to lowest order,

$$\begin{aligned} j^{\mu a}(k)|_{\mathcal{O}(gy^2)} &= gf^{abc}\int d^dx e^{ik\cdot x}\Phi^{\tilde{a}b}(x)D^\mu\Phi^{\tilde{a}c}(x) \\ &= gf^{abc}\int d^dx e^{ik\cdot x}\Phi^{\tilde{a}b}(x)|_{\mathcal{O}(g\tilde{g})}\partial^\mu\Phi^{\tilde{a}c}(x)|_{\mathcal{O}(g\tilde{g})}. \end{aligned} \tag{4.104}$$

Once again, the lowest-order field solutions are plugged in to find

$$j^{\mu a}(k)|_{\mathcal{O}(gy^2)} = gy^2\sum_{\substack{\alpha=1\\ \beta\neq\alpha}}^{N} if^{abc}c_\alpha^b c_\beta^c c_\alpha^{\tilde{a}}c_\beta^{\tilde{a}}\int_{l_\alpha,l_\beta}\mu_{\alpha,\beta}(k)l_\alpha^\mu, \tag{4.105}$$

To prove that the algebraic method presented above agrees with the radiative Feynman rules, diagram (3c) is computed in Section (A.3) from the three-point vertex with two biadjoint scalars and one adjoint vector.

Summing up the three diagrams (3a)–(3c) gives $\hat{J}^{\mu a}(k)|_{\mathcal{O}(gy^2)}$,

$$\begin{aligned}\hat{J}^{\mu a}(k)|_{\mathcal{O}(gy^2)} &= -gy^2 \sum_{\substack{\alpha=1 \\ \beta\neq\alpha}}^{N} c_\alpha^{\tilde{a}} c_\beta^{\tilde{a}} \int_{l_\alpha, l_\beta} \mu_{\alpha,\beta}(k) \\ &\quad \times \left[\frac{c_\alpha^b c_\beta^b}{m_\alpha} \frac{l_\alpha^2 c_\alpha^a}{k\cdot v_\alpha} \left(\frac{k\cdot l_\beta}{k\cdot v_\alpha} v_\alpha^\mu - l_\beta^\mu \right) + i f^{abc} c_\alpha^b c_\beta^c \left(\frac{l_\alpha^2}{k\cdot v_\alpha} v_\alpha^\mu - l_\alpha^\mu \right) \right] \end{aligned} \tag{4.106}$$

The radiative field must be gauge invariant and the above expression satisfies the Ward identity $k_\mu \hat{J}^{\mu a}(k)|_{\mathcal{O}(gy^2)} = 0$, as the identity must be satisfied order by order. Adding the above contributions to Eq. (4.27) gives the total source, $\hat{J}^{\mu a}$. Integrating this over all frequencies as shown in Eq. (4.28) includes the biadjoint-scalar contribution to vector boson radiation.

4.4 Gravitational Radiation in Einstein-Yang-Mills Theory

4.4.1 Equations of Motion and Initial Conditions

The action for the Einstein-Yang-Mills-scalar theory in consideration is

$$S = \int d^d x \sqrt{-g} \left[-\frac{2}{\kappa^2} R - \frac{1}{4} g^{\mu\rho} g^{\nu\sigma} F_{\mu\nu}^{\tilde{a}} F_{\rho\sigma}^{\tilde{a}} + \frac{2}{\kappa^2} (d-2) g^{\mu\nu} \partial_\mu \phi \partial_\nu \phi \right] - m \int d\tau e^\phi, \tag{4.107}$$

where ϕ is the dilaton field and $d\tau = \sqrt{g_{\mu\nu} dx^\mu dx^\nu}$. By varying the action above, the energy-momentum pseudotensor contributions from the Yang-Mills field and the dilaton are given by

$$\begin{aligned} 8\pi G T_{\mu\nu} &= R_{\mu\nu} - \frac{1}{2} g_{\mu\nu} R + 8\pi G \left(g^{\rho\sigma} F_{\mu\rho}^{\tilde{a}} F_{\nu\sigma}^{\tilde{a}} - \frac{1}{4} g_{\mu\nu} g^{\rho\sigma} g^{\lambda\tau} F_{\rho\lambda}^{\tilde{a}} F_{\sigma\tau}^{\tilde{a}} \right) \\ &\quad - (d-2) \left(\partial_\mu \phi \partial_\nu \phi - \frac{1}{2} g_{\mu\nu} g^{\rho\sigma} \partial_\rho \phi \partial_\sigma \phi \right). \end{aligned} \tag{4.108}$$

After expanding, the Yang-Mills contribution to the pseudotensor is

$$t^{\mu\nu}|_{\Delta A} = -F^{\mu\rho\tilde{a}} F^{\nu\ \tilde{a}}_{\ \rho} + \frac{1}{4} \eta^{\mu\nu} F^{\rho\sigma\tilde{a}} F_{\rho\sigma}^{\tilde{a}} - \kappa \left(h_{\rho\sigma} F^{\mu\rho\tilde{a}} F^{\nu\sigma\tilde{a}} - \frac{1}{2} \eta^{\mu\nu} h_{\rho\sigma} F^{\rho\tau\tilde{a}} F_{\ \tau}^{\sigma\ \tilde{a}} + \frac{1}{4} h^{\mu\nu} F^{\rho\sigma\tilde{a}} F_{\rho\sigma}^{\tilde{a}} \right), \tag{4.109}$$

where the first two terms give the non-Abelian extension of the well-known electromagnetic energy-momentum tensor, and the other terms represent interactions between the Yang-Mills field and the gravitational field.

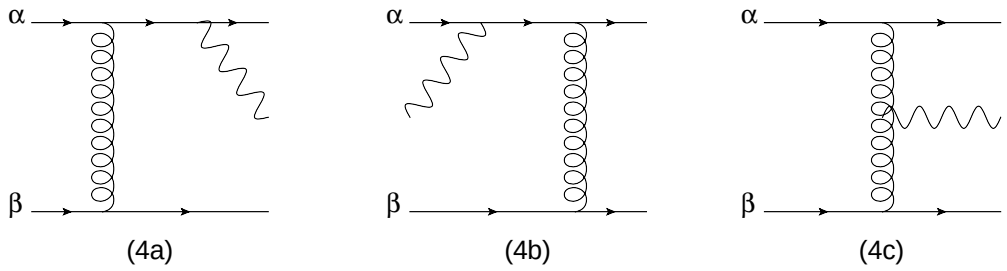

Figure 4.4: Diagrams (4a) and (4b) correspond to $\sqrt{|g|}T^{\mu\nu}|_{\Delta A}$ and diagram (4c) corresponds to $\hat{t}^{\mu\nu}|_{\Delta A}$. The curly lines represent Yang-Mills fields and the wavy lines represent gravitational fields.

In addition to the six diagrams found in Fig. (4.2), three additional diagrams (4a), (4b), and (4c) are shown in Fig. (4.4), which contribute to gravitational radiation for Einstein-Yang-Mills theory. Keeping the lower order term of the non-Abelian energy-momentum tensor gives

$$t^{\mu\nu}|_{\Delta A} = -F^{\mu\rho\tilde{a}}F_{\rho}^{\nu\ \tilde{a}} + \frac{1}{4}\eta^{\mu\nu}F^{\rho\sigma\tilde{a}}F^{\tilde{a}}_{\rho\sigma}. \tag{4.110}$$

Similar to the previous section, we will assume that the position of the particle is given by

$$x^{\mu}_{\alpha}(\tau) = b^{\mu}_{\alpha} + v^{\mu}_{\alpha}\tau + z^{\mu}_{\alpha}(\tau) + \tilde{z}^{\mu}_{\alpha}(\tau), \tag{4.111}$$

where $z^{\mu}_{\alpha}(\tau)$ is the correction due to the graviton and dilaton already computed, and $\tilde{z}^{\mu}_{\alpha}(\tau)$ is the correction due to the gauge field $A^{\mu\tilde{a}}$. The matter is assumed to have a color charge $c^{\tilde{a}}_{\alpha}(\tau)$, but their corrections do not source the lowest-order gravitational radiation field. The force due to the gauge field is

$$m_{\alpha}\frac{d^2\tilde{z}^{\mu}_{\alpha}(\tau)}{d\tau^2} = \tilde{g}c^{\tilde{a}}_{\alpha}F^{\mu\nu\tilde{a}}v_{\alpha\nu}(\tau). \tag{4.112}$$

4.4.2 Solutions of the Radiation Fields

Reusing a result from a previous section to find $A^{\tilde{a}}_{\mu}$ gives

$$A^{\mu\tilde{a}}(x)|_{\mathcal{O}(\tilde{g})} = -\tilde{g}\sum_{\alpha=1}^{N}\int_{l}(2\pi)\delta(l\cdot v_{\alpha})\frac{e^{-il\cdot(x-b_{\alpha})}}{l^2}c^{\tilde{a}}_{\alpha}v^{\mu}_{\alpha}. \tag{4.113}$$

The deflection caused by Yang-Mills is given by

$$m_\alpha \frac{d^2 \tilde{z}^\mu_\alpha(\tau)}{d\tau^2} = \tilde{g} c^{\tilde{a}}_\alpha F^{\mu\nu\tilde{a}} v_{\alpha\nu}(\tau). \tag{4.114}$$

Plugging the lowest-order field solution into the deflection gives

$$\left.\frac{d^2 \tilde{z}^\mu_\alpha}{d\tau^2}\right|_{\mathcal{O}(g^2)} = i\tilde{g}^2 \sum_{\beta\neq\alpha} \frac{c^{\tilde{a}}_\alpha c^{\tilde{a}}_\beta}{m_\alpha} \int_l (2\pi)\delta(l\cdot v_\beta) \frac{e^{-il\cdot(b_{\alpha\beta}+v_\alpha\tau)}}{l^2} \left[(v_\alpha\cdot v_\beta) l^\mu - (l\cdot v_\alpha) v^\mu_\beta\right]. \tag{4.115}$$

Focusing on the energy-momentum tensor $\sqrt{|g|}T^{\mu\nu}$,

$$\sqrt{|g|}T^{\mu\nu} = \sum_{\alpha=1}^N m_\alpha \int d\tau e^{ik\cdot x_\alpha(\tau)} \left(v^\mu_\alpha + \frac{dz^\mu_\alpha(\tau)}{d\tau} + \frac{d\tilde{z}^\mu_\alpha(\tau)}{d\tau}\right)\left(v^\nu_\alpha + \frac{dz^\nu_\alpha(\tau)}{d\tau} + \frac{d\tilde{z}^\nu_\alpha(\tau)}{d\tau}\right). \tag{4.116}$$

The corrections to the position are useful for finding $\sqrt{|g|}T^{\mu\nu}|_{\Delta A}$, given by

$$\sqrt{|g|}T^{\mu\nu}(k)|_{\Delta A} = \sum_{\alpha=1}^N m_\alpha \int d\tau e^{ik\cdot(b_\alpha+v_\alpha\tau)} \left[ik\cdot\tilde{z}_\alpha(\tau) v^\mu_\alpha v^\nu_\alpha + \frac{d\tilde{z}^\mu_\alpha(\tau)}{d\tau} v^\nu_\alpha + v^\mu_\alpha \frac{d\tilde{z}^\nu_\alpha(\tau)}{d\tau}\right], \tag{4.117}$$

Similar to the previous section, corrections from the gravitational, dilaton, gauge fields can be separated. The deflection $\tilde{z}^\mu_\alpha$ contributes to the source by

$$\begin{aligned}\sqrt{|g|}T^{\mu\nu}(k)|_{\Delta A} &= \tilde{g}^2 \sum_{\substack{\alpha=1\\ \beta\neq\alpha}}^N c^{\tilde{a}}_\alpha c^{\tilde{a}}_\beta \int_{l_\alpha, l_\beta} \mu_{\alpha,\beta}(k) \frac{l^2_\alpha}{k\cdot v_\alpha} \left[v^\mu_\alpha v^\nu_\alpha \left(v_\alpha\cdot v_\beta \frac{k\cdot l_\beta}{k\cdot v_\alpha} - k\cdot v_\beta\right)\right. \\ &\quad \left. + (v^\mu_\alpha v^\nu_\beta + v^\nu_\alpha v^\mu_\beta)(k\cdot v_\alpha) - (v^\mu_\alpha l^\nu_\beta + v^\nu_\alpha l^\mu_\beta)(v_\alpha\cdot v_\beta)\right].\end{aligned} \tag{4.118}$$

When calculated algebraically from Eq. (4.110), the diagram with internal gauge bosons gives

$$\begin{aligned}\hat{t}^{\mu\nu}(k)|_{\Delta A} &= \tilde{g}^2 \sum_{\substack{\alpha=1\\ \beta\neq\alpha}}^N c^{\tilde{a}}_\alpha c^{\tilde{a}}_\beta \int_{l_\alpha, l_\beta} \mu_{\alpha,\beta}(k) \left[\frac{1}{2}\left(v^\mu_\alpha v^\nu_\beta + v^\nu_\alpha v^\mu_\alpha\right) l_\alpha\cdot l_\beta \right. \\ &\quad \left. + (v^\mu_\alpha l^\nu_\alpha + v^\nu_\alpha l^\mu_\alpha)\, k\cdot v_\beta - l^\mu_\alpha l^\nu_\alpha v_\alpha\cdot v_\beta - \frac{1}{2}\eta^{\mu\nu}\left(k\cdot v_\alpha k\cdot v_\beta + v_\alpha\cdot v_\beta l_\alpha\cdot l_\beta\right)\right].\end{aligned} \tag{4.119}$$

Calculated in Section (A.3), the radiative Feynman rules for the Einstein-Yang-Mills three-point vertex diagram are shown to agree with the algebraic result above. Similar to the dilaton, $\hat{t}^{\mu\nu}|_{\Delta A} = t^{\mu\nu}|_{\Delta A}$, as the difference between $\hat{t}^{\mu\nu}$ and $t^{\mu\nu}$ only depends on the gravita-

tional field $h^{\mu\nu}$, not $A^{\mu\tilde{a}}$. Adding $\sqrt{|g|}T^{\mu\nu}|_{\Delta A}$ and $\hat{t}^{\mu\nu}|_{\Delta A}$ gives

$$\begin{aligned}\tilde{T}^{\mu\nu}|_{\mathcal{O}(\tilde{g}^2)} &= \tilde{g}^2 \sum_{\substack{\alpha=1\\ \beta\neq\alpha}}^{N} \int_{l_\alpha, l_\beta} \mu_{\alpha,\beta}(k) \left[v_\alpha^\mu v_\alpha^\nu \left(v_\alpha \cdot v_\beta \frac{k\cdot l_\beta}{(k\cdot v_\alpha)^2} - \frac{k\cdot v_\beta}{k\cdot v_\alpha} \right) l_\alpha^2 + \frac{1}{2}(v_\alpha^\mu v_\beta^\nu + v_\alpha^\nu v_\beta^\mu) l_\alpha^2 \right. \\ &\quad \left. + (v_\alpha^\mu l_\alpha^\nu + v_\alpha^\nu l_\alpha^\mu) \left(\frac{l_\alpha^2 v_\alpha \cdot v_\beta}{k\cdot v_\alpha} + k\cdot v_\beta \right) - l_\alpha^\mu l_\alpha^\nu v_\alpha \cdot v_\beta - \frac{1}{2}\eta^{\mu\nu}\left(k\cdot v_\alpha k\cdot v_\beta + l_\alpha^2 v_\alpha \cdot v_\beta \right) \right]. \end{aligned} \tag{4.120}$$

Adding this result to $\tilde{T}^{\mu\nu}|_{\mathcal{O}(\kappa^2)}$, calculated in Eq. (4.61), gives the total source for gravitational radiation for Einstein-Yang-Mills theory. Next, we show that this result agrees precisely with what is found with the radiative double-copy method.

4.4.3 The Radiative Double Copy

In order to use the double copy to find gravitational radiation in Einstein-Yang-Mills theory, the same replacement rules used for general relativity may be used with the radiation found in Yang-Mills-biadjoint-scalar theory. Applying the double copy replacement rules in Eq. (4.63) to Eq. (4.106) in addition to sending $y \to \tilde{g}$ gives

$$\begin{aligned}\hat{T}^{\mu\nu}(k)|_{\tilde{g}^2} &= \tilde{g}^2 \sum_{\substack{\alpha=1\\ \beta\neq\alpha}}^{N} m_\alpha m_\beta c_\alpha^{\tilde{a}} c_\beta^{\tilde{a}} \int_{l_\alpha, l_\beta} \mu_{\alpha,\beta}(k) \left[v_\alpha \cdot v_\beta \frac{l_\alpha^2 v_\alpha^\nu}{k\cdot v_\alpha} \left(\frac{k\cdot l_\beta}{k\cdot v_\alpha} v_\alpha^\mu - l_\beta^\mu \right) \right. \\ &\quad \left. - \frac{1}{2}\left(2k\cdot v_\beta v_\alpha^\nu - 2k\cdot v_\alpha v_\beta^\nu + v_\alpha \cdot v_\beta (l_\beta - l_\alpha)^\nu \right) \left(\frac{l_\alpha^2}{k\cdot v_\alpha} v_\alpha^\mu - l_\alpha^\mu \right) \right] \end{aligned} \tag{4.121}$$

Shifting $l_\beta^\mu \to (l_\beta - l_\alpha)^\mu/2$ gives the gauge invariant $\hat{T}^{\mu\nu}$,

$$\begin{aligned}\hat{T}^{\mu\nu}(k)|_{\mathcal{O}(\tilde{g}^2)} &= \tilde{g}^2 \sum_{\substack{\alpha=1\\ \beta\neq\alpha}}^{N} m_\alpha m_\beta c_\alpha^{\tilde{a}} c_\beta^{\tilde{a}} \int_{l_\alpha, l_\beta} \mu_{\alpha,\beta}(k) \\ &\quad \times \left[v_\alpha \cdot v_\beta \frac{l_\alpha^2 v_\alpha^\nu}{k\cdot v_\alpha} \left(\frac{k\cdot l_\beta}{k\cdot v_\alpha} v_\alpha^\mu - \frac{1}{2}(l_\beta - l_\alpha)^\mu \right) \right. \\ &\quad \left. - \frac{1}{2}\left(2k\cdot v_\beta v_\alpha^\nu - 2k\cdot v_\alpha v_\beta^\nu + v_\alpha \cdot v_\beta (l_\beta - l_\alpha)^\nu \right) \left(\frac{l_\alpha^2}{k\cdot v_\alpha} v_\alpha^\mu - l_\alpha^\mu \right) \right] \end{aligned} \tag{4.122}$$

Symmetrizing this result gives the appropriate final expression for $\hat{T}^{\mu\nu}$,

$$\begin{aligned}\hat{T}^{\mu\nu}|_{\mathcal{O}(\tilde{g}^2)} &= -\tilde{g}^2\left(\frac{\kappa}{2}\right)^2\sum_{\substack{\alpha=1\\\beta\neq\alpha}}^{N} m_\alpha m_\beta c_\alpha^{\tilde{a}} c_\beta^{\tilde{a}} \int_{l_\alpha,l_\beta} \mu_{\alpha,\beta}(k) \\ &\quad\times\left[v_\alpha^\mu v_\alpha^\nu\left(\frac{k\cdot v_\beta}{k\cdot v_\alpha}-\frac{v_\alpha\cdot v_\beta}{(k\cdot v_\alpha)^2}k\cdot l_\beta\right)l_\alpha^2-\frac{1}{2}(v_\alpha^\mu v_\beta^\nu+v_\alpha^\nu v_\beta^\mu)l_\alpha^2\right. \\ &\quad\left.-(v_\alpha^\mu l_\alpha^\nu+v_\alpha^\nu l_\alpha^\mu)\left(\frac{v_\alpha\cdot v_\beta}{k\cdot v_\alpha}l_\alpha^2+k\cdot v_\beta\right)+l_\alpha^\mu l_\alpha^\nu(v_\alpha\cdot v_\beta)+\frac{1}{2}\eta^{\mu\nu}l_\alpha^2(v_\alpha\cdot v_\beta)\right],\end{aligned}$$

where the gauge condition allows for $v_\alpha^\mu k^\nu = \frac{1}{2}\eta^{\mu\nu}k\cdot v_\alpha$. This result agrees precisely with what was found in Eq. (4.120), demonstrating that the radiative double copy holds for Einstein-Yang-Mills theory.

4.4.4 Einstein-Maxwell Theory

Since it is more physically relevant to scatter massive point particles with electric charge rather than particles with weak-isospin or color, an Abelian $U(1)$ gauge symmetry is also worth studying. The action for fields in Einstein-Maxwell theory is

$$S=\int d^dx\sqrt{|g|}\left(-\frac{2}{\kappa^2}R-\frac{1}{4}g^{\mu\rho}g^{\nu\sigma}F_{\mu\nu}F_{\rho\sigma}\right). \tag{4.123}$$

When comparing with Einstein-Yang-Mills theory, the Maxwell field A^μ can be recovered from a single component of the Yang-Mills field $A^{\mu\tilde{a}}$. In order to find results in Einstein-Maxwell theory from Einstein-Yang-Mills theory, care must be taken with the coupling constants. For exampe, the Maxwell current density for point particles is given by

$$J^\mu(x)=e\sum_{\alpha=1}^{N}q_\alpha\int d\tau v_\alpha^\mu(\tau)\delta^d(x-x_\alpha(\tau)), \tag{4.124}$$

where $q_\alpha = -1$ for electrons, such that eq_α represents the electric charge of particle α. In order to recover Einstein-Maxwell theory from Einstein-Yang-Mills, one must substitute $\tilde{g}\to e$ and $c_\alpha^{\tilde{a}}\to q_\alpha$, given our conventions for $\tilde{g}$ and the normalization of the Lagrangian given in Eq. (4.107). Applying these substitutions to Eq. (4.120) would give gravitational radiation in Einstein-Maxwell theory. At higher orders, $f^{\tilde{a}\tilde{b}\tilde{c}}$ would be sent to zero as well.

In terms of the radiative double copy, an adjoint scalar field Φ^a could also be seen as a single component of the biadjoint scalar feld $\Phi^{\tilde{a}a}$. Results for Yang-Mills-adjoint-scalar

theory can easily be found from Eq. (4.106) by properly sending $c_\alpha^{\tilde{a}} \to q_\alpha$ and reinterpreting y as the coupling constant of the adjoint scalar theory. It is straightforward to see that the double copy of Yang-Mills-adjoint-scalar theory gives solutions in Einstein-Maxwell theory with the replacement rules shown in Eq. (4.63) and $y \to e$.

CHAPTER 5

Conclusions

This thesis explores methods in quantum scattering amplitudes and classical radiation solutions. In particular, the BCJ relations are connected to color-kinematics duality in scattering amplitudes, which becomes evident when factoring the amplitude in to color and kinematic numerators. Chapter 2 applies the tree-level BCJ relations to give loop-level integral coefficient relations. The double copy refers to replacing the non-Abelian charge factor with a kinematic one, which allows for solutions in gravity theories to be found from solutions in gauge theories.

To bridge the gap between quantum scattering amplitudes and classical radiation field solutions, Chapter 3 introduced the study of gravitational waves in linearized gravity. In the pursuit of a radiative double copy, the Lienard-Wiechert potentials of electrodynamics were studied, which motivates the inclusion of a Lienard-Wiechert metric for linearized gravity. While the energy-momentum tensor for free particles did not exhibit a double copy with the electromagnetic current for particles, an effective energy-momentum tensor for interacting point particles was found. Within the context of the classical double copy for linearized gravity, this energy-momentum tensor for interacting point particles can be thought of as a double copy of the electromagnetic current for particles. It was shown that the Lienard-Wiechert metric of linearized gravity reduces to the quadrupole moment method for point particles when taking the nonrelativistic limit.

In Chapter 4, the classical double copy for nonlinear theories is investigated. In previous work, the double copy has been applied to gravitational radiation in general relativity with a dilaton, which suggested that schematic radiative diagrams may be useful for depicting sources of radiation [92]. Similarly, it was shown that the same replacement rules can be

used to find Yang-Mills radiation from biadjoint-scalar radiation [134]. Building off of the initial work of Goldberger and Ridgway, gravitational radiation produced by colliding color charges was found within the context of Einstein-Yang-Mills theory. Our results demonstrate that the double copy can be used to find radiation in Einstein-Yang-Mills theory from Yang-Mills-biadjoint-scalar theory. Also, scalar ghost fields were introduced to remove the dilaton, as shown in Ref. [139], except our results were found in a formalism closer to Refs. [92, 134]. All radiation was derived algebraically, which provided insight on how a radiative diagrammatic scheme closer to Feynman diagrams used for scattering amplitudes may be possible. Furthermore, radiation in Einstein-Maxwell theory can be found via similar methods.

This thesis suggests that it is possible to develop systematic rules to calculate radiation to higher orders. In order to apply a diagrammatic scheme, it appears that Feynman rules for worldline propagators would be needed, in addition to the typical rules used for scattering amplitudes. A radiative double copy to higher orders may be possible, which would provide new calculational tools for precision gravitational wave emission processes.

In future work, it would be interesting to investigate if the radiative double copy holds for higher orders, as the precise replacement rules are not yet known. Additional efforts to perform the integrals are also needed. Studying the formation of bound states at higher orders would also be important [135]. Initial conditions with angular momentum could also be considered. The gravitational interactions between the quantized spin of Dirac particles would also be an interesting theoretical challenge, while considering the scattering of macroscopic mass distributions with classical angular momentum would be more applicable for experiments such as LIGO.

APPENDIX A

Additional Details of Nonlinear Radiation

A.1 Conventions for Yang-Mills-Biadjoint-Scalar Theory

In this section, the conventions used for Yang-Mills-biadjoint-scalar theory are provided. The non-Abelian field strength can be defined up to a sign s_1 as

$$F^a_{\mu\nu} = \partial_\mu A^a_\nu - \partial_\nu A^a_\mu + s_1 g f^{abc} A^b_\mu A^c_\nu, \tag{A.1}$$

where Peskin and Schroeder and Chiodaroli et al. choose $s_1 = +1$ [73, 233]. The vacuum equations for Yang-Mills are typically $D^\mu F^a_{\mu\nu} = 0$. By varying the Lagrangian, we find that this equation of motion is satisfied when

$$D^\mu F^a_{\mu\nu} = \partial^\mu F^a_{\mu\nu} + s_1 g f^{abc} A^{\mu b} F^c_{\mu\nu}, \tag{A.2}$$

where Goldberger and Ridgway have chosen $s_1 = -1$ [92]. Finally, the vector current J^a_μ can be added as a source to the vacuum equations, such that

$$D_\mu F^{\mu\nu a} = s_2 J^{\mu a}, \tag{A.3}$$

where Goldberger and Ridgway choose $s_2 = +1$, while some other sources choose $c_2 = -1$. Finally, different authors choose a different sign convention for the D'Alebertian operator,

$$\Box = s_3 \partial_\mu \partial^\mu, \tag{A.4}$$

where Goldberger and Ridgway choose $s_3 = +1$, a common choice with this metric.

In summary, Goldberger and Ridgway [92] choose conventions such that $(s_1, s_2, s_3) = (-1, +1, +1)$, and we use these conventions in order to not add any minus signs in the radiative double copy replacement rules. The only major difference in our conventions is

that a factor of κ is taken out of $h_{\mu\nu}$, such that $g_{\mu\nu} = \eta_{\mu\nu} + \kappa h_{\mu\nu}$. To keep the same replacement rules, g is absorbed into $J^{\mu a}$, such that $D_\mu F^{\mu\nu a} = J^{\nu a}$ instead of $gJ^{\nu a}$.

A.2 Derivation of Gravitational Radiation from Pseudotensor

In this section, the steps for deriving the gravitational radiation coming from nonlinear gravitational interactions are provided. In Section (4.4), Einstein's field equations to first order for weak gravitational fields was found to be

$$\Box \bar{h}^{\mu\nu} = -\frac{\kappa}{2}\left(T^{\mu\nu} + \hat{t}^{\mu\nu}\right), \tag{A.5}$$

where the energy-momentum pseudotensor $\hat{T}^{\mu\nu} = T^{\mu\nu} + t^{\mu\nu} = \sqrt{|g|}T^{\mu\nu} + \hat{t}^{\mu\nu}$ contains the nonlinear corrections to the linearized field equations, such that the purely gravitational component of the pseudotensor $t^{\mu\nu}$ is given by Eq. (4.45)

$$\begin{aligned} t^{\mu\nu} &= 2h_{\rho\sigma}\left(h^{\mu\rho,\nu\sigma} + h^{\nu\sigma,\mu\rho} - h^{\mu\nu,\rho\sigma} - h^{\rho\sigma,\mu\nu}\right) + h^{\mu\nu}\Box h - 2h^{\mu\rho}\Box h^{\nu}_{\rho} - 2h^{\nu\rho}\Box h^{\mu}_{\rho} \\ &\quad - 2h^{\mu\rho,\sigma}\left(h^{\nu}_{\rho,\sigma} - h^{\nu}_{\sigma,\rho}\right) - h^{\rho\sigma,\mu}h_{\rho\sigma}^{,\nu} + \eta^{\mu\nu}\left[2h^{\rho\sigma}\Box h_{\rho\sigma} + h_{\rho\sigma,\lambda}\left(\frac{3}{2}h^{\rho\sigma,\lambda} - h^{\rho\lambda,\sigma}\right)\right]. \end{aligned} \tag{A.6}$$

In order to solve for this, the lowest-order solution of the gravitational field is used

$$h^{\mu\nu}(x) = \frac{\kappa}{2}\sum_{\alpha=1}^{N} m_\alpha \int_{l_\alpha} (2\pi)\delta(l_\alpha \cdot v_\alpha)\frac{e^{-il_\alpha\cdot(x-b_\alpha)}}{l_\alpha^2}\left(v_\alpha^\mu v_\alpha^\nu - \frac{\eta^{\mu\nu}}{d-2}\right), \tag{A.7}$$

which gives rise to a source for the nonlinear gravitational interaction via $t^{\mu\nu}$. Each term in $t^{\mu\nu}$ is second order in $h^{\mu\nu}$, so one is related to particle α and another to particle β, giving a double sum. The summation and integrals on all terms will have the following form

$$t^{\mu\nu} = \left(\frac{\kappa}{2}\right)^2 \sum_{\substack{\alpha=1 \\ \beta\neq\alpha}}^{N} m_\alpha m_\beta \int_{l_\alpha, l_\beta} \mu_{\alpha,\beta}(k) I^{\mu\nu}, \tag{A.8}$$

where $I^{\mu\nu}$ is the integrand containing many terms. For the integrand, focusing on the $(v_\alpha^\mu v_\alpha^\nu - \eta^{\mu\nu}/(d-2))$ portion of the solution to $h^{\mu\nu}$ and manually plug these pieces into

Eq. (A.6) gives

$$
\begin{aligned}
I^{\mu\nu} &= 2\left(v_{\beta\rho}v_{\beta\sigma}-\frac{\eta_{\rho\sigma}}{d-2}\right)\left[-l_\alpha^\nu l_\alpha^\sigma\left(v_\alpha^\mu v_\alpha^\rho-\frac{\eta^{\mu\rho}}{d-2}\right)-l_\alpha^\mu l_\alpha^\rho\left(v_\alpha^\nu v_\alpha^\sigma-\frac{\eta^{\nu\sigma}}{d-2}\right)\right.\\
&\qquad\left.+\,l_\alpha^\rho l_\alpha^\sigma\left(v_\alpha^\mu v_\alpha^\nu-\frac{\eta^{\mu\nu}}{d-2}\right)+l_\alpha^\mu l_\alpha^\nu\left(v_\alpha^\rho v_\alpha^\sigma-\frac{\eta^{\rho\sigma}}{d-2}\right)\right]-l_\beta^2\left(v_\alpha^\mu v_\alpha^\nu-\frac{\eta^{\mu\nu}}{d-2}\right)\left(\frac{-2}{d-2}\right)\\
&\quad+2l_\alpha^2\left(v_\beta^\mu v_\beta^\rho-\frac{\eta^{\mu\rho}}{d-2}\right)\left(v_{\alpha\rho}v_\alpha^\nu-\frac{\eta_\rho^\nu}{d-2}\right)+2l_\alpha^2\left(v_\beta^\nu v_\beta^\rho-\frac{\eta^{\nu\rho}}{d-2}\right)\left(v_{\alpha\rho}v_\alpha^\mu-\frac{\eta_\rho^\mu}{d-2}\right)\\
&\quad-2il_\alpha^\sigma\left(v_\alpha^\mu v_\alpha^\rho-\frac{\eta^{\mu\rho}}{d-2}\right)\left[il_{\beta\sigma}\left(v_\beta^\nu v_{\beta\rho}-\frac{\eta_\rho^\nu}{d-2}\right)-il_{\beta\rho}\left(v_\beta^\nu v_{\beta\sigma}-\frac{\eta_\sigma^\nu}{d-2}\right)\right]\\
&\quad+l_\alpha^\mu l_\beta^\nu\left(v_\alpha^\rho v_\alpha^\sigma-\frac{\eta^{\rho\sigma}}{d-2}\right)\left(v_{\beta\rho}v_{\beta\sigma}-\frac{\eta_{\rho\sigma}}{d-2}\right)\\
&\quad+\eta^{\mu\nu}\left\{-2l_\alpha^2\left(v_\alpha^\rho v_\alpha^\sigma-\frac{\eta^{\rho\sigma}}{d-2}\right)\left(v_{\beta\rho}v_{\beta\sigma}-\frac{\eta_{\rho\sigma}}{d-2}\right)\right.\\
&\quad\left.+il_{\alpha\lambda}\left(v_{\alpha\rho}v_{\alpha\sigma}-\frac{\eta_{\rho\sigma}}{d-2}\right)\left[\frac{3}{2}il_\beta^\lambda\left(v_\beta^\rho v_\beta^\sigma-\frac{\eta^{\rho\sigma}}{d-2}\right)-il_\beta^\sigma\left(v_\beta^\rho v_\beta^\lambda-\frac{\eta^{\rho\lambda}}{d-2}\right)\right]\right\}. \qquad \text{(A.9)}
\end{aligned}
$$

Distributing these factors and reorganizing all of the terms with the same tensor index structure gives

$$
\begin{aligned}
t^{\mu\nu} &\propto v_\alpha^\mu v_\alpha^\nu\left(2(k\cdot v_\beta)^2-\frac{2l_\alpha^2}{d-2}+\frac{2l_\beta^2}{d-2}-\frac{4l_\alpha^2+4l_\beta^2}{d-2}-\frac{4l_\alpha\cdot l_\beta}{d-2}\right)\\
&\quad+\left(v_\alpha^\mu v_\beta^\nu+v_\alpha^\nu v_\beta^\mu\right)\left(2l_\alpha^2(v_\alpha\cdot v_\beta)+l_\alpha\cdot l_\beta(v_\alpha\cdot v_\beta)-k\cdot v_\alpha k\cdot v_\beta\right)\\
&\quad+(v_\alpha^\mu l_\alpha^\nu+v_\alpha^\nu l_\alpha^\mu)\left(-2(v_\alpha\cdot v_\beta)k\cdot v_\beta+\frac{2k\cdot v_\alpha}{d-2}\right)+(v_\alpha^\mu l_\beta^\nu+v_\alpha^\nu l_\beta^\mu)\left(\frac{2k\cdot v_\alpha}{d-2}\right)\\
&\quad+l_\alpha^\mu l_\alpha^\nu\left(-\frac{4}{(d-2)^2}+2(v_\alpha\cdot v_\beta)^2-\frac{4}{d-2}+\frac{2d}{(d-2)^2}\right)\\
&\quad+(l_\alpha^\mu l_\beta^\nu+l_\alpha^\nu l_\beta^\mu)\left(-\frac{1}{(d-2)^2}+\frac{1}{2}(v_\alpha\cdot v_\beta)^2-\frac{1}{d-2}+\frac{d}{2(d-2)^2}\right)\\
&\quad+\eta^{\mu\nu}\left[-\frac{2(k\cdot v_\beta)^2}{d-2}+\frac{2l_\alpha^2}{(d-2)^2}-\frac{2l_\beta^2}{(d-2)^2}+\frac{4l_\alpha^2}{(d-2)^2}+\frac{2l_\alpha\cdot l_\beta}{(d-2)^2}\right.\\
&\qquad-\left(2l_\alpha^2+\frac{3}{2}l_\alpha\cdot l_\beta\right)\left((v_\alpha\cdot v_\beta)^2-\frac{2}{d-2}+\frac{d}{(d-2)^2}\right)\\
&\qquad\left.+\left(v_\alpha\cdot v_\beta k\cdot v_\alpha k\cdot v_\beta+\frac{l_\alpha\cdot l_\beta}{(d-2)^2}\right)\right]. \qquad \text{(A.10)}
\end{aligned}
$$

Next, the relation $k^2 = l_\alpha^2 + 2l_\alpha\cdot l_\beta + l_\beta^2 = 0$ is used to simplify further. The identity $a^\mu l_\beta^\nu = a^\mu k^\nu - a^\mu l_\alpha^\nu$ and the gauge condition of the gravitational field allows for the gauge-invariant shift $a^\mu l_\beta^\nu \to \frac{1}{2}a\cdot k\eta^{\mu\nu} - a^\mu l_\alpha^\nu$, since dotting this expression with the polarization

tensor would give the same radiation amplitude. Making such changes gives

$$\begin{aligned} t^{\mu\nu} \propto\ & v_\alpha^\mu v_\alpha^\nu \left(2(k\cdot v_\beta)^2 - \frac{4l_\alpha^2}{d-2}\right) + (v_\alpha^\mu v_\beta^\nu + v_\alpha^\nu v_\beta^\mu)\left(l_\alpha^2(v_\alpha\cdot v_\beta) - k\cdot v_\alpha k\cdot v_\beta\right) \\ & - 2(v_\alpha\cdot v_\beta)k\cdot v_\beta(v_\alpha^\mu l_\alpha^\nu + v_\alpha^\nu l_\alpha^\mu) + l_\alpha^\mu l_\alpha^\nu\left((v_\alpha\cdot v_\beta)^2 - \frac{1}{d-2}\right) \\ & + \eta^{\mu\nu}\left(\frac{2(k\cdot v_\alpha)^2}{d-2} + \frac{k\cdot l_\alpha}{2}(v_\alpha\cdot v_\beta)^2 - \frac{k\cdot l_\alpha}{2(d-2)}\right) \\ & + \eta^{\mu\nu}\left[-\frac{2(k\cdot v_\beta)^2}{d-2} + \frac{2l_\alpha^2}{(d-2)^2} - \frac{2l_\beta^2}{(d-2)^2} + \frac{4l_\alpha^2}{(d-2)^2} + \frac{2l_\alpha\cdot l_\beta}{(d-2)^2}\right. \\ & \quad - \left(2l_\alpha^2 + \frac{3}{2}l_\alpha\cdot l_\beta\right)\left((v_\alpha\cdot v_\beta)^2 - \frac{2}{d-2} + \frac{d}{(d-2)^2}\right) \\ & \quad \left. + \left(v_\alpha\cdot v_\beta k\cdot v_\alpha k\cdot v_\beta + \frac{l_\alpha\cdot l_\beta}{(d-2)^2}\right)\right]. \end{aligned} \tag{A.11}$$

By considering that α and β are symmetric, all particle labels may be switched for any term, which allows further simplification to give the final result

$$\begin{aligned} t^{\mu\nu} \propto\ & v_\alpha^\mu v_\alpha^\nu \left(2(k\cdot v_\beta)^2 - \frac{4l_\alpha^2}{d-2}\right) + (v_\alpha^\mu v_\beta^\nu + v_\alpha^\nu v_\beta^\mu)\left(l_\alpha^2(v_\alpha\cdot v_\beta) - k\cdot v_\alpha k\cdot v_\beta\right) \\ & - 2(v_\alpha\cdot v_\beta)k\cdot v_\beta(v_\alpha^\mu l_\alpha^\nu + v_\alpha^\nu l_\alpha^\mu) + l_\alpha^\mu l_\alpha^\nu\left((v_\alpha\cdot v_\beta)^2 - \frac{1}{d-2}\right) \\ & + \eta^{\mu\nu}\left(v_\alpha\cdot v_\beta k\cdot v_\alpha k\cdot v_\beta - \frac{l_\alpha^2}{2}\left((v_\alpha\cdot v_\beta)^2 - \frac{1}{d-2}\right)\right). \end{aligned} \tag{A.12}$$

To more easily compare with the diagrammatic method, $\hat{t}^{\mu\nu}$ is found by adding the lowest-order term of $\left(1-\sqrt{|g|}\right)T^{\mu\nu}$, where

$$\begin{aligned} T^{\mu\nu}(x) &\approx \sum_{\alpha=1}^{N} m_\alpha \int_{l_\alpha} (2\pi)\delta(v_\alpha\cdot l_\alpha)e^{-il_\alpha\cdot(x-b_\alpha)}v_\alpha^\mu v_\alpha^\nu, \\ h(x) &\approx \frac{-\kappa}{d-2}\sum_{\beta\neq\alpha} m_\beta \int_{l_\beta} (2\pi)\delta(l_\beta\cdot v_\beta)\frac{e^{-il_\beta\cdot(x-b_\beta)}}{l_\beta^2}, \\ \left(1-\sqrt{|g|}\right)T^{\mu\nu} &\approx \frac{1}{d-2}\left(\frac{\kappa}{2}\right)^2 \sum m_\alpha m_\beta \int_{l_\alpha,l_\beta} \mu_{\alpha,\beta}(k) 2l_\alpha^2 v_\alpha^\mu v_\alpha^\nu. \end{aligned} \tag{A.13}$$

Adding this to $t^{\mu\nu}$ gives

$$\begin{aligned} \hat{t}^{\mu\nu} \propto\ & v_\alpha^\mu v_\alpha^\nu \left(2(k\cdot v_\beta)^2 - \frac{2l_\alpha^2}{d-2}\right) + (v_\alpha^\mu v_\beta^\nu + v_\alpha^\nu v_\beta^\mu)\left(l_\alpha^2(v_\alpha\cdot v_\beta) - k\cdot v_\alpha k\cdot v_\beta\right) \\ & - 2(v_\alpha\cdot v_\beta)k\cdot v_\beta(v_\alpha^\mu l_\alpha^\nu + v_\alpha^\nu l_\alpha^\mu) + l_\alpha^\mu l_\alpha^\nu\left((v_\alpha\cdot v_\beta)^2 - \frac{1}{d-2}\right) \\ & + \eta^{\mu\nu}\left(v_\alpha\cdot v_\beta k\cdot v_\alpha k\cdot v_\beta - \frac{l_\alpha^2}{2}\left((v_\alpha\cdot v_\beta)^2 - \frac{1}{d-2}\right)\right). \end{aligned} \tag{A.14}$$

As shown in the next section, this result agrees precisely with a diagram involving the three-point graviton vertex.

A.3 Some Radiative Feynman Rules

A.3.1 Yang-Mills and Biadjoint-Scalar Theory

A Feynman diagram approach can be used to find the results for diagrams (1c) and (3c), shown in Figs (4.1) and (4.3). We will briefly describe this method, as it could be useful for organizing higher order corrections. It can also be utilized in conjunction with the algebraic approach to make sure the results are self-consistent. Expanding the kinetic term of the Lagrangian, the $\mathcal{O}(A^3)$ term corresponding to the three-point vector boson interaction is

$$-\frac{1}{4}F^a_{\mu\nu}F^{\mu\nu a} = -\partial_\mu A^a_\nu g f^{abc} A^{\mu b} A^{\nu c} + \dots . \tag{A.15}$$

This term in the Lagrangian gives the textbook non-Abelian three-point vector boson vertex, given by

$$\Gamma^{\mu a,\nu b,\rho c}(k,p,q) = g f^{abc}\left((k^\nu - q^\nu)\eta^{\mu\rho} + (p^\rho - k^\rho)\eta^{\nu\mu} + (q^\mu - p^\mu)\eta^{\rho\nu}\right), \tag{A.16}$$

where A^a_μ is associated with the momentum k, A^b_ν is associated with p, and A^c_ρ is associated with q.

The three-point vertex for two biadjoint scalars and one adjoint vector field can be used to efficiently calculate a piece radiation, which comes from the kinetic term of the biadjoint scalar. Focusing on the terms in the Lagrangian to $\mathcal{O}(\Phi^2 A)$,

$$\frac{1}{2}(D_\mu \Phi^{\tilde{a}})^a (D^\mu \Phi^{\tilde{b}})^a \delta^{\tilde{a}\tilde{b}} = g f^{abc}\delta^{\tilde{a}\tilde{c}}(\partial_\mu \Phi^{\tilde{a}a}) A^{\mu b}\Phi^{\tilde{c}c} + \dots . \tag{A.17}$$

Taking the appropriate functional derivatives and properly symmetrizing gives the three-point vertex for two scalars and one vector, giving

$$\Gamma^{\tilde{a}a,\nu b,\tilde{c}c}(k,p,q) = g f^{abc}\delta^{\tilde{a}\tilde{c}}\left(k^\nu - q^\nu\right). \tag{A.18}$$

The three-point vertices above can be used to find diagrams (1c) and (3c) shown in Figs. (4.1) and (4.3), giving

$$(1c)^{\mu a}(k) = \frac{1}{2}\int_{l_\alpha,l_\beta} A^b_\nu(l_\alpha)|_{\mathcal{O}(g^1)} i\Gamma^{\mu a,\nu b,\rho c}(-k,l_\alpha,l_\beta)A^c_\rho(l_\beta)|_{\mathcal{O}(g^1)}(2\pi)^d\delta^d(k-l_\alpha-l_\beta),$$
$$(1f)^{\mu a}(k) = \frac{1}{2}\int_{l_\alpha,l_\beta} \Phi^{\tilde{b}b}(l_\alpha)|_{\mathcal{O}(y^1)} i\Gamma^{\tilde{b}b,\mu a,\tilde{c}c}(l_\alpha,-k,l_\beta)\Phi^{\tilde{c}c}(l_\beta)|_{\mathcal{O}(y^1)}(2\pi)^d\delta^d(k-l_\alpha-l_\beta), \quad (A.19)$$

where a symmetry factor of 1/2 has been added.

The solutions needed for these diagrams were found in Eqs. (4.13) and (4.94), giving

$$\begin{aligned} A^{\mu a}(l_\alpha)|_{\mathcal{O}(g^1)} &= -g\sum_{\alpha=1}^{N}(2\pi)\delta(l_\alpha\cdot v_\alpha)\frac{e^{il_\alpha\cdot b_\alpha}}{l_\alpha^2}v_\alpha^\mu c_\alpha^a, \\ \Phi^{a\tilde{a}}(l_\alpha)|_{\mathcal{O}(y^1)} &= -y\sum_{\alpha=1}^{N}(2\pi)\delta(l_\alpha\cdot v_\alpha)\frac{e^{il_\alpha\cdot b_\alpha}}{l_\alpha^2}c_\alpha^a c_\alpha^{\tilde{a}}. \end{aligned} \quad (A.20)$$

Plugging in these solutions gives

$$\begin{aligned} (1c)^{\mu a}(k) &= \frac{g^3}{2}\sum_{\alpha\neq\beta} if^{abc}c_\alpha^b c_\beta^c\int_{l_\alpha,l_\beta}\mu_{\alpha,\beta}(k)\left[-2k\cdot v_\alpha v_\beta^\mu + 2k\cdot v_\beta v_\alpha^\mu + v_\alpha\cdot v_\beta(l_\beta-l_\alpha)^\mu\right], \\ (1f)^{\mu a}(k) &= \frac{gy^2}{2}\sum_{\beta\neq\alpha} if^{abc}c_\alpha^b c_\beta^c c_\alpha^{\tilde{a}}c_\beta^{\tilde{a}}\int_{l_\alpha,l_\beta}\mu_{\alpha,\beta}(k)(l_\alpha-l_\beta)^\mu. \end{aligned} \quad (A.21)$$

Due to the antisymmetry of $f^{abc}c_\alpha^b c_\beta^c$, switching $\alpha\leftrightarrow\beta$ for a term multiplied by this factor introduces a minus sign, allowing further simplification,

$$\begin{aligned} (1c)^{\mu a}(k) &= g^3\sum_{\alpha\neq\beta} if^{abc}c_\alpha^b c_\beta^c\int_{l_\alpha,l_\beta}\mu_{\alpha,\beta}(k)\left[2k\cdot v_\beta v_\alpha^\mu - (v_\alpha\cdot v_\beta)l_\alpha^\mu\right], \\ (1f)^{\mu a}(k) &= gy^2\sum_{\beta\neq\alpha} if^{abc}c_\alpha^b c_\beta^c c_\alpha^{\tilde{a}}c_\beta^{\tilde{a}}\int_{l_\alpha,l_\beta}\mu_{\alpha,\beta}(k)l_\alpha^\mu. \end{aligned} \quad (A.22)$$

Note how this result agrees with the algebraic method found in Eqs. (4.26) and (4.105).

A.3.2 General Relativity and Einstein-Yang-Mills Theory

Next, the three-point graviton vertex will be used to stitch together lower order gravitational field solutions to generate a piece of the gravitational radiation field. The three-point graviton

vertex from DeWitt [234] and utilized by Sannan [235] is

$$
\begin{aligned}
V_{\mu\alpha,\nu\beta,\sigma\gamma}(k_1,k_2,k_3) \;=\; & \text{sym}\left[-\frac{1}{2}P_3(k_1\cdot k_2\eta_{\mu\alpha}\eta_{\nu\beta}\eta_{\sigma\gamma}) - \frac{1}{2}P_6(k_{1\nu}k_{1\beta}\eta_{\mu\alpha}\eta_{\sigma\gamma})\right. \\
& + \frac{1}{2}P_3(k_1\cdot k_2\eta_{\mu\nu}\eta_{\alpha\beta}\eta_{\sigma\gamma}) + P_6(k_1\cdot k_2\eta_{\mu\alpha}\eta_{\nu\sigma}\eta_{\beta\gamma}) + 2P_3(k_{1\nu}k_{1\gamma}\eta_{\mu\alpha}\eta_{\beta\sigma}) \\
& - P_3(k_{1\beta}k_{2\mu}\eta_{\alpha\nu}\eta_{\sigma\gamma}) + P_3(k_{1\sigma}k_{2\gamma}\eta_{\mu\nu}\eta_{\alpha\beta}) + P_6(k_{1\sigma}k_{1\gamma}\eta_{\mu\nu}\eta_{\alpha\beta}) \\
& \left. + 2P_6(k_{1\nu}k_{2\gamma}\eta_{\beta\mu}\eta_{\alpha\sigma}) + 2P_3(k_{1\nu}k_{2\mu}\eta_{\beta\sigma}\eta_{\gamma\alpha}) - 2P_3(k_1\cdot k_2\eta_{\alpha\nu}\eta_{\beta\sigma}\eta_{\gamma\mu})\right],
\end{aligned}
\tag{A.23}
$$

where P_3 and P_6 refers to a permutation of k_1, k_2, and k_3 resulting in 3 or 6 terms, respectively, and sym applies a symmetrization across $\mu\alpha$, $\nu\beta$, and $\sigma\gamma$. For example,

$$
\begin{aligned}
P_3(k_1\cdot k_2\eta_{\mu\nu}\eta_{\alpha\beta}\eta_{\sigma\gamma}) \;&=\; k_1\cdot k_2\eta_{\mu\nu}\eta_{\alpha\beta}\eta_{\sigma\gamma} + k_2\cdot k_3\eta_{\nu\sigma}\eta_{\beta\gamma}\eta_{\mu\alpha} + k_3\cdot k_1\eta_{\mu\sigma}\eta_{\alpha\gamma}\eta_{\nu\beta}, \\
\text{sym}[\eta_{\mu\nu}\eta_{\alpha\beta}] \;&=\; \frac{1}{4}\left(\eta_{\mu\nu}\eta_{\alpha\beta} + \eta_{\mu\beta}\eta_{\nu\alpha} + \eta_{\nu\alpha}\eta_{\mu\beta} + \eta_{\alpha\beta}\eta_{\mu\nu}\right).
\end{aligned}
\tag{A.24}
$$

Expanding P_3 and P_6 gives

$$
\begin{aligned}
V^{\mu\alpha,\nu\beta,\sigma\gamma}(k_1,k_2,k_3) \;=\; & \text{sym}\left[-\frac{1}{2}\left(k_1\cdot k_2 + k_2\cdot k_3 + k_3\cdot k_1\right)\eta^{\mu\alpha}\eta^{\nu\beta}\eta^{\sigma\gamma}\right. \\
& - \frac{1}{2}\left(k_1^\nu k_1^\beta\eta^{\mu\alpha}\eta^{\sigma\gamma} + k_1^\sigma k_1^\gamma\eta^{\mu\alpha}\eta^{\nu\beta}k_2^\mu k_2^\alpha\eta^{\nu\beta}\eta^{\sigma\gamma}\right. \\
& \left. + k_2^\sigma k_2^\gamma\eta^{\mu\alpha}\eta^{\nu\beta} + k_3^\mu k_3^\alpha\eta^{\nu\beta}\eta^{\gamma\sigma} + k_3^\nu k_3^\beta\eta^{\mu\alpha}\eta^{\gamma\sigma}\right) \\
& + \frac{1}{2}\left(k_1\cdot k_2\eta^{\mu\nu}\eta^{\alpha\beta}\eta^{\sigma\gamma} + k_2\cdot k_3\eta^{\nu\sigma}\eta^{\beta\gamma}\eta^{\mu\alpha} + k_3\cdot k_1\eta^{\mu\sigma}\eta^{\alpha\gamma}\eta^{\nu\beta}\right) \\
& + \left(k_1\cdot k_2\eta^{\mu\alpha}\eta^{\nu\sigma}\eta^{\beta\gamma} + k_1\cdot k_2\eta^{\nu\beta}\eta^{\mu\sigma}\eta^{\alpha\gamma} + k_2\cdot k_3\eta^{\nu\beta}\eta^{\mu\sigma}\eta^{\alpha\gamma}\right. \\
& \left. + k_2\cdot k_3\eta^{\sigma\gamma}\eta^{\mu\nu}\eta^{\alpha\beta} + k_3\cdot k_1\eta^{\sigma\gamma}\eta^{\mu\nu}\eta^{\alpha\beta} + k_3\cdot k_1\eta^{\mu\alpha}\eta^{\nu\sigma}\eta^{\beta\gamma}\right) \\
& + 2\left(k_1^\nu k_1^\gamma\eta^{\mu\alpha}\eta^{\beta\sigma} + k_2^\sigma k_2^\mu\eta^{\nu\beta}\eta^{\gamma\mu} + k_3^\mu k_3^\beta\eta^{\sigma\gamma}\eta^{\alpha\nu}\right) \\
& - \left(k_1^\beta k_2^\mu\eta^{\alpha\nu}\eta^{\sigma\gamma} + k_2^\gamma k_3^\nu\eta^{\beta\sigma}\eta^{\mu\alpha} + k_3^\beta k_1^\mu\eta^{\gamma\mu}\eta^{\nu\beta}\right) \\
& + \left(k_1^\sigma k_2^\gamma\eta^{\mu\nu}\eta^{\alpha\beta} + k_2^\mu k_3^\alpha\eta^{\nu\sigma}\eta^{\beta\gamma} + k_3^\nu k_1^\beta\eta^{\sigma\mu}\eta^{\gamma\alpha}\right) \\
& + \left(k_1^\sigma k_1^\gamma\eta^{\mu\nu}\eta^{\alpha\beta} + k_1^\nu k_1^\beta\eta^{\mu\sigma}\eta^{\alpha\gamma} + k_2^\mu k_2^\alpha\eta^{\nu\sigma}\eta^{\beta\gamma}\right. \\
& \left. + k_2^\sigma k_2^\gamma\eta^{\nu\mu}\eta^{\gamma\alpha} + k_3^\nu k_3^\beta\eta^{\sigma\mu}\eta^{\gamma\alpha} + k_3^\mu k_3^\alpha\eta^{\sigma\nu}\eta^{\alpha\beta}\right) \\
& + 2\left(k_1^\nu k_2^\gamma\eta^{\beta\mu}\eta^{\alpha\sigma} + k_1^\mu k_2^\gamma\eta^{\alpha\nu}\eta^{\beta\sigma} + k_2^\sigma k_3^\alpha\eta^{\gamma\nu}\eta^{\beta\mu}\right. \\
& \left. + k_2^\nu k_3^\alpha\eta^{\beta\sigma}\eta^{\gamma\mu} + k_3^\mu k_1^\beta\eta^{\alpha\sigma}\eta^{\gamma\nu} + k_3^\sigma k_1^\beta\eta^{\gamma\mu}\eta^{\alpha\sigma}\right) \\
& + 2\left(k_1^\nu k_2^\mu\eta^{\beta\sigma}\eta^{\gamma\alpha} + k_2^\sigma k_3^\nu\eta^{\gamma\mu}\eta^{\alpha\beta} + k_3^\mu k_1^\sigma\eta^{\alpha\nu}\eta^{\beta\gamma}\right) \\
& \left. - 2\left(k_1\cdot k_2\eta^{\alpha\nu}\eta^{\beta\sigma}\eta^{\gamma\mu} + k_2\cdot k_3\eta^{\beta\sigma}\eta^{\gamma\mu}\eta^{\alpha\nu} + k_3\cdot k_1\eta^{\gamma\mu}\eta^{\alpha\nu}\eta^{\gamma\sigma}\right)\right].
\end{aligned}
\tag{A.25}
$$

To find the radiative field contribution from this three-point vertex, two instances of the lowest-order field solution will be stitched together with this vertex to find a higher order contribution. The lowest-order field in momentum space is given by

$$h^{\rho\sigma}(l_\alpha) = \frac{\kappa}{2}\sum_\alpha^N m_\alpha \frac{e^{il_\alpha\cdot b_\alpha}}{l_\alpha^2}(2\pi)\delta(l_\alpha\cdot v_\alpha)\left[v_\alpha^\rho v_\alpha^\sigma - \frac{\eta^{\rho\sigma}}{d-2}\right]. \tag{A.26}$$

The three-point vertex allows for a purely gravitational source to be found, which corresponds to a component of the pseudotensor, $t^{\mu\nu}$. This component of the source that generates radiation is given by

$$t^{\sigma\lambda}(k) = \frac{1}{2}\int_{l_\alpha,l_\beta} V^{\mu\rho,\nu\tau,\sigma\lambda}(-l_\alpha,-l_\beta,k)h_{\mu\rho}(l_\alpha)h_{\nu\tau}(l_\beta)\delta^d(k-l_\alpha-l_\beta). \tag{A.27}$$

Since the lowest-order solutions for l_α and l_β are symmetric, the symmetrization is only needed for indices σ and λ in $V^{\mu\rho,\nu\tau,\sigma\lambda}$. Focusing on the integrand and breaking down the two lowest-order solutions into four terms gives

$$h^{\mu\rho}(l_\alpha)h^{\nu\tau}(l_\beta) \propto \left[v_\alpha^\mu v_\alpha^\rho v_\beta^\nu v_\beta^\tau - \frac{1}{d-2}\left(v_\alpha^\mu v_\alpha^\rho \eta^{\nu\tau} + v_\beta^\nu v_\beta^\tau \eta^{\mu\rho}\right) + \frac{1}{(d-2)^2}\left(\eta^{\mu\rho}\eta^{\nu\tau}\right)\right]. \tag{A.28}$$

It is straightforward to perform the index contractions with Mathematica to simplify the result, giving

$$\begin{aligned} V^{\mu\rho,\nu\tau,\sigma\lambda}h_{\mu\rho}h_{\nu\tau} \quad \propto \quad & \left[2v_\alpha^\sigma v_\alpha^\lambda\left((k\cdot v_\beta)^2 - \frac{l_\alpha^2}{d-2}\right) + \left(v_\alpha^\sigma v_\beta^\lambda + v_\alpha^\lambda v_\beta^\sigma\right)\left(l_\alpha^2 v_\alpha\cdot v_\beta - k\cdot v_\alpha k\cdot v_\beta\right)\right. \\ & - 2\left(v_\alpha^\sigma l_\alpha^\lambda + v_\alpha^\lambda l_\alpha^\sigma\right)(v_\alpha\cdot v_\beta k\cdot v_\beta) + l_\alpha^\sigma l_\alpha^\lambda\left((v_\alpha\cdot v_\beta)^2 - \frac{1}{d-2}\right) \\ & \left. + \eta^{\sigma\lambda}\left(k\cdot v_\alpha k\cdot v_\beta v_\alpha\cdot v_\beta - \frac{l_\alpha^2}{2}\left((v_\alpha\cdot v_\beta)^2 - \frac{1}{d-2}\right)\right)\right], \end{aligned} \tag{A.29}$$

where this result gives the integrand of the diagram (2c).

For calculating the additional gravitational radiation diagrams due to Yang-Mills contributions, the Feynman rules for scattering outlined by Rodigast's thesis give the necessary three-point vertex [236, 237]. The Feynman rule for the three-point vertex with two gluons and one graviton can be found from the interaction term in the Lagrangian,

$$\begin{aligned} \mathcal{L} &= \sqrt{-g}g^{\mu\rho}g^{\nu\sigma}\partial_\mu A_\nu^a \partial_{[\rho}A_{\sigma]}^a + \ldots \\ &\approx \kappa\left(\eta^{\mu\tau}\eta^{\rho\lambda}\eta^{\nu\sigma} + \eta^{\mu\rho}\eta^{\nu\tau}\eta^{\sigma\lambda} - \frac{1}{2}\eta^{\tau\lambda}\eta^{\mu\rho}\eta^{\nu\sigma}\right)h_{\tau\lambda}\partial_\mu A_\nu^a\partial_{[\rho}A_{\sigma]}^a. \end{aligned} \tag{A.30}$$

Taking the functional derivatives and properly symmetrizing over all indices and momenta gives

$$\begin{aligned}\Gamma^{\tau\lambda,\mu\tilde{a},\nu\tilde{b}}(k,p,q) &= -2i\delta^{\tilde{a}\tilde{b}}\left(p^{(\tau}q^{\lambda)}\eta^{\mu\nu}+\frac{1}{2}p\cdot q(\eta^{\tau\mu}\eta^{\lambda\nu}\eta^{\tau\nu}\eta^{\lambda\mu}-\eta^{\tau\lambda}\eta^{\mu\nu})\right.\\ &\quad\left.+\frac{1}{2}\eta^{\tau\lambda}p^{\nu}q^{\mu}-q^{\mu}\eta^{\nu(\lambda}p^{\tau)}-p^{\nu}\eta^{\mu(\tau}q^{\lambda)}\right),\end{aligned} \tag{A.31}$$

where a factor of $2/\kappa$ was added to have the same conventions as DeWitt's three-point vertex. This allows us to use the same formula for calculating the contribution to the radiation source. By reusing the lowest-order result for $A^{\mu a}(l)|_{\mathcal{O}(g^1)}$ and switching $a \to \tilde{a}$, the solution to diagram (4c) is

$$(2\mathrm{i})^{\mu\nu} = \frac{1}{2}\int_{l_\alpha,l_\beta} i\Gamma^{\mu\nu,\rho\tilde{a},\sigma\tilde{b}}(-k,l_\alpha,l_\beta)A^{\tilde{a}}_{\rho}(l_\alpha)|_{\mathcal{O}(g^1)}A^{\tilde{b}}_{\sigma}(l_\beta)|_{\mathcal{O}(g^1)}\delta^d(k-l_\alpha-l_\beta). \tag{A.32}$$

Plugging in the lowest-order solution gives

$$\begin{aligned}(2\mathrm{i})^{\mu\nu} &= \tilde{g}^2\sum_{\substack{\alpha=1\\ \beta\neq\alpha}}^{N}\int_{l_\alpha,l_\beta}\mu_{\alpha,\beta}(k)c^{\tilde{a}}_{\alpha}c^{\tilde{a}}_{\beta}\left[\frac{1}{2}(v^{\mu}_{\alpha}v^{\nu}_{\beta}+v^{\nu}_{\alpha}v^{\mu}_{\beta}-\eta^{\mu\nu}v_\alpha\cdot v_\beta)l_\alpha\cdot l_\beta\right.\\ &\quad\left.+v_\alpha\cdot v_\beta l^{(\mu}_{\alpha}l^{\nu)}_{\beta}+\frac{1}{2}\eta^{\mu\nu}k\cdot v_\alpha k\cdot v_\beta-k\cdot v_\beta v^{(\mu}_{\alpha}l^{\nu)}_{\beta}-k\cdot v_\alpha v^{(\mu}_{\beta}l^{\nu)}_{\alpha}\right],\end{aligned} \tag{A.33}$$

which can be shown to agree with the algebraic result found in Eq. (4.120).

Bibliography

[1] H. Kawai, D. C. Lewellen, and S. H. H. Tye. A Relation Between Tree Amplitudes of Closed and Open Strings. *Nucl. Phys.*, B269:1–23, 1986.

[2] Frits A. Berends, W. T. Giele, and H. Kuijf. On relations between multi - gluon and multigraviton scattering. *Phys. Lett.*, B211:91–94, 1988.

[3] Zvi Bern, Lance J. Dixon, David C. Dunbar, and David A. Kosower. One loop n point gauge theory amplitudes, unitarity and collinear limits. *Nucl.Phys.*, B425:217–260, 1994.

[4] Zvi Bern, Lance J. Dixon, David C. Dunbar, and David A. Kosower. Fusing gauge theory tree amplitudes into loop amplitudes. *Nucl.Phys.*, B435:59–101, 1995.

[5] Z. Bern, Lance J. Dixon, D. C. Dunbar, M. Perelstein, and J. S. Rozowsky. On the relationship between Yang-Mills theory and gravity and its implication for ultraviolet divergences. *Nucl. Phys.*, B530:401–456, 1998.

[6] Z. Bern, Lance J. Dixon, M. Perelstein, and J. S. Rozowsky. One loop n point helicity amplitudes in (selfdual) gravity. *Phys. Lett.*, B444:273–283, 1998.

[7] Z. Bern, Lance J. Dixon, M. Perelstein, and J. S. Rozowsky. Multileg one loop gravity amplitudes from gauge theory. *Nucl. Phys.*, B546:423–479, 1999.

[8] Z. Bern and Aaron K. Grant. Perturbative gravity from QCD amplitudes. *Phys. Lett.*, B457:23–32, 1999.

[9] Z. Bern, J. J. Carrasco, Lance J. Dixon, Henrik Johansson, D. A. Kosower, and R. Roiban. Three-Loop Superfiniteness of N=8 Supergravity. *Phys. Rev. Lett.*, 98:161303, 2007.

[10] Z. Bern, J. J. Carrasco, D. Forde, H. Ita, and Henrik Johansson. Unexpected Cancellations in Gravity Theories. *Phys. Rev.*, D77:025010, 2008.

[11] Stephen J. Parke and T.R. Taylor. An Amplitude for n Gluon Scattering. *Phys.Rev.Lett.*, 56:2459, 1986.

[12] Zhan Xu, Da-Hua Zhang, and Lee Chang. Helicity Amplitudes for Multiple Bremsstrahlung in Massless Nonabelian Gauge Theories. *Nucl. Phys.*, B291:392, 1987.

[13] Michelangelo L. Mangano and Stephen J. Parke. Quark - Gluon Amplitudes in the Dual Expansion. *Nucl. Phys.*, B299:673, 1988.

[14] Michelangelo L. Mangano, Stephen J. Parke, and Zhan Xu. Duality and Multi - Gluon Scattering. *Nucl. Phys.*, B298:653, 1988.

[15] F.A. Berends and W.T. Giele. Recursive calculations for processes with n gluons. *Nuclear Physics B*, 306(4):759 – 808, 1988.

[16] Edward Witten. Perturbative gauge theory as a string theory in twistor space. *Commun. Math. Phys.*, 252:189–258, 2004.

[17] Ruth Britto, Freddy Cachazo, and Bo Feng. New recursion relations for tree amplitudes of gluons. *Nucl.Phys.*, B715:499–522, 2005.

[18] Ruth Britto, Freddy Cachazo, Bo Feng, and Edward Witten. Direct proof of tree-level recursion relation in Yang-Mills theory. *Phys. Rev. Lett.*, 94:181602, 2005.

[19] F. Cachazo, P. Svrcek, and E. Witten. MHV Vertices And Tree Amplitudes In Gauge Theory. *Journal of High Energy Physics*, 9:006, September 2004.

[20] Kasper Risager. A Direct proof of the CSW rules. *JHEP*, 12:003, 2005.

[21] Carola F. Berger, Zvi Bern, Lance J. Dixon, Darren Forde, and David A. Kosower. Bootstrapping One-Loop QCD Amplitudes with General Helicities. *Phys. Rev.*, D74:036009, 2006.

[22] Giovanni Ossola, Costas G. Papadopoulos, and Roberto Pittau. Reducing full one-loop amplitudes to scalar integrals at the integrand level. *Nucl.Phys.*, B763:147–169, 2007.

[23] C.F. Berger, Z. Bern, L.J. Dixon, F. Febres Cordero, D. Forde, et al. An Automated Implementation of On-Shell Methods for One-Loop Amplitudes. *Phys.Rev.*, D78:036003, 2008.

[24] Carola F. Berger, Vittorio Del Duca, and Lance J. Dixon. Recursive Construction of Higgs-Plus-Multiparton Loop Amplitudes: The Last of the Phi-nite Loop Amplitudes. *Phys. Rev.*, D74:094021, 2006. [Erratum: Phys. Rev.D76,099901(2007)].

[25] R. Keith Ellis, W. T. Giele, and Z. Kunszt. A Numerical Unitarity Formalism for Evaluating One-Loop Amplitudes. *JHEP*, 03:003, 2008.

[26] C. F. Berger, Z. Bern, L. J. Dixon, F. Febres Cordero, D. Forde, T. Gleisberg, H. Ita, D. A. Kosower, and D. Maître. Next-to-leading order QCD predictions for W + 3-jet distributions at hadron colliders. *Phys. Rev. D*, 80:074036, Oct 2009.

[27] C. F. Berger, Z. Bern, Lance J. Dixon, F. Febres Cordero, D. Forde, T. Gleisberg, H. Ita, D. A. Kosower, and D. Maitre. Precise Predictions for W + 4 Jet Production at the Large Hadron Collider. *Phys. Rev. Lett.*, 106:092001, 2011.

[28] Georges Aad et al. Observation of a new particle in the search for the Standard Model Higgs boson with the ATLAS detector at the LHC. *Phys. Lett.*, B716:1–29, 2012.

[29] Serguei Chatrchyan et al. Observation of a new boson at a mass of 125 GeV with the CMS experiment at the LHC. *Phys. Lett.*, B716:30–61, 2012.

[30] Z. Bern, J.J.M. Carrasco, and Henrik Johansson. New Relations for Gauge-Theory Amplitudes. *Phys.Rev.*, D78:085011, 2008.

[31] Yi-Xin Chen, Yi-Jian Du, and Bo Feng. A Proof of the Explicit Minimal-basis Expansion of Tree Amplitudes in Gauge Field Theory. *JHEP*, 02:112, 2011.

[32] Leonardo de la Cruz, Alexander Kniss, and Stefan Weinzierl. Proof of the fundamental BCJ relations for QCD amplitudes. *JHEP*, 09:197, 2015.

[33] Z. Bern, J. J. M. Carrasco, Lance J. Dixon, Henrik Johansson, and R. Roiban. Manifest Ultraviolet Behavior for the Three-Loop Four-Point Amplitude of N=8 Supergravity. *Phys. Rev.*, D78:105019, 2008.

[34] Z. Bern, J. J. Carrasco, Lance J. Dixon, H. Johansson, and R. Roiban. The Ultraviolet Behavior of N=8 Supergravity at Four Loops. *Phys. Rev. Lett.*, 103:081301, 2009.

[35] Zvi Bern, John Joseph M. Carrasco, and Henrik Johansson. Perturbative Quantum Gravity as a Double Copy of Gauge Theory. *Phys. Rev. Lett.*, 105:061602, 2010.

[36] Zvi Bern, Tristan Dennen, Yu-tin Huang, and Michael Kiermaier. Gravity as the Square of Gauge Theory. *Phys. Rev.*, D82:065003, 2010.

[37] Z. Bern, C. Boucher-Veronneau, and H. Johansson. N $\geq$ 4 Supergravity Amplitudes from Gauge Theory at One Loop. *Phys. Rev.*, D84:105035, 2011.

[38] John Joseph M. Carrasco and Henrik Johansson. Generic multiloop methods and application to N=4 super-Yang-Mills. *J. Phys.*, A44:454004, 2011.

[39] John JosephM. Carrasco and Henrik Johansson. Five-Point Amplitudes in N=4 Super-Yang-Mills Theory and N=8 Supergravity. *Phys. Rev.*, D85:025006, 2012.

[40] John Joseph M. Carrasco, Marco Chiodaroli, Murat Günaydin, and Radu Roiban. One-loop four-point amplitudes in pure and matter-coupled N ¡= 4 supergravity. *JHEP*, 03:056, 2013.

[41] Yu-tin Huang and Henrik Johansson. Equivalent D=3 Supergravity Amplitudes from Double Copies of Three-Algebra and Two-Algebra Gauge Theories. *Phys. Rev. Lett.*, 110:171601, 2013.

[42] Yu-tin Huang, Henrik Johansson, and Sangmin Lee. On Three-Algebra and Bi-Fundamental Matter Amplitudes and Integrability of Supergravity. *JHEP*, 11:050, 2013.

[43] Zvi Bern, Scott Davies, Tristan Dennen, Yu-tin Huang, and Josh Nohle. Color-Kinematics Duality for Pure Yang-Mills and Gravity at One and Two Loops. *Phys. Rev.*, D92(4):045041, 2015.

[44] L. Borsten, M. J. Duff, L. J. Hughes, and S. Nagy. Magic Square from Yang-Mills Squared. *Phys. Rev. Lett.*, 112(13):131601, 2014.

[45] Alexander Ochirov and Piotr Tourkine. BCJ duality and double copy in the closed string sector. *JHEP*, 05:136, 2014.

[46] A. Anastasiou, L. Borsten, M. J. Duff, L. J. Hughes, and S. Nagy. A magic pyramid of supergravities. *JHEP*, 04:178, 2014.

[47] A. Anastasiou, L. Borsten, M. J. Duff, L. J. Hughes, and S. Nagy. Yang-Mills origin of gravitational symmetries. *Phys. Rev. Lett.*, 113(23):231606, 2014.

[48] A. Anastasiou, L. Borsten, M. J. Hughes, and S. Nagy. Global symmetries of Yang-Mills squared in various dimensions. *JHEP*, 01:148, 2016.

[49] Lance J. Dixon. Ultraviolet Behavior of $\mathcal{N} = 8$ Supergravity. *Subnucl. Ser.*, 47:1–39, 2011.

[50] Pierre Vanhove. The Critical ultraviolet behaviour of N=8 supergravity amplitudes. 2010.

[51] Z. Bern, J. J. M. Carrasco, L. J. Dixon, H. Johansson, and R. Roiban. Simplifying Multiloop Integrands and Ultraviolet Divergences of Gauge Theory and Gravity Amplitudes. *Phys. Rev.*, D85:105014, 2012.

[52] Zvi Bern, Scott Davies, Tristan Dennen, Alexander V. Smirnov, and Vladimir A. Smirnov. Ultraviolet Properties of N=4 Supergravity at Four Loops. *Phys. Rev. Lett.*, 111(23):231302, 2013.

[53] Zvi Bern, Scott Davies, and Tristan Dennen. Enhanced ultraviolet cancellations in $\mathcal{N} = 5$ supergravity at four loops. *Phys. Rev.*, D90(10):105011, 2014.

[54] Gang Yang. Color-Kinematics Duality and Sudakov Form Factor at Five Loops for $\mathcal{N} = 4$ Supersymmetric Yang-Mills Theory. *Phys. Rev. Lett.*, 117:271602, Dec 2016.

[55] Zvi Bern, John Joseph Carrasco, Wei-Ming Chen, Alex Edison, Henrik Johansson, Julio Parra-Martinez, Radu Roiban, and Mao Zeng. Ultraviolet Properties of $\mathcal{N} = 8$ Supergravity at Five Loops. 2018.

[56] S. Stieberger. Open & Closed vs. Pure Open String Disk Amplitudes. 2009.

[57] N. E. J. Bjerrum-Bohr, Poul H. Damgaard, and Pierre Vanhove. Minimal Basis for Gauge Theory Amplitudes. *Phys. Rev. Lett.*, 103:161602, 2009.

[58] Carlos R. Mafra. Simplifying the Tree-level Superstring Massless Five-point Amplitude. *JHEP*, 01:007, 2010.

[59] Carlos R. Mafra, Oliver Schlotterer, Stephan Stieberger, and Dimitrios Tsimpis. Six Open String Disk Amplitude in Pure Spinor Superspace. *Nucl. Phys.*, B846:359–393, 2011.

[60] S. H. Henry Tye and Yang Zhang. Dual Identities inside the Gluon and the Graviton Scattering Amplitudes. *JHEP*, 06:071, 2010. [Erratum: JHEP04,114(2011)].

[61] N. E. J. Bjerrum-Bohr, Poul H. Damgaard, Thomas Sondergaard, and Pierre Vanhove. Monodromy and Jacobi-like Relations for Color-Ordered Amplitudes. *JHEP*, 06:003, 2010.

[62] N. E. J. Bjerrum-Bohr, Poul H. Damgaard, Bo Feng, and Thomas Sondergaard. New Identities among Gauge Theory Amplitudes. *Phys. Lett.*, B691:268–273, 2010.

[63] Carlos R. Mafra, Oliver Schlotterer, and Stephan Stieberger. Explicit BCJ Numerators from Pure Spinors. *JHEP*, 07:092, 2011.

[64] Song He and Oliver Schlotterer. New Relations for Gauge-Theory and Gravity Amplitudes at Loop Level. *Phys. Rev. Lett.*, 118(16):161601, 2017.

[65] Piotr Tourkine and Pierre Vanhove. Higher-loop amplitude monodromy relations in string and gauge theory. *Phys. Rev. Lett.*, 117(21):211601, 2016.

[66] Oliver Schlotterer. Amplitude relations in heterotic string theory and Einstein-Yang-Mills. *JHEP*, 11:074, 2016.

[67] Gang Chen and Yi-Jian Du. Amplitude Relations in Non-linear Sigma Model. *JHEP*, 01:061, 2014.

[68] Freddy Cachazo, Song He, and Ellis Ye Yuan. Scattering Equations and Matrices: From Einstein To Yang-Mills, DBI and NLSM. *JHEP*, 07:149, 2015.

[69] Yi-Jian Du, Fei Teng, and Yong-Shi Wu. Direct Evaluation of n-point single-trace MHV amplitudes in 4d Einstein-Yang-Mills theory using the CHY Formalism. *JHEP*, 09:171, 2016.

[70] Yi-Jian Du and Chih-Hao Fu. Explicit BCJ numerators of nonlinear simga model. *JHEP*, 09:174, 2016.

[71] Clifford Cheung, Grant N. Remmen, Chia-Hsien Shen, and Congkao Wen. Pions as Gluons in Higher Dimensions. *JHEP*, 04:129, 2018.

[72] Marco Chiodaroli, Murat Günaydin, Henrik Johansson, and Radu Roiban. Scattering amplitudes in $\mathcal{N} = 2$ Maxwell-Einstein and Yang-Mills/Einstein supergravity. *JHEP*, 01:081, 2015.

[73] Marco Chiodaroli, Murat Gunaydin, Henrik Johansson, and Radu Roiban. Spontaneously Broken Yang-Mills-Einstein Supergravities as Double Copies. *JHEP*, 06:064, 2017.

[74] Marco Chiodaroli. Simplifying amplitudes in Maxwell-Einstein and Yang-Mills-Einstein supergravities. 2016.

[75] Freddy Cachazo, Song He, and Ellis Ye Yuan. Scattering of Massless Particles in Arbitrary Dimensions. *Phys. Rev. Lett.*, 113(17):171601, 2014.

[76] Freddy Cachazo, Song He, and Ellis Ye Yuan. Scattering of Massless Particles: Scalars, Gluons and Gravitons. *JHEP*, 07:033, 2014.

[77] N. E. J. Bjerrum-Bohr, Jacob L. Bourjaily, Poul H. Damgaard, and Bo Feng. Manifesting Color-Kinematics Duality in the Scattering Equation Formalism. *JHEP*, 09:094, 2016.

[78] Freddy Cachazo, Song He, and Ellis Ye Yuan. Einstein-Yang-Mills Scattering Amplitudes From Scattering Equations. *JHEP*, 01:121, 2015.

[79] Dhritiman Nandan, Jan Plefka, Oliver Schlotterer, and Congkao Wen. Einstein-Yang-Mills from pure Yang-Mills amplitudes. *JHEP*, 10:070, 2016.

[80] Leonardo de la Cruz, Alexander Kniss, and Stefan Weinzierl. Relations for Einstein–Yang–Mills amplitudes from the CHY representation. *Phys. Lett.*, B767:86–90, 2017.

[81] Clifford Cheung, Chia-Hsien Shen, and Congkao Wen. Unifying Relations for Scattering Amplitudes. *JHEP*, 02:095, 2018.

[82] John Joseph M. Carrasco, Carlos R. Mafra, and Oliver Schlotterer. Abelian Z-theory: NLSM amplitudes and α'-corrections from the open string. *JHEP*, 06:093, 2017.

[83] John Joseph M. Carrasco, Carlos R. Mafra, and Oliver Schlotterer. Semi-abelian Z-theory: NLSM+ϕ^3 from the open string. *JHEP*, 08:135, 2017.

[84] Carlos R. Mafra and Oliver Schlotterer. Non-abelian Z-theory: Berends-Giele recursion for the α'-expansion of disk integrals. *JHEP*, 01:031, 2017.

[85] Ricardo Monteiro and Donal O'Connell. The Kinematic Algebra From the Self-Dual Sector. *JHEP*, 07:007, 2011.

[86] Ricardo Monteiro and Donal O'Connell. The Kinematic Algebras from the Scattering Equations. *JHEP*, 03:110, 2014.

[87] Clifford Cheung and Grant N. Remmen. Twofold Symmetries of the Pure Gravity Action. *JHEP*, 01:104, 2017.

[88] Clifford Cheung and Chia-Hsien Shen. Symmetry for Flavor-Kinematics Duality from an Action. *Phys. Rev. Lett.*, 118(12):121601, 2017.

[89] Clifford Cheung and Grant N. Remmen. Hidden Simplicity of the Gravity Action. *JHEP*, 09:002, 2017.

[90] Ricardo Monteiro, Donal O'Connell, and Chris D. White. Black holes and the double copy. *JHEP*, 12:056, 2014.

[91] Andrés Luna, Ricardo Monteiro, Isobel Nicholson, Donal O'Connell, and Chris D. White. The double copy: Bremsstrahlung and accelerating black holes. *JHEP*, 06:023, 2016.

[92] Walter D. Goldberger and Alexander K. Ridgway. Radiation and the classical double copy for color charges. *Phys. Rev.*, D95(12):125010, 2017.

[93] Zvi Bern, Scott Davies, and Josh Nohle. Double-Copy Constructions and Unitarity Cuts. *Phys. Rev.*, D93(10):105015, 2016.

[94] M. Maggiore. *Gravitational Waves: Volume 1: Theory and Experiments*. Gravitational Waves. Oxford University Press, 2008.

[95] L. Blanchet and T. Damour. Radiative gravitational fields in general relativity I. General structure of the field outside the source. *Philosophical Transactions of the Royal Society of London A: Mathematical, Physical and Engineering Sciences*, 320(1555):379–430, 1986.

[96] Luc Blanchet, Thibault Damour, and Bala R. Iyer. Gravitational waves from inspiralling compact binaries: Energy loss and waveform to second-post-Newtonian order. *Phys. Rev. D*, 51:5360–5386, May 1995.

[97] Luc Blanchet. Energy losses by gravitational radiation in inspiraling compact binaries to $\frac{5}{2}$ post-Newtonian order. *Phys. Rev. D*, 54:1417–1438, Jul 1996.

[98] Luc Blanchet and Guillaume Faye. General relativistic dynamics of compact binaries at the third post-Newtonian order. *Phys. Rev. D*, 63:062005, Feb 2001.

[99] Toshifumi Futamase and Yousuke Itoh. The Post-Newtonian Approximation for Relativistic Compact Binaries. *Living Reviews in Relativity*, 10(1):2, Mar 2007.

[100] Luc Blanchet, Guillaume Faye, Bala R. Iyer, and Benoit Joguet. Gravitational-wave inspiral of compact binary systems to 7/2 post-Newtonian order. *Phys. Rev. D*, 65:061501, Feb 2002.

[101] Luc Blanchet, Thibault Damour, Gilles Esposito-Farèse, and Bala R. Iyer. Gravitational Radiation from Inspiralling Compact Binaries Completed at the Third Post-Newtonian Order. *Phys. Rev. Lett.*, 93:091101, Aug 2004.

[102] Luc Blanchet, Guillaume Faye, Bala R Iyer, and Siddhartha Sinha. The third post-Newtonian gravitational wave polarizations and associated spherical harmonic modes for inspiralling compact binaries in quasi-circular orbits. *Classical and Quantum Gravity*, 25(16):165003, 2008.

[103] Luc Blanchet. Gravitational Radiation from Post-Newtonian Sources and Inspiralling Compact Binaries. *Living Rev. Rel.*, 17:2, 2014.

[104] Alan G. Wiseman and Clifford M. Will. Christodoulou's nonlinear gravitational-wave memory: Evaluation in the quadrupole approximation. *Phys. Rev. D*, 44:R2945–R2949, Nov 1991.

[105] Clifford M. Will and Alan G. Wiseman. Gravitational radiation from compact binary systems: Gravitational waveforms and energy loss to second post-Newtonian order. *Phys. Rev. D*, 54:4813–4848, Oct 1996.

[106] Michael E. Pati and Clifford M. Will. Post-Newtonian gravitational radiation and equations of motion via direct integration of the relaxed Einstein equations: Foundations. *Phys. Rev. D*, 62:124015, Nov 2000.

[107] Michael E. Pati and Clifford M. Will. Post-Newtonian gravitational radiation and equations of motion via direct integration of the relaxed Einstein equations. II. Two-body equations of motion to second post-Newtonian order, and radiation reaction to 3.5 post-Newtonian order. *Phys. Rev. D*, 65:104008, Apr 2002.

[108] Stefano Foffa and Riccardo Sturani. Dynamics of the gravitational two-body problem at fourth post-Newtonian order and at quadratic order in the Newton constant. *Phys. Rev.*, D87(6):064011, 2013.

[109] Piotr Jaranowski and Gerhard Schafer. Towards the 4th post-Newtonian Hamiltonian for two-point-mass systems. *Phys. Rev.*, D86:061503, 2012.

[110] Piotr Jaranowski and Gerhard Schäfer. Dimensional regularization of local singularities in the 4th post-Newtonian two-point-mass Hamiltonian. *Phys. Rev.*, D87:081503, 2013.

[111] Thibault Damour, Piotr Jaranowski, and Gerhard Schäfer. Nonlocal-in-time action for the fourth post-Newtonian conservative dynamics of two-body systems. *Phys. Rev.*, D89(6):064058, 2014.

[112] Thibault Damour, Piotr Jaranowski, and Gerhard Schäfer. Fourth post-Newtonian effective one-body dynamics. *Phys. Rev.*, D91(8):084024, 2015.

[113] Laura Bernard, Luc Blanchet, Alejandro Bohé, Guillaume Faye, and Sylvain Marsat. Fokker action of nonspinning compact binaries at the fourth post-Newtonian approximation. *Phys. Rev.*, D93(8):084037, 2016.

[114] Piotr Jaranowski and Gerhard Schäfer. Derivation of local-in-time fourth post-Newtonian ADM Hamiltonian for spinless compact binaries. *Phys. Rev.*, D92(12):124043, 2015.

[115] Rafael A. Porto and Ira Z. Rothstein. Apparent ambiguities in the post-Newtonian expansion for binary systems. *Phys. Rev.*, D96(2):024062, 2017.

[116] Laura Bernard, Luc Blanchet, Guillaume Faye, and Tanguy Marchand. Center-of-Mass Equations of Motion and Conserved Integrals of Compact Binary Systems at the Fourth Post-Newtonian Order. 2017.

[117] K. Westpfahl and M. Goller. Gravitational scattering of two relativistic particles in post-linear approximation. *Lettere al Nuovo Cimento (1971-1985)*, 26(17):573–576, Dec 1979.

[118] Westpfahl Konradin. High-Speed Scattering of Charged and Uncharged Particles in General Relativity. *Fortschritte der Physik/Progress of Physics*, 33(8):417–493, 1985.

[119] K Westpfahl, R Mohles, and H Simonis. Energy-momentum conservation for gravitational two-body scattering in the post-linear approximation. *Classical and Quantum Gravity*, 4(5):L185, 1987.

[120] Tomá š Ledvinka, Gerhard Schäfer, and Ji ří Bičák. Relativistic Closed-Form Hamiltonian for Many-Body Gravitating Systems in the Post-Minkowskian Approximation. *Phys. Rev. Lett.*, 100:251101, Jun 2008.

[121] Thibault Damour. Gravitational scattering, post-Minkowskian approximation and Effective One-Body theory. *Phys. Rev.*, D94(10):104015, 2016.

[122] Donato Bini and Thibault Damour. Gravitational spin-orbit coupling in binary systems, post-Minkowskian approximation and effective one-body theory. *Phys. Rev.*, D96(10):104038, 2017.

[123] Thibault Damour. High-energy gravitational scattering and the general relativistic two-body problem. 2017.

[124] Justin Vines. Scattering of two spinning black holes in post-Minkowskian gravity, to all orders in spin, and effective-one-body mappings. *Classical and Quantum Gravity*, 35(8):084002, 2018.

[125] Alexander K. Ridgway and Mark B. Wise. Static Spherically Symmetric Kerr-Schild Metrics and Implications for the Classical Double Copy. 2015.

[126] Andrés Luna, Ricardo Monteiro, Donal O'Connell, and Chris D. White. The classical double copy for Taub–NUT spacetime. *Phys. Lett.*, B750:272–277, 2015.

[127] Lee Smolin. The Plebanski action extended to a unification of gravity and Yang-Mills theory. *Phys. Rev.*, D80:124017, 2009.

[128] A. Garrett Lisi, Lee Smolin, and Simone Speziale. Unification of gravity, gauge fields, and Higgs bosons. *J. Phys.*, A43:445401, 2010.

[129] A. Garrett Lisi. Lie Group Cosmology. 2015.

[130] Chris D. White. Exact solutions for the biadjoint scalar field. 2016.

[131] Nadia Bahjat-Abbas, Andrés Luna, and Chris D. White. The Kerr-Schild double copy in curved spacetime. 2017.

[132] Mariana Carrillo-González, Riccardo Penco, and Mark Trodden. The classical double copy in maximally symmetric spacetimes. *JHEP*, 04:028, 2018.

[133] Tim Adamo, Eduardo Casali, Lionel Mason, and Stefan Nekovar. Scattering on plane waves and the double copy. 2017.

[134] Walter D. Goldberger, Siddharth G. Prabhu, and Jedidiah O. Thompson. Classical gluon and graviton radiation from the bi-adjoint scalar double copy. *Phys. Rev.*, D96(6):065009, 2017.

[135] Walter D. Goldberger and Alexander K. Ridgway. Bound states and the classical double copy. 2017.

[136] Walter D. Goldberger, Jingping Li, and Siddharth G. Prabhu. Spinning particles, axion radiation, and the classical double copy. 2017.

[137] Jingping Li and Siddharth G. Prabhu. Gravitational radiation from the classical spinning double copy. 2018.

[138] Andrés Luna, Ricardo Monteiro, Isobel Nicholson, Alexander Ochirov, Donal O'Connell, Niclas Westerberg, and Chris D. White. Perturbative spacetimes from Yang-Mills theory. *JHEP*, 04:069, 2017.

[139] Andrés Luna, Isobel Nicholson, Donal O'Connell, and Chris D. White. Inelastic Black Hole Scattering from Charged Scalar Amplitudes. 2017.

[140] David Chester. Bern-Carrasco-Johansson relations for one-loop QCD integral coefficients. *Phys. Rev. D*, 93:065047, Mar 2016.

[141] Michelangelo L. Mangano and Stephen J. Parke. Multiparton amplitudes in gauge theories. *Phys.Rept.*, 200:301–367, 1991.

[142] Lance J. Dixon. Calculating scattering amplitudes efficiently. 1996.

[143] Ronald Kleiss and Hans Kuijf. Multi - Gluon Cross-sections and Five Jet Production at Hadron Colliders. *Nucl.Phys.*, B312:616, 1989.

[144] Yin Jia, Rijun Huang, and Chang-Yong Liu. $U(1)$-decoupling, KK and BCJ relations in $\mathcal{N} = 4$ SYM. *Phys.Rev.*, D82:065001, 2010.

[145] Z. Bern and A. G. Morgan. Massive loop amplitudes from unitarity. *Nucl. Phys.*, B467:479–509, 1996.

[146] Zvi Bern, Lance J. Dixon, David C. Dunbar, and David A. Kosower. One loop selfdual and N=4 superYang-Mills. *Phys. Lett.*, B394:105–115, 1997.

[147] Charalampos Anastasiou, Ruth Britto, Bo Feng, Zoltan Kunszt, and Pierpaolo Mastrolia. D-dimensional unitarity cut method. *Phys. Lett.*, B645:213–216, 2007.

[148] Walter T. Giele, Zoltan Kunszt, and Kirill Melnikov. Full one-loop amplitudes from tree amplitudes. *JHEP*, 04:049, 2008.

[149] S. D. Badger. Direct Extraction Of One Loop Rational Terms. *JHEP*, 01:049, 2009.

[150] Harald Ita. Susy Theories and QCD: Numerical Approaches. *J.Phys.*, A44:454005, 2011.

[151] N. E. J. Bjerrum-Bohr, Poul H. Damgaard, Thomas Sondergaard, and Pierre Vanhove. Monodromy and Jacobi-like Relations for Color-Ordered Amplitudes. *JHEP*, 06:003, 2010.

[152] Rutger H. Boels and Reinke Sven Isermann. New relations for scattering amplitudes in Yang-Mills theory at loop level. *Phys. Rev.*, D85:021701, 2012.

[153] Rutger H. Boels and Reinke Sven Isermann. Yang-Mills amplitude relations at loop level from non-adjacent BCFW shifts. *JHEP*, 03:051, 2012.

[154] Simon Badger, Gustav Mogull, Alexander Ochirov, and Donal O'Connell. A Complete Two-Loop, Five-Gluon Helicity Amplitude in Yang-Mills Theory. *JHEP*, 10:064, 2015.

[155] D. Maitre and P. Mastrolia. S@M, a Mathematica Implementation of the Spinor-Helicity Formalism. *Comput.Phys.Commun.*, 179:501–574, 2008.

[156] Brecht Truijen. Britto-Cachazo-Feng-Witten Recursion: An Introduction. Master's thesis, Utrecht University Institute for Theoretical Physics, August 2012.

[157] D. B. Melrose. Reduction of Feynman diagrams. *Nuovo Cim.*, 40:181–213, 1965.

[158] W. L. van Neerven and J. A. M. Vermaseren. Large Loop Integrals. *Phys. Lett.*, B137:241, 1984.

[159] Zvi Bern, Lance J. Dixon, and David A. Kosower. Dimensionally regulated pentagon integrals. *Nucl. Phys.*, B412:751–816, 1994.

[160] Ruth Britto, Freddy Cachazo, and Bo Feng. Generalized unitarity and one-loop amplitudes in N=4 super-Yang-Mills. *Nucl.Phys.*, B725:275–305, 2005.

[161] Darren Forde. Direct extraction of one-loop integral coefficients. *Phys.Rev.*, D75:125019, 2007.

[162] Kasper Risager. Unitarity and On-Shell Recursion Methods for Scattering Amplitudes. 2008.

[163] Scott Davies. One-Loop QCD and Higgs to Partons Processes Using Six-Dimensional Helicity and Generalized Unitarity. *Phys.Rev.*, D84:094016, 2011.

[164] Amedeo Primo and William J. Torres Bobadilla. BCJ Identities and d-Dimensional Generalized Unitarity. *JHEP*, 04:125, 2016.

[165] Gerard 't Hooft and M. J. G. Veltman. One loop divergencies in the theory of gravitation. *Ann. Inst. H. Poincare Phys. Theor.*, A20:69–94, 1974.

[166] J. Scherk and J.H. Schwarz. Dual models and the geometry of space-time. *Physics Letters B*, 52(3):347 – 350, 1974.

[167] Oscar Castillo-Felisola, Cristobal Corral, Sergey Kovalenko, Ivan Schmidt, and Valery E. Lyubovitskij. Axions in gravity with torsion. *Phys. Rev.*, D91(8):085017, 2015.

[168] R. J. Petti. Derivation of Einstein-Cartan theory from general relativity. *ArXiv e-prints*, January 2013.

[169] Andrzej Trautman. Einstein-Cartan theory. 2006.

[170] Nikodem J. Poplawski. Nonsingular Dirac particles in spacetime with torsion. *Phys. Lett.*, B690:73–77, 2010. [Erratum: Phys. Lett.B727,575(2013)].

[171] Joseph Anthony Harrison. Einstein-Cartan Theory and Its Formulation as a Quantum Field Theory, 2013.

[172] Echehard W. Mielke. Is Einstein-Cartan Theory Coupled to Light Fermions Asymptotically Safe? *Journal of Gravity*, 2013, 2013.

[173] J. E. Daum and M. Reuter. Einstein-Cartan gravity, Asymptotic Safety, and the running Immirzi parameter. *Annals Phys.*, 334:351–419, 2013.

[174] Carlo Pagani and Roberto Percacci. Quantum gravity with torsion and non-metricity. *Class. Quant. Grav.*, 32(19):195019, 2015.

[175] Abhay Ashtekar, Martin Reuter, and Carlo Rovelli. From General Relativity to Quantum Gravity. 2014.

[176] Carlo Pagani and Martin Reuter. Finite Entanglement Entropy in Asymptotically Safe Quantum Gravity. 2018.

[177] Nikodem J. Poplawski. Torsion as electromagnetism and spin. *Int. J. Theor. Phys.*, 49:1481–1488, 2010.

[178] H. Dehnen and E. Hitzer. SU(2)×U(1) gauge gravity. *International Journal of Theoretical Physics*, 34(9):1981–2001, Sep 1995.

[179] Jens Boos and Friedrich W. Hehl. Gravity-induced four-fermion contact interaction implies gravitational intermediate W and Z type gauge bosons. *Int. J. Theor. Phys.*, 56(3):751–756, 2017.

[180] A.V. Minkevich. Accelerating Universe with spacetime torsion but without dark matter and dark energy. *Physics Letters B*, 678(5):423 – 426, 2009.

[181] Nikodem J. Poplawski. Four-fermion interaction from torsion as dark energy. *Gen. Rel. Grav.*, 44:491–499, 2012.

[182] Andre Tilquin and Thomas Schucker. Torsion, an alternative to dark matter? *Gen. Rel. Grav.*, 43:2965–2978, 2011.

[183] Carl F. Diether and Joy Christian. On the Role of Einstein-Cartan Gravity in Fundamental Particle Physics. 2017.

[184] B. P. et al. Abbott. Observation of Gravitational Waves from a Binary Black Hole Merger. *Phys. Rev. Lett.*, 116:061102, Feb 2016.

[185] C. K. Whitney. On the Lienard-Wiechert potentials. *Hadronic Journal*, 11(5):257–261, 1988.

[186] C. K. Whitney. Generalized functions in relativistic potential theory. *Hadronic Journal*, 10:289–290, 1987.

[187] C. K. Whitney. Field lines in classical theory. *Hadronic Journal*, 10:91–93, 1987.

[188] C. K. Whitney. Operator noncommutation in classical field theory. *Hadronic Journal*, 11:101–107, 1988.

[189] C. K. Whitney. Limiting cases in relativistic field theory. *Hadronic Journal*, 11:147–151, 1988.

[190] J. H. Field. Space-time transformation properties of inter-charge forces and dipole radiation: Breakdown of the classical field concept in relativistic electrodynamics. *ArXiv Physics e-prints*, April 2006.

[191] J. H. Field. Retarded electric and magnetic fields of a moving charge: Feynman's derivation of Lienard-Wiechert potentials revisited. *ArXiv e-prints*, April 2007.

[192] J. H. Field. Forces Between Electric Charges in Motion:. Rutherford Scattering, Circular Keplerian Orbits, Action-At and Newton's Third Law in Relativistic Classical Electrodynamics. *International Journal of Modern Physics A*, 23:327–351, 2008.

[193] Andrew E. Chubykalo and Roman Smirnov-Rueda. Action at a distance as a full-value solution of Maxwell equations: The basis and application of the separated-potentials method. *Phys. Rev.*, E53(5):5373–5381, 1996.

[194] John David Jackson. Criticism of 'Necessity of simultaneous coexistence of instantaneous and retarded interactions in classical electrodynamics'. *Int. J. Mod. Phys.*, A17:3975–3979, 2002.

[195] Ljuba Skovrlj and Tomislav Ivezic. About the simultaneous coexistence of instantaneous and retarded interactions in classical electrodynamics. *Int. J. Mod. Phys.*, A17:2513–2518, 2002.

[196] H. Aspden. Instantaneous electrodynamic potential with retarded energy transfer. *Hadronic Journal*, 11:107–113, 1988.

[197] John Archibald Wheeler and Richard Phillips Feynman. Interaction with the Absorber as the Mechanism of Radiation. *Rev. Mod. Phys.*, 17:157–181, Apr 1945.

[198] A. K. Assis. *Weber's Electrodynamics*. Fundamental Theories of Physics. Springer, 1994.

[199] A. Lukyanov and S. Molokov. Do we need to recourse to Ampere-Neumann electrodynamics to explain wire fragmentation in the solid state? *ArXiv Physics e-prints*, December 2000.

[200] J.D. Jackson. *Classical Electrodynamics, 3rd Ed.* Wiley, 1998.

[201] Marcelo Bueno and A. K. Assis. Proof of the identity between Ampère and Grassmann's forces. *Physica Scripta*, 56(6):554, 1997.

[202] Tom Banks, W. Fischler, S. H. Shenker, and Leonard Susskind. M theory as a matrix model: A Conjecture. *Phys. Rev.*, D55:5112–5128, 1997. [,435(1996)].

[203] Leonard Susskind. The World as a hologram. *J. Math. Phys.*, 36:6377–6396, 1995.

[204] Raphael Bousso. The holographic principle for general backgrounds. *Classical and Quantum Gravity*, 17(5):997, 2000.

[205] Frank Ferrari. Gauge Theories, D-Branes and Holography. *Nucl. Phys.*, B880:247–289, 2014.

[206] Roman Tomaschitz. Tachyons and the Wheeler-Feynman absorber theory. *Classical and Quantum Gravity*, 18(21):4395, 2001.

[207] E. V. Stefanovich. Relativistic Quantum Dynamics: A non-traditional perspective on space, time, particles, fields, and action-at-a-distance. *ArXiv Physics e-prints*, April 2005.

[208] Elie Cartan. Sur les variétés à connexion affine et la théorie de la relativité généralisée (première partie). *Annales scientifiques de lÉcole normale supérieure*, 40:325–412, 1923.

[209] Kurt Friedrichs. Eine invariante formulierung des newtonschen gravitationsgesetzes und des grenzüberganges vom einsteinschen zum newtonschen gesetz. *Mathematische Annalen*, 98(1):566–575, Mar 1928.

[210] W. G. Dixon. On the uniqueness of the newtonian theory as a geometric theory of gravitation. *Communications in Mathematical Physics*, 45(2):167–182, Jun 1975.

[211] C. Duval, G. Burdet, H. P. Künzle, and M. Perrin. Bargmann structures and newton-cartan theory. *Phys. Rev. D*, 31:1841–1853, Apr 1985.

[212] Walter D. Goldberger. AdS/CFT duality for non-relativistic field theory. *JHEP*, 03:069, 2009.

[213] F.G. Friedlander, P.V. Landshoff, D.R. Nelson, S. Weinberg, and D.W. Sciama. *The Wave Equation on a Curved Space-Time*. Cambridge Monographs on Mathematical Physics. Cambridge University Press, 1975.

[214] David Chester. Radiative double copy for Einstein-Yang-Mills theory. *Phys. Rev. D*, 97:084025, Apr 2018.

[215] Nima Arkani-Hamed, Freddy Cachazo, Clifford Cheung, and Jared Kaplan. A Duality For The S Matrix. *JHEP*, 03:020, 2010.

[216] Song He, Oliver Schlotterer, and Yong Zhang. New BCJ representations for one-loop amplitudes in gauge theories and gravity. 2017.

[217] Tim Adamo, Eduardo Casali, Kai A. Roehrig, and David Skinner. On tree amplitudes of supersymmetric Einstein-Yang-Mills theory. *JHEP*, 12:177, 2015.

[218] Stephan Stieberger and Tomasz R. Taylor. New relations for Einstein–Yang–Mills amplitudes. *Nucl. Phys.*, B913:151–162, 2016.

[219] Freddy Cachazo, Song He, and Ellis Ye Yuan. Scattering equations and Kawai-Lewellen-Tye orthogonality. *Phys. Rev.*, D90(6):065001, 2014.

[220] A. Anastasiou, L. Borsten, M. J. Duff, A. Marrani, S. Nagy, and M. Zoccali. Are all supergravity theories Yang-Mills squared? 2017.

[221] Henrik Johansson and Josh Nohle. Conformal Gravity from Gauge Theory. 2017.

[222] C.W. Misner, K.S. Thorne, and J.A. Wheeler. *Gravitation*. Number pt. 3 in Gravitation. W. H. Freeman, 1973.

[223] Yi-Zen Chu. More On Cosmological Gravitational Waves And Their Memories. *Class. Quant. Grav.*, 34(19):194001, 2017.

[224] Eanna E. Flanagan and Scott A. Hughes. The Basics of gravitational wave theory. *New J. Phys.*, 7:204, 2005.

[225] Alejandro Bohé et al. Improved effective-one-body model of spinning, nonprecessing binary black holes for the era of gravitational-wave astrophysics with advanced detectors. *Phys. Rev.*, D95(4):044028, 2017.

[226] Jordan Moxon and Éanna Flanagan. Radiation-Reaction Force on a Small Charged Body to Second Order. 2017.

[227] P. Sikivie and N. Weiss. Classical Yang-Mills theory in the presence of external sources. *Phys. Rev. D*, 18:3809–3821, Nov 1978.

[228] S. K. Wong. Field and particle equations for the classical Yang-Mills field and particles with isotopic spin. *Il Nuovo Cimento A (1965-1970)*, 65(4):689–694, Feb 1970.

[229] F. W. Hehl and B. K. Datta. Nonlinear Spinor Equation and Asymmetric Connection in General Relativity. *Journal of Mathematical Physics*, 12:1334–1339, July 1971.

[230] Friedrich W. Hehl, Paul von der Heyde, and G. David Kerlick. General relativity with spin and torsion and its deviations from Einstein's theory. *Phys. Rev. D*, 10:1066–1069, Aug 1974.

[231] P.A.M. Dirac. *General Theory of Relativity.* Physics Notes. Princeton University Press, 1975.

[232] L.D. Landau and E.M. Lifshitz. Chaper 11 - The Gravitational Field Equations. In L.D. Landau and E.M. Lifshitz, editors, *The Classical Theory of Fields (Fourth Edition)*, volume 2 of *Course of Theoretical Physics*, pages 259 – 294. Pergamon, Amsterdam, fourth edition edition, 1975.

[233] Michael E. Peskin and Daniel V. Schroeder. *An Introduction to quantum field theory.* Addison-Wesley, Reading, USA, 1995.

[234] Bryce S. DeWitt. Quantum theory of gravity. iii. applications of the covariant theory. *Phys. Rev.*, 162:1239–1256, Oct 1967.

[235] Sigurd Sannan. Gravity as the limit of the type-II superstring theory. *Phys. Rev. D*, 34:1749–1758, Sep 1986.

[236] Dietmar Ebert, Jan Plefka, and Andreas Rodigast. Absence of gravitational contributions to the running Yang-Mills coupling. *Phys. Lett.*, B660:579–582, 2008.

[237] Andreas Rodigast. *One-Loop Divergences of the Yang-Mills Theory Coupled to Gravitation.* PhD thesis, Humboldt University, August 2008.